

PDF hosted at the Radboud Repository of the Radboud University Nijmegen

The following full text is a publisher's version.

For additional information about this publication click this link.

<http://hdl.handle.net/2066/92741>

Please be advised that this information was generated on 2021-11-06 and may be subject to change.

**The role of DC-STAMP and its interacting
partners LUMAN and OS9 in dendritic cell
immunobiology
STAMPing the way to Golgi**

Anna Sanecka-Duin

The research described in this thesis was performed at the Department of Tumor Immunology of the Nijmegen Centre for Molecular Life Sciences (NCMLS), Radboud University Nijmegen Medical Centre, the Netherlands, and was supported by grant 912-02-34 and VICI grant 918-66-615 (awarded to G.J.A) from the Netherlands Organisation for Scientific Research (NWO).

ISBN: 978-90-8570-982-4

© 2012 by Anna Sanecka-Duin

The image of the Mandelbrot fractal on the cover was generated with the use of www.fractalposter.com

Page design and lay-out: Patrick Duin and Anna Sanecka-Duin

Printed by: Wöhrmann print service, the Netherlands

**The role of DC-STAMP and its interacting
partners LUMAN and OS9 in dendritic cell
immunobiology
STAMPing the way to Golgi**

Een wetenschappelijke proeve op het gebied van de
Medische Wetenschappen

Proefschrift

ter verkrijging van de graad van doctor
aan de Radboud Universiteit Nijmegen,
op gezag van rector magnificus, prof. mr. S.C.J.J. Kortmann,
volgens besluit van het college van decanen
in het openbaar te verdedigen op vrijdag 23 maart 2012
om 10:30 uur precies

door

Anna Sanecka-Duin

geboren op 6 maart 1981
te Staszów, Polen

Promotor:

Prof. Dr. Gosse J. Adema

Leden manuscriptcommissie:

Prof. Dr. Ad Geurts van Kessel (voorzitter)

Prof. Dr. Teunis B. H. Geijtenbeek (AMC Amsterdam)

Dr. Bert van der Reijden

Table of contents

Abbreviations	7
Chapter 1 General introduction	11
Chapter 2 OS9 interacts with DC-STAMP and modulates its intracellular localization in response to TLR ligation <i>Molecular Immunology 46 (2009) 505–515</i>	31
Chapter 3 DC-STAMP interacts with ER-resident transcription factor LUMAN which becomes activated during DC maturation <i>Molecular Immunology 47 (2010) 1963–1973</i>	57
Chapter 4 DC-STAMP knock-down deregulates cytokine production and T-cell stimulatory capacity of LPS-matured dendritic cells <i>BMC Immunology (2011), 12:57</i>	85
Chapter 5 Analysis of genes regulated by the transcription factor LUMAN identifies ApoA4 as a target gene in dendritic cells <i>Molecular Immunology (2011), doi:10.1016/j.molimm.2011.12.003</i>	107
Chapter 6 General discussion and future perspectives	129
Summary	145
Samenvatting	147
Podsumowanie	149
Acknowledgements	153
Curriculum Vitae	157
List of publications	159

Abbreviations

APC	antigen presenting cell
Apo	apolipoprotein
ATF6	activating transcription factor 6
BfA	brefeldin A
cDC	conventional DCs
C/EBP	CCAAT/enhancer binding protein
CFSE	carboxyfluorescein succinimidyl ester
CLSM	confocal laser scanning microscopy
CRE	cAMP response element
D2SC/1	dendritic cell-like cell line
DAMP	danger associated molecular patterns
DC	dendritic cell
DC-STAMP	DC-specific transmembrane protein
EDEM	ER degradation-enhancing alpha-mannosidase-like
ELISA	enzyme-linked immunosorbent assay
ER	endoplasmic reticulum
ERAD	ER associated degradation
FACS	fluorescence-activated cell sorting
GFP	green fluorescent protein
GM-CSF	granulocytes monocyte-colony stimulating factor
HCF	host cell factor
Herp	homocysteine-induced ER protein
HIF1 α	hypoxia-inducible 1 alpha
IL	interleukin
IP	immunoprecipitation
LPS	lipopolysaccharide
mBMDC	mouse bone marrow-derived DC
MEP1B	meprin A subunit beta
MFI	mean fluorescence intensity
MHC	major histocompatibility complex
MLR	mixed lymphocyte reaction
MOI	multiplicity of infection
ND	not detectable
NGFR	nerve growth factor receptor
OS9	amplified in osteosarcoma 9
PAGE	polyacrylamide gel electrophoresis
PAMPs	pathogen associated molecular patterns
PBGD	porphobilinogen deaminase
PCR	polymerase chain reaction
pDC	plasmacytoid DC
PDI	protein disulfide isomerase
PRR	pattern recognition receptor
qPCR	quantitative PCR
RIP	regulated intramembrane proteolysis
RT-PCR	reverse transcriptase PCR
shRNA	short hairpin RNA
SREBP	sterol regulatory binding protein
TF	transcription factor
TFBS	TF binding site
TG	thapsigargin

Th	T helper cell
TLR	toll-like receptor
Tm	tunicamycin
tNGFR	truncated nerve growth factor receptor
Treg	regulatory T cell
TRPV4	vanilloid transient receptor potential protein 4
TSS	transcription start site
TU	transfection unit
UPRE	unfolded protein response element
Y-2-H	yeast-2-hybrid

CHAPTER 1

General introduction

Immune system

Our body is constantly challenged by invasion of pathogenic bacteria, viruses, fungi and parasites. The immune system is our armour against it. The cells of the immune system evolved to fight the invasion of the infectious intruders while being able to recognize the non-infectious self antigens that should be left in peace¹. The immune system can be divided into innate and adaptive immune responses. Innate immunity serves as a first line of defence while the adaptive immune system protects us from re-infection². Innate immune responses do not require prior exposure to certain pathogen and are often called unspecific ones. Nevertheless, activation of innate immune cells depend on recognition of specific pathogen associated molecular patterns (PAMPs) by a wide range of pattern recognition receptors (PRR). Mast cells, macrophages, dendritic cells, natural killer cells and granulocytes are the mediators of the innate immunity³⁻⁷. The innate immune responses create an essential foundation for the initiation of adaptive immunity. In the adaptive immune response, antigen-specific lymphocytes proliferate and differentiate into effector cells that eliminate pathogens. B cells and T cells are the key players in adaptive immunity. They circulate between blood and lymph until they come across their specific antigen. After encountering antigen, B cells become activated and differentiate into memory B cells or plasma cells that produce pathogen specific antibodies. Antibody mediated immunity is known as humoral immunity and provides the defence mechanism against the extracellular pathogens^{8,9}. Each T cell express a unique receptor that recognizes peptide fragment presented in the context of a major histocompatibility complex (MHC) molecule¹⁰. There are two classes of MHC molecules that can present peptides to the two distinct T cell types. MHC class I molecules present peptide to CD8 positive T cells known as the cytotoxic T cells¹¹. The cytotoxic T cells are specialized in killing cells that present the MHC peptide specific for its T cell receptor. As peptides presented in the context of MHC class I come mostly from inside the cell the CD8⁺ T cells are an efficient defence mechanism against intracellular pathogens. MHC class II molecules are expressed uniquely by antigen presenting cells (APC) like dendritic cells, macrophages and B cells¹². Peptides bound to MHC class II are predominantly delivered from exogenous proteins. CD4 positive T cells can recognize peptides that are presented in the context of MHC class II molecules. The peptide recognition with an appropriate second signal and cytokine stimulation will lead to a differentiation of the naïve T cell into T helper cell (Th). Activated Th cells can differentiate into different subsets - that is, Th1, Th2, and Th17 cells - that drive different classes of specific immune responses¹³ (Fig. 1). The Th1 subset secretes mainly IL-2 and IFN- γ

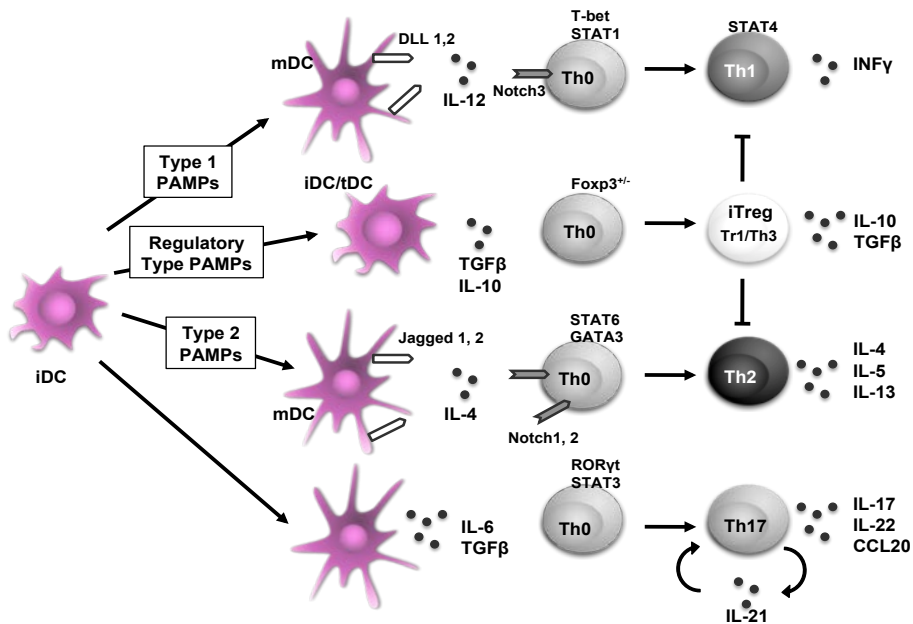


Figure 1. Schematic representation of the functional plasticity of DCs to polarize naïve T cells. According to the type of pathogen and the presence of a variety of surrounding tissue factors DCs via expression of particular cytokines profiles or cell surface molecules regulate the naïve T cell differentiation. Different Th-cell lineages are specialized in the eradication of specific pathogens (Th1, Th2, Th17) or maintaining homeostasis (Treg).

giving support to cytotoxic T cells and activating macrophages. Th2 cells simulate humoral responses by providing help to the B cells^{14,15}. Recently, a new Th17 subset that produces high levels of IL-17 has been described^{16,17}. This subset is implicated in regulation of inflammatory responses¹⁸. An additional subset of T cells that can suppress proliferation of all above-mentioned subsets and prevent excessive immune responses that may result in autoimmunity is known as regulatory T cells (Treg)¹⁹. Several types of Treg cells have been described on the basis of their origin, generation and mechanism of action. These cells can be broadly subdivided into two groups: endogenous, known also as naturally occurring Treg cells (nTreg cells), and inducible Treg cells (iTreg cells) also described as adaptive Treg cells²⁰. The naturally occurring Treg cells originate from thymus and express the transcription factor Foxp3^{21,22}. The suppressive activity of these cells is known to be antigen non-specific and involves cell contact-dependent mechanisms²³. Adaptive Treg cells that develop in the periphery can be divided into at least two types: interleukin 10 (IL-10)-producing, Foxp3 negative Tr1 cells²⁴ and Foxp3 positive Th3 cells producing

high amounts of TGF- β ^{25,26}. The precise mechanisms by which these cells function to maintain the balance between immunity and tolerance are not fully understood. It is presumed that crosstalk among these various Treg cell populations is required for the integrated control of the immune responses²⁷.

Dendritic cells

Dendritic cells (DCs) are professional antigen presenting cells that play a key role in maintenance of the balance between immunity and tolerance in our body²⁸. They link innate and adaptive immunity and are important in both initiation and modulation of the immune response²⁹. DCs are widely distributed between different tissues at the contact sites with the external milieu, such as the skin, gut or lungs where they constantly scavenge the environment for the presence of invading pathogens.

DC subsets

DCs represent a widely distributed population of bone marrow derived cells. Although they share many common features, multiple subtypes of DCs with distinct functions have been identified³⁰. Two major intrinsically different subpopulations of DCs are the conventional DCs (cDCs), and the plasmacytoid DCs (pDCs). Both of them can arise from common myeloid and lymphoid precursor but their function, activating cytokines and markers are different³¹. Plasmacytoid DCs are the front line in anti-viral immunity as they rapidly produce high amounts of type I interferon in response to viruses³². On the other hand, conventional DC subsets have ability to respond to different microbial structures and to direct T cell differentiation. Conventional DCs can be subdivided into migratory DCs, which traffic from peripheral tissues to the lymph nodes, and lymphoid-organ-resident DCs, which develop from bone-marrow precursors within the lymphoid organs³³. Migratory DCs can be further divided into three major groups: interstitial DCs (dermal DCs), CD103⁺ DCs and Langerhans cells. Lymphoid-organ-resident DCs can be categorized into three subsets in the spleen on the basis of their expression of CD4 and CD8 α : CD4⁺ DCs, CD8⁺ DCs and CD4⁻CD8⁻ (double negative) DCs. Additionally, a subset of monocyte-derived DCs, commonly used in human and mouse studies of DC biology is considered as a precursor of migratory or so called emergency DCs. Different subset of DCs differ in their ability to capture and process antigens. Migratory DC types are more specialized in antigen transport from peripheral tissues to secondary lymphoid tissues, whereas lymphoid-organ-residing DCs are specialized at generation and

display of peptide/MHC complexes to naive T cells that reside within lymph nodes. All dendritic cells (DCs) have functional MHC class I and MHC class II presentation pathways. It was suggested that the migratory DC subsets CD103⁺ DCs are mainly responsible for MHC class I restricted presentation, whereas dermal DCs control MHC class II restricted presentation³⁴. Ability to deliver exogenous antigens to the MHC class I pathway, known as a cross-presentation is restricted to some DC types. The role of the different subsets of DCs in antigen cross-presentation has been studied extensively in mice. Murine CD8⁺ DCs are more efficient in cross-presentation than CD8⁻ DCs^{35,36}. In general CD8⁺ DCs are better in presenting the antigens in the context of MHC class I than CD8⁻ DCs superior in MHC class II restricted presentation³³. Human equivalent of CD8⁺ DCs was recently identified as a CD141⁺ DC subset³⁷⁻⁴¹.

DC life cycle

Migratory DCs residing in non-lymphoid peripheral tissues in the immune steady state are considered as immature. These cells have unique ability to recognize and take up antigens. Antigen uptake in the presence of danger signal and inflammation leads to maturation of dendritic cell. Mature DC migrates to secondary lymphoid organs to stimulate T cells. Lymphoid-organ-resident DCs do not conform to the described above Langerhans cell paradigm; they develop from bone-marrow precursors within the lymphoid organs without previously trafficking through peripheral tissues. In the absence of infection, the resident DCs maintain an immature phenotype throughout their entire lifespan⁴². As resident DCs do not migrate out of lymphoid organs antigen has to be delivered to them by other cells of the immune system or lymph itself.

Expression of Pattern Recognition Receptors (PRRs) by DCs

Immature DCs express large array of PRRs including Toll-like receptors (TLRs), C-type lectins, NOD-like receptors and RIG-like helicases. TLRs are transmembrane receptors present on the plasma membrane or within the endosomal compartment that recognize a variety of PAMPs, like specific structures of microbial lipoproteins, glycolipins, CpG DNA, RNA and lipopolysaccharides⁴³⁻⁴⁵. Another class of PRRs present on the surface of immature DCs are C-type lectins, which recognize carbohydrate structures on pathogens⁴⁶. RIG-like helicases and NOD-like receptors are present in the cytosol and are involved in sensing the intracellular pathogens. RIG-like helicases bind mainly viral RNA⁴⁷. NOD-like receptors beside binding diverse PAMPs also bind endogenous danger associated molecular patterns (DAMPs)⁴⁸. DAMPs are the molecules that can be released from the cell or cell compartment upon tissue or cell damage. They can initiate and propagate immune responses. DNA, uric acid and

ATP as well as heat-shock proteins (HSP) and high-mobility group box 1 (HMGB1) can act as these danger signals⁴⁹⁻⁵¹. Some of the NOD-like receptors are crucial components of an inflammasome⁵². The inflammasome represents a high molecular weight complex that activates inflammatory caspases and activates cytokines of the IL-1 family.

Multiple PRRs are differentially expressed between different DC subtypes. Differential expression of these receptors can provide each DC subset with distinct capacities to capture and initiate responses against specific pathogens.

Binding of the PAMPs and DAMPs to PRRs induce various intracellular signaling pathways including NF κ B, AKT/PI3K, and MAPK pathways leading to inflammatory responses⁵³. As cross talk between different PRRs exist, combined activation of different receptors results in distinct intensities and the nature of the response⁵⁴. This cross talk adds another dimension to already great competence of DCs to sense the environment and establish the specific immune response directed at clearing the pathogen.

Antigen uptake and presentation by DCs

Equipped with this very efficient sensing mechanism immature DCs patrol the body tissues in search for non-self antigens. Once in contact with such, they use different phagocytic pathways to engulf it. Uptake of the antigens can occur via specific receptor-mediated endocytosis or unspecific phagocytosis and macropinocytosis⁵⁵. Taken up antigens must be processed before can be presented to T cells. In the endosomal compartment variety of exogenous antigens may be degraded and resulting peptides are loaded on MHC class II molecules accumulated in the same compartment. In general, MHC class I molecules are loaded with peptides derived from cytosolic proteins in the endoplasmic reticulum (ER). However, exogenous antigens may be also loaded on MHC class I molecules in the process known as cross presentation⁵⁶.

Maturation of DC can be triggered by binding of different PAMPs and DAMPs to the PRRs, inflammatory cytokines (e.g. TNF α and IL-1 β) or the ligation of surface expressed activating receptors like CD40⁵⁷⁻⁵⁹. In the process of maturation DCs transform from highly phagocytic stationary cell into migratory ones. They lose ability to efficiently take up and process antigens. Instead, they start to express CCR7, which enables them to migrate towards lymphatic tissues to T cell-rich areas⁶⁰. Additionally, DCs upregulate whole set of genes involved in antigen presentation and costimulation including MHC class II, CD40, CD80, CD86 as well as cytokines that

promote and modulate inflammation and effector cells function²⁹. These changes are necessary for DCs to initiate T cell responses.

Three simultaneous signals are necessary for the activation of T cells. Beside antigen presented in the context of MHC second signal must be derived from binding the costimulatory molecules⁶¹. One of the best-characterized costimulatory receptors expressed by T cells is CD28, which interacts with CD80 (B7-1) and CD86 (B7-2) on the membrane of APCs. Another molecular pair found to be essential for costimulation is CD40/CD154. CD40 is continuously expressed on the APC, and the expression of CD154 can be induced on the T cell upon activation via CD28 receptor⁶². Third signal is provided by cytokines produced by DCs or other microenvironmental sources. Next to T cell activation, DCs regulate also a differentiation of T cells into the appropriate subset of T helper cells. Sensing the environment via PRRs and cytokine receptors incite DCs to switch into a suitable program. These pre-programmed DCs will produce the set of cytokines and express the correct array of costimulatory molecules to instruct the effector T cell development (Fig. 1). For instance, IL-12 producing DCs will induce differentiation of naïve CD4⁺ cells into Th1 subset⁶³. pDCs delivered from solid tumours were shown to secrete IL-4 directing development of Th2 lineage^{14,15,64}. There is also cytokine independent, differential Notch ligation dependent stimulation of subset differentiation of naïve T cells into Th1 and Th2 effector cells by DCs⁶⁵. Notch 1-4 receptors are present on naïve T cells. If DCs will be stimulated by type 1 pathogen (viruses, bacteria) they will upregulate Delta-like ligand (DLL) on their surface that will bind to Notch 3 on naïve T cell and induce differentiation into Th1. Activation of DCs by type 2 pathogens like parasites or allergens will lead to upregulation of another Notch ligand called Jagged. Ligation of Jagged by Notch 1 and 2 on naïve T cell will lead to differentiation into Th2 subset. Binding of Jagged to Notch will induce Th2 differentiation. Notch directs Th2 differentiation by inducing GATA3 and by directly regulating *il4* gene transcription⁶⁶. Th17 subset development is supported by IL-6 and TGF- β ⁶⁷. Tolerogenic DCs that produce TGF- β and IL-10 will stimulate expansion of Tregs. The sentinels qualifications of the DCs are so high that even the same pathogen in the different life stage will evoke a different program in DCs, e.g., stimulation of DCs with the yeast form of *C. albicans* leads to IL-12 production and Th1 responses, while its hyphae stage stimulates DCs to produce IL-4 and a Th2 responses⁶⁸.

DCs and tolerance

Recognition of non-self molecules by DCs drives inflammation and adaptive immunity responses to pathogens. However, DCs also play a very important role in maintaining tolerance to self-antigens. They contribute to the deletion of autoreactive lymphocytes during maturation in the central lymphoid organs, as well as suppress the autoreactive lymphocytes, which have escaped elimination in the periphery⁶⁹. These two processes are referred to as central and peripheral tolerance. In the thymus, DCs presenting tissue specific antigens (TSA) to autoreactive T cells supply the negative selection signal or directed them to the Treg lineage⁷⁰⁻⁷³. Generation of tolerance in the periphery is mediated mostly by so-called tolerogenic DCs. Tolerogenic DCs can induce or enhance the suppressive function of existing Tregs and convert activated T cells into Tregs. Immature DCs are typically tolerogenic. Presentation of the antigen to the T cells in the periphery by immature DCs without delivery of costimulatory signals will result in T cell apoptosis or anergy, or might give rise to immunosuppressive Tregs⁷⁴⁻⁷⁶. DCs can also acquire the tolerogenic phenotype by phagocytosis of apoptotic cells in a steady state or in presence of IL-10 or TGF- β cytokines in the microenvironment⁷⁷⁻⁸⁰.

Defects in the cross-tolerance via DCs may result in accumulation of autoreactive T cells and lead to autoimmune diseases. Signals that tolerogenic DCs use to broadcast their suppressive message to T cells are still incompletely understood. A better understanding of these issues may offer new opportunities for the treatment of autoimmunity, allograft rejection, allergy, asthma and various forms of hypersensitivity.

DC-associated molecules

The central role of DC in the initiation of the immune responses and in the maintenance of the balance between the immunity and tolerance is currently exploited to treat cancer, autoimmune diseases and to prevent the transplant rejection⁸¹⁻⁸⁵. Fundamental knowledge on factors that determine DC function is necessary for further development of DC-based therapies. Identification and characterisation of novel DC-associated molecules like DC-SIGN⁸⁶, DC-CK1⁸⁷, DCIR⁸⁸, Dectin-1 and -2^{89,90}, DEC205⁹¹ and DC-SCRIPT^{92,93} have already provided new insight in DC immunobiology. In this thesis we make effort to unravel the role of Dendritic Cells Specific TrAnsMembrane Protein (DC-STAMP) in DCs.

DC-STAMP was first identified in dendritic cells⁹⁴ and IL-4 stimulated macrophages⁹⁵. Further research demonstrated expression of DC-STAMP also in

osteoclasts⁹⁶. DC-STAMP is highly conserved between different species. Human DC-STAMP has 81% of homology on mRNA level and 95% homology on protein level with murine DC-STAMP⁹⁷. Protein contains 479 amino acids and has from 4 to 7 putative transmembrane domains and three N-linked glycosylation sites⁹⁴, and localizes to the endoplasmic reticulum (ER) in DCs⁹⁷ (Fig. 2). Human *DC-STAMP* gene localizes to chromosome 8q23 and consists of four exons⁹⁸. Mouse *DC-STAMP* gene localizes to chromosome 15 and its organisation is conserved with the human one⁹⁷. DC-STAMP was shown to be necessary for fusion of osteoclasts and foreign body giant cells⁹⁹ but its function in DCs is only recently emerging. In the following chapters of this thesis we characterised two binding partners of DC-STAMP: LUMAN and OS9. LUMAN is a type II transmembrane protein that belongs to the bZIP family of transcription factors and resides in ER. OS9 is also an ER associated protein implicated in ER-to-Golgi transport and ER-associated degradation.

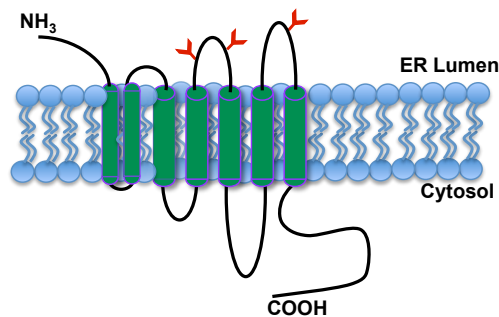


Figure 2. Model of DC-STAMP structure. DC-STAMP localizes to the ER membranes in immature DCs. Putative 7-transmembrane domain model is based on hydrophobicity analysis of the sequence. C-terminal tail of DC-STAMP is present on cytoplasmic site of the ER. Glycosylation sites are depicted (↗).

Signalling from the ER and its cross-talk with immune response pathways

The ER responds to and regulates many aspects of cellular metabolism and homeostasis. It is the main site for calcium storage and signalling, lipid biosynthesis, and protein synthesis and folding. Almost all secretory and membrane proteins are folded and assembled in the lumen of ER. Newly synthesised polypeptides translocate to the lumen of the ER and attain a three-dimensional conformation after undergoing of protein folding and posttranslational modifications. Improper protein folding can lead to the accumulation of misfolded proteins resulting in ER-stress. To dampen this ER stress, eukaryotic cells make use of an unfolded protein response (UPR).

UPR was first described in yeast cells, which possess a single UPR signalling pathway¹⁰⁰. In eukaryotic organism this mechanism evolved to the three-arm UPR signal-transduction pathway mediated by three distinct transmembrane proteins: inositol-requiring transmembrane kinase/endonuclease 1 (IRE1), pancreatic ER kinase (PERK) and activating transcription factor 6 (ATF6)¹⁰¹⁻¹⁰⁵. In the absence of ER stress, IRE1, PERK and ATF6 are sequestered in inactive complexes with GRP78/BIP chaperone. ER stress results in dissociation of BIP from these complexes allowing activation of the all three UPR signalling pathways.

The ER associated degradation (ERAD) and regulated intramembrane proteolysis (RIP) are also components of UPR. ERAD is a secretory protein quality control process that results in the removal of aberrant proteins from the ER¹⁰⁶. ERAD substrates are recognized by molecular chaperones in the lumen of ER and after retro-translocation to the cytoplasm degraded by ubiquitin-proteasome machinery¹⁰⁷.

RIP is the process regulating the activity of the membrane-associated transcription factors in the ER and ATF6 is one of them¹⁰⁸. The key components of RIP comprise a distinct class of membrane associated transcription factors, anchoring partners that localize the factors to the ER, and proteases that are located in the Golgi compartment. The transcription factors are inserted in the ER membranes with DNA-binding and transcriptional-activation domains oriented towards cytosolic face of the membrane. The main step in the controlling the activity of these factors in specific pathways appears to reside in their regulated release from the ER in response to the specific stimuli. They are then transported to the Golgi where they are cleaved in a site-specific manner by resident proteases. This results in the release of the cytosolic domain, which is transported to the nucleus to effect transcription of specific target gene and orchestrate an adaptive response

to the stress or imbalance encountered^{107,109,110}. RIP was first described for sterol regulatory element binding proteins, SREBP 1 and 2^{111,112}. SREBPs control genes involved in cholesterol and fatty acids metabolism^{113,114}. They are retained in the ER in a complex with multimembrane spanning protein SCAP^{115,116}. SCAP senses lower cholesterol levels in ER membranes and in response escorts SREBPs to the Golgi, where they are cleaved by Golgi proteases, S1P and S2P, thus liberating the SREBP N-terminal transactivation domain of the protein.

Recently, the concept of the cross-talk between UPR and immune response pathways started to emerge indicating the importance of the UPR in the immune system¹¹⁷.

Initially, intact UPR was described as necessary for plasma cell differentiation^{118,119} and dendritic cells survival and function¹²⁰. Recently, research by Martinon *et al.* showed that TLR ligands (LPS, Pam₃CK₄) can selectively activate one of the branches of UPR pathways in macrophages, namely IRE/XBP1¹²¹. As a result of this activation, alternatively spliced XBP1 influences the NF- κ B driven cytokine

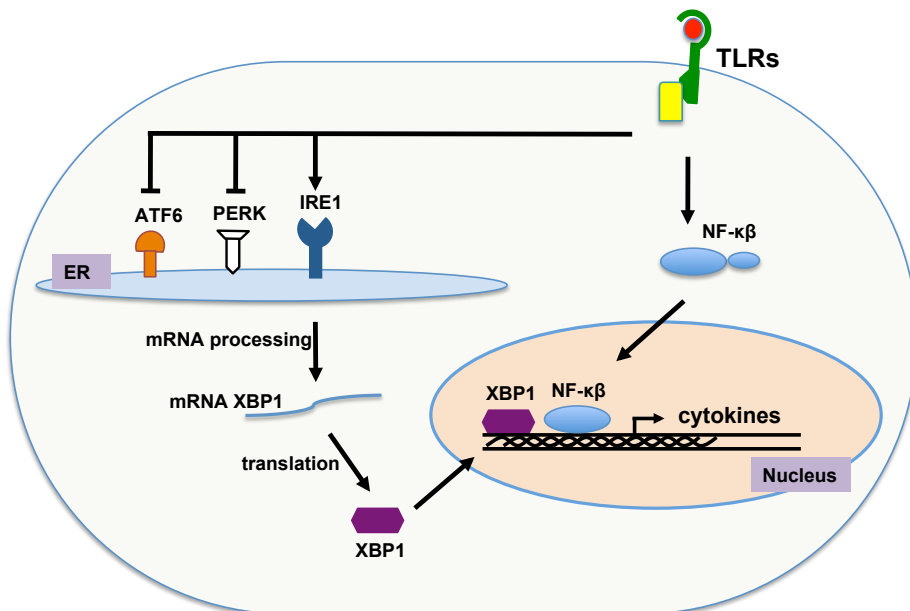


Figure 3. Activation of UPR sensors after TLR stimulation. Stimulation of macrophages with TLR ligands results in activation of IRE1 and production of the spliced form of the XBP1 transcription factor. XBP1 can enhance the transcription of inflammatory cytokines. In contrast to IRE1, the PERK and ATF6 sensors are negatively regulated by TLR ligation. Figure adapted from^{117,126}.

production, enhancing the effect of TLR ligation (Fig. 3). A different group described that proinflammatory cytokines could induce UPR in the liver tissue¹²², pointing at another intersection of UPR with the innate immune responses. In addition, ER-stress was also reported to impair the MHC class I presentation, thus, influencing the adaptive immune responses¹²³. Finally, malfunctions in UPR system can negatively influence immune responses, which potentially contribute to the development of the autoimmunity^{117,121,124,125}. The growing knowledge about importance of the cross-talk between UPR and immune system directs current attention of the immunologists towards processes taking place in the ER.

Scope of this thesis

DCs are important players of the immune system. The aim of this thesis is to better understand DCs at the molecular level by investigating the role of DC-STAMP and its interacting partners LUMAN and OS9 in DC immunobiology. The knowledge about interacting proteins can shed a light on their function. Yeast-2-hybrid analysis was performed to identify binding partners of DC-STAMP. Two proteins which interact with cytoplasmic tail of DC-STAMP were identified: OS9 and LUMAN.

In **Chapter 2** we describe the interaction of DC-STAMP with OS9 in dendritic cells. OS9 is the ER-resident protein previously implicated in ER-to-Golgi transport and unfolding protein responses (UPR). We show that DC-STAMP colocalizes with OS9 in immature DCs. Upon maturation DC-STAMP translocates towards Golgi compartment while OS9 stays in ER. We demonstrate that OS9 play a crucial role in facilitating this translocation, suggesting a novel role of OS9 in DCs.

In **Chapter 3** interaction of DC-STAMP with transcription factor LUMAN is described. LUMAN is an ER-resident transcription factor, which for its activation needs to be translocated to Golgi compartment. Golgi residing proteases can cleave the LUMAN and liberated active N-terminal part of LUMAN will translocate to the nucleus to activate its target genes. This study for the first time shows expression of LUMAN protein in DCs and demonstrate its activation in mature DCs. Our data suggest DC-STAMP being an important factor in this activation.

In **Chapter 4** we use a gene silencing approach to identify the role of DC-STAMP in dendritic cells. We show that knock-down of DC-STAMP in murine bone marrow-derived DCs (mBMDCs) leads to deregulation of cytokine and chemokine production upon LPS stimulation. As DC-STAMP knock-down mBMDC have impaired ability to stimulate Th1 lineage development we postulate an importance of DC-STAMP in immune responses to LPS.

In **Chapter 5** we performed microarray experiment to identify target genes of LUMAN in DCs. By lentiviral overexpression of active form of LUMAN in DCs we identify ApolipoproteinA4 (ApoA4) as a novel target gene of LUMAN. As ApoA4 is described as an anti-inflammatory protein we suggest the role of LUMAN in DCs may involve quenching the inflammation.

In **Chapter 6** we summarized our finding, discuss their implication in understanding the DC immunobiology and suggest future work.

References

1. Janeway, C.A., Jr. The immune system evolved to discriminate infectious nonself from noninfectious self. *Immunol Today* **13**, 11-16 (1992).
2. Janeway, C.A., Jr., Travers, P., Walport, M. & Shlomchik, M.J. *Immunobiology: the immune system in health and disease*, (Garland science, New York and London 2005).
3. Erb, K.J., Holloway, J.W. & Le Gros, G. Mast cells in the front line. Innate immunity. *Curr Biol* **6**, 941-942 (1996).
4. Weissmann, G., Smolen, J.E. & Korchak, H.M. Release of inflammatory mediators from stimulated neutrophils. *N Engl J Med* **303**, 27-34 (1980).
5. Trinchieri, G. Natural killer cells wear different hats: effector cells of innate resistance and regulatory cells of adaptive immunity and of hematopoiesis. *Semin Immunol* **7**, 83-88 (1995).
6. Hirai, K., Miyamasu, M., Takaishi, T. & Morita, Y. Regulation of the function of eosinophils and basophils. *Crit Rev Immunol* **17**, 325-352 (1997).
7. Mosser, D.M. & Edwards, J.P. Exploring the full spectrum of macrophage activation. *Nat Rev Immunol* **8**, 958-969 (2008).
8. Yoshida, T., *et al.* Memory B and memory plasma cells. *Immunol Rev* **237**, 117-139 (2010).
9. Calame, K.L. Plasma cells: finding new light at the end of B cell development. *Nat Immunol* **2**, 1103-1108 (2001).
10. Germain, R.N. MHC-dependent antigen processing and peptide presentation: providing ligands for T lymphocyte activation. *Cell* **76**, 287-299 (1994).
11. Monaco, J.J. A molecular model of MHC class-I-restricted antigen processing. *Immunol Today* **13**, 173-179 (1992).
12. Cresswell, P. Assembly, transport, and function of MHC class II molecules. *Annu Rev Immunol* **12**, 259-293 (1994).
13. Abbas, A.K., Murphy, K.M. & Sher, A. Functional diversity of helper T lymphocytes. *Nature* **383**, 787-793 (1996).
14. Kopf, M., *et al.* Disruption of the murine IL-4 gene blocks Th2 cytokine responses. *Nature* **362**, 245-248 (1993).
15. Le Gros, G., Ben-Sasson, S.Z., Seder, R., Finkelman, F.D. & Paul, W.E. Generation of interleukin 4 (IL-4)-producing cells in vivo and in vitro: IL-2 and IL-4 are required for in vitro generation of IL-4-producing cells. *J Exp Med* **172**, 921-929 (1990).
16. Stockinger, B. & Veldhoen, M. Differentiation and function of Th17 T cells. *Curr Opin Immunol* **19**, 281-286 (2007).
17. Laurence, A. & O'Shea, J.J. T(H)-17 differentiation: of mice and men. *Nat Immunol* **8**, 903-905 (2007).
18. Bettelli, E., *et al.* Reciprocal developmental pathways for the generation of pathogenic effector TH17 and regulatory T cells. *Nature* **441**, 235-238 (2006).
19. Sakaguchi, S., Yamaguchi, T., Nomura, T. & Ono, M. Regulatory T cells and immune tolerance. *Cell* **133**, 775-787 (2008).
20. van Maren, W.W., Jacobs, J.F., de Vries, I.J., Nierkens, S. & Adema, G.J. Toll-like receptor signalling on Tregs: to suppress or not to suppress? *Immunology* **124**, 445-452 (2008).
21. Sakaguchi, S. Naturally arising Foxp3-expressing CD25+CD4+ regulatory T cells in immunological tolerance to self and non-self. *Nat Immunol* **6**, 345-352 (2005).
22. Hori, S., Nomura, T. & Sakaguchi, S. Control of regulatory T cell development by the transcription factor Foxp3. *Science* **299**, 1057-1061 (2003).
23. Thornton, A.M. & Shevach, E.M. Suppressor effector function of CD4+CD25+ immunoregulatory T cells is antigen nonspecific. *J Immunol* **164**, 183-190 (2000).
24. Roncarolo, M.G., *et al.* Interleukin-10-secreting type 1 regulatory T cells in rodents and humans. *Immunol Rev* **212**, 28-50 (2006).
25. Chen, W., *et al.* Conversion of peripheral CD4+CD25- naive T cells to CD4+CD25+ regulatory T cells by TGF-beta induction of transcription factor Foxp3. *J Exp Med* **198**, 1875-1886 (2003).
26. Sun, C.M., *et al.* Small intestine lamina propria dendritic cells promote de novo generation of Foxp3 T reg cells via retinoic acid. *J Exp Med* **204**, 1775-1785 (2007).
27. Belkaid, Y. & Chen, W. Regulatory ripples. *Nat Immunol* **11**, 1077-1078 (2010).
28. Palucka, K. & Banchereau, J. Dendritic cells: a link between innate and adaptive immunity. *J Clin Immunol* **19**,

- 12-25 (1999).
29. Banchereau, J. & Steinman, R.M. Dendritic cells and the control of immunity. *Nature* **392**, 245-252 (1998).
 30. Wu, L. & Liu, Y.J. Development of dendritic-cell lineages. *Immunity* **26**, 741-750 (2007).
 31. D'Amico, A. & Wu, L. The early progenitors of mouse dendritic cells and plasmacytoid predendritic cells are within the bone marrow hemopoietic precursors expressing Flt3. *J Exp Med* **198**, 293-303 (2003).
 32. Siegal, F.P., *et al.* The nature of the principal type 1 interferon-producing cells in human blood. *Science* **284**, 1835-1837 (1999).
 33. Villadangos, J.A. & Schnorrer, P. Intrinsic and cooperative antigen-presenting functions of dendritic-cell subsets in vivo. *Nat Rev Immunol* **7**, 543-555 (2007).
 34. Bedoui, S., *et al.* Cross-presentation of viral and self antigens by skin-derived CD103+ dendritic cells. *Nat Immunol* **10**, 488-495 (2009).
 35. Pooley, J.L., Heath, W.R. & Shortman, K. Cutting edge: intravenous soluble antigen is presented to CD4 T cells by CD8- dendritic cells, but cross-presented to CD8 T cells by CD8+ dendritic cells. *J Immunol* **166**, 5327-5330 (2001).
 36. Schnorrer, P., *et al.* The dominant role of CD8+ dendritic cells in cross-presentation is not dictated by antigen capture. *Proc Natl Acad Sci U S A* **103**, 10729-10734 (2006).
 37. Villadangos, J.A. & Shortman, K. Found in translation: the human equivalent of mouse CD8+ dendritic cells. *J Exp Med* **207**, 1131-1134 (2010).
 38. Bachem, A., *et al.* Superior antigen cross-presentation and XCR1 expression define human CD11c+CD141+ cells as homologues of mouse CD8+ dendritic cells. *J Exp Med* **207**, 1273-1281 (2010).
 39. Crozat, K., *et al.* The XC chemokine receptor 1 is a conserved selective marker of mammalian cells homologous to mouse CD8alpha+ dendritic cells. *J Exp Med* **207**, 1283-1292 (2010).
 40. Jongbloed, S.L., *et al.* Human CD141+ (BDCA-3)+ dendritic cells (DCs) represent a unique myeloid DC subset that cross-presents necrotic cell antigens. *J Exp Med* **207**, 1247-1260 (2010).
 41. Poulin, L.F., *et al.* Characterization of human DNGR-1+ BDCA3+ leukocytes as putative equivalents of mouse CD8alpha+ dendritic cells. *J Exp Med* **207**, 1261-1271 (2010).
 42. Wilson, N.S., *et al.* Most lymphoid organ dendritic cell types are phenotypically and functionally immature. *Blood* **102**, 2187-2194 (2003).
 43. Akira, S., Takeda, K. & Kaisho, T. Toll-like receptors: critical proteins linking innate and acquired immunity. *Nat Immunol* **2**, 675-680 (2001).
 44. Medzhitov, R. Toll-like receptors and innate immunity. *Nat Rev Immunol* **1**, 135-145 (2001).
 45. Medzhitov, R., Preston-Hurlburt, P. & Janeway, C.A., Jr. A human homologue of the Drosophila Toll protein signals activation of adaptive immunity. *Nature* **388**, 394-397 (1997).
 46. Figdor, C.G., van Kooyk, Y. & Adema, G.J. C-type lectin receptors on dendritic cells and Langerhans cells. *Nat Rev Immunol* **2**, 77-84 (2002).
 47. Pichlmair, A. & Reis e Sousa, C. Innate recognition of viruses. *Immunity* **27**, 370-383 (2007).
 48. Martinon, F. & Tschopp, J. NLRs join TLRs as innate sensors of pathogens. *Trends Immunol* **26**, 447-454 (2005).
 49. Klune, J.R., Dhupar, R., Cardinal, J., Billiar, T.R. & Tsung, A. HMGB1: endogenous danger signaling. *Mol Med* **14**, 476-484 (2008).
 50. Tsan, M.F. Heat shock proteins and high mobility group box 1 protein lack cytokine function. *J Leukoc Biol* **89**, 847-853 (2011).
 51. Bianchi, M.E. DAMPs, PAMPs and alarmins: all we need to know about danger. *J Leukoc Biol* **81**, 1-5 (2007).
 52. Martinon, F. & Tschopp, J. Inflammatory caspases: linking an intracellular innate immune system to autoinflammatory diseases. *Cell* **117**, 561-574 (2004).
 53. Lee, M.S. & Kim, Y.J. Signaling pathways downstream of pattern-recognition receptors and their cross talk. *Annu Rev Biochem* **76**, 447-480 (2007).
 54. Hajishengallis, G. & Lambris, J.D. Microbial manipulation of receptor crosstalk in innate immunity. *Nat Rev Immunol* **11**, 187-200 (2011).
 55. Sallusto, F., Cella, M., Danieli, C. & Lanzavecchia, A. Dendritic cells use macropinocytosis and the mannose receptor to concentrate macromolecules in the major histocompatibility complex class II compartment: downregulation by cytokines and bacterial products. *J Exp Med* **182**, 389-400 (1995).
 56. Heath, W.R., *et al.* Cross-presentation, dendritic cell subsets, and the generation of immunity to cellular antigens. *Immunol Rev* **199**, 9-26 (2004).

57. Matzinger, P. The danger model: a renewed sense of self. *Science* **296**, 301-305 (2002).
58. Jonuleit, H., *et al.* Pro-inflammatory cytokines and prostaglandins induce maturation of potent immunostimulatory dendritic cells under fetal calf serum-free conditions. *Eur J Immunol* **27**, 3135-3142 (1997).
59. Elgueta, R., *et al.* Molecular mechanism and function of CD40/CD40L engagement in the immune system. *Immunol Rev* **229**, 152-172 (2009).
60. Yanagihara, S., Komura, E., Nagafune, J., Watarai, H. & Yamaguchi, Y. EB1/CCR7 is a new member of dendritic cell chemokine receptor that is up-regulated upon maturation. *J Immunol* **161**, 3096-3102 (1998).
61. Liu, Y. & Janeway, C.A., Jr. Cells that present both specific ligand and costimulatory activity are the most efficient inducers of clonal expansion of normal CD4 T cells. *Proc Natl Acad Sci U S A* **89**, 3845-3849 (1992).
62. Grewal, I.S. & Flavell, R.A. CD40 and CD154 in cell-mediated immunity. *Annu Rev Immunol* **16**, 111-135 (1998).
63. Macatonia, S.E., *et al.* Dendritic cells produce IL-12 and direct the development of Th1 cells from naive CD4+ T cells. *J Immunol* **154**, 5071-5079 (1995).
64. Cox, K., *et al.* Plasmacytoid dendritic cells (PDC) are the major DC subset innately producing cytokines in human lymph nodes. *J Leukoc Biol* **78**, 1142-1152 (2005).
65. Amsen, D., Antov, A. & Flavell, R.A. The different faces of Notch in T-helper-cell differentiation. *Nat Rev Immunol* **9**, 116-124 (2009).
66. Amsen, D., *et al.* Instruction of distinct CD4 T helper cell fates by different notch ligands on antigen-presenting cells. *Cell* **117**, 515-526 (2004).
67. Veldhoen, M., Hocking, R.J., Atkins, C.J., Locksley, R.M. & Stockinger, B. TGFbeta in the context of an inflammatory cytokine milieu supports de novo differentiation of IL-17-producing T cells. *Immunity* **24**, 179-189 (2006).
68. d'Ostiani, C.F., *et al.* Dendritic cells discriminate between yeasts and hyphae of the fungus *Candida albicans*. Implications for initiation of T helper cell immunity in vitro and in vivo. *J Exp Med* **191**, 1661-1674 (2000).
69. Wallet, M.A., Sen, P. & Tisch, R. Immunoregulation of dendritic cells. *Clin Med Res* **3**, 166-175 (2005).
70. Brocker, T., Riedinger, M. & Karjalainen, K. Targeted expression of major histocompatibility complex (MHC) class II molecules demonstrates that dendritic cells can induce negative but not positive selection of thymocytes in vivo. *J Exp Med* **185**, 541-550 (1997).
71. Wu, L. & Shortman, K. Heterogeneity of thymic dendritic cells. *Semin Immunol* **17**, 304-312 (2005).
72. Griesemer, A.D., Sorenson, E.C. & Hardy, M.A. The role of the thymus in tolerance. *Transplantation* **90**, 465-474 (2010).
73. Watanabe, N., *et al.* Hassall's corpuscles instruct dendritic cells to induce CD4+CD25+ regulatory T cells in human thymus. *Nature* **436**, 1181-1185 (2005).
74. Hawiger, D., *et al.* Dendritic cells induce peripheral T cell unresponsiveness under steady state conditions in vivo. *J Exp Med* **194**, 769-779 (2001).
75. Steinman, R.M., Hawiger, D. & Nussenzweig, M.C. Tolerogenic dendritic cells. *Annu Rev Immunol* **21**, 685-711 (2003).
76. Cools, N., Ponsaerts, P., Van Tendeloo, V.F. & Berneman, Z.N. Balancing between immunity and tolerance: an interplay between dendritic cells, regulatory T cells, and effector T cells. *J Leukoc Biol* **82**, 1365-1374 (2007).
77. Liu, K., *et al.* Immune tolerance after delivery of dying cells to dendritic cells in situ. *J Exp Med* **196**, 1091-1097 (2002).
78. Steinman, R.M., Turley, S., Mellman, I. & Inaba, K. The induction of tolerance by dendritic cells that have captured apoptotic cells. *J Exp Med* **191**, 411-416 (2000).
79. Haase, C., Jorgensen, T.N. & Michelsen, B.K. Both exogenous and endogenous interleukin-10 affects the maturation of bone-marrow-derived dendritic cells in vitro and strongly influences T-cell priming in vivo. *Immunology* **107**, 489-499 (2002).
80. Yang, A.S. & Lattime, E.C. Tumor-induced interleukin 10 suppresses the ability of splenic dendritic cells to stimulate CD4 and CD8 T-cell responses. *Cancer Res* **63**, 2150-2157 (2003).
81. Tacken, P.J. & Figdor, C.G. Targeted antigen delivery and activation of dendritic cells in vivo: Steps towards cost effective vaccines. *Semin Immunol* **23**, 12-20 (2010).
82. Palucka, K., Ueno, H. & Banchereau, J. Recent developments in cancer vaccines. *J Immunol* **186**, 1325-1331 (2010).
83. Natarajan, S. & Thomson, A.W. Tolerogenic dendritic cells and myeloid-derived suppressor cells: potential for regulation and therapy of liver auto- and alloimmunity. *Immunobiology* **215**, 698-703 (2010).

84. Mukherjee, G. & Dilenzo, T.P. The immunotherapeutic potential of dendritic cells in type 1 diabetes. *Clin Exp Immunol* **161**, 197-207 (2010).
85. Ehser, S., et al. Suppressing dendritic cells as a tool for controlling allograft rejection in organ transplantation: promises and difficulties. *Hum Immunol* **69**, 165-173 (2008).
86. Geijtenbeek, T.B., et al. Identification of DC-SIGN, a novel dendritic cell-specific ICAM-3 receptor that supports primary immune responses. *Cell* **100**, 575-585 (2000).
87. Adema, G.J., et al. A dendritic-cell-derived C-C chemokine that preferentially attracts naive T cells. *Nature* **387**, 713-717 (1997).
88. Bates, E.E., et al. APCs express DCIR, a novel C-type lectin surface receptor containing an immunoreceptor tyrosine-based inhibitory motif. *J Immunol* **163**, 1973-1983 (1999).
89. Ariizumi, K., et al. Cloning of a second dendritic cell-associated C-type lectin (dectin-2) and its alternatively spliced isoforms. *J Biol Chem* **275**, 11957-11963 (2000).
90. Ariizumi, K., et al. Identification of a novel, dendritic cell-associated molecule, dectin-1, by subtractive cDNA cloning. *J Biol Chem* **275**, 20157-20167 (2000).
91. Jiang, W., et al. The receptor DEC-205 expressed by dendritic cells and thymic epithelial cells is involved in antigen processing. *Nature* **375**, 151-155 (1995).
92. Triantis, V., et al. Molecular characterization of the murine homologue of the DC-derived protein DC-SCRIPT. *J Leukoc Biol* **79**, 1083-1091 (2006).
93. Triantis, V., et al. Identification and characterization of DC-SCRIPT, a novel dendritic cell-expressed member of the zinc finger family of transcriptional regulators. *J Immunol* **176**, 1081-1089 (2006).
94. Hartgers, F.C., et al. DC-STAMP, a novel multimembrane-spanning molecule preferentially expressed by dendritic cells. *Eur J Immunol* **30**, 3585-3590 (2000).
95. Staeger, H., Brauchlin, A., Schoedon, G. & Schaffner, A. Two novel genes FIND and LIND differentially expressed in deactivated and Listeria-infected human macrophages. *Immunogenetics* **53**, 105-113 (2001).
96. Kukita, T., et al. RANKL-induced DC-STAMP is essential for osteoclastogenesis. *J Exp Med* **200**, 941-946 (2004).
97. Eleveld-Trancikova, D., et al. The dendritic cell-derived protein DC-STAMP is highly conserved and localizes to the endoplasmic reticulum. *J Leukoc Biol* **77**, 337-343 (2005).
98. Hartgers, F.C., et al. Genomic organization, chromosomal localization, and 5' upstream region of the human DC-STAMP gene. *Immunogenetics* **53**, 145-149 (2001).
99. Yagi, M., et al. DC-STAMP is essential for cell-cell fusion in osteoclasts and foreign body giant cells. *J Exp Med* **202**, 345-351 (2005).
100. Patil, C. & Walter, P. Intracellular signaling from the endoplasmic reticulum to the nucleus: the unfolded protein response in yeast and mammals. *Curr Opin Cell Biol* **13**, 349-355 (2001).
101. Harding, H.P., Zhang, Y. & Ron, D. Protein translation and folding are coupled by an endoplasmic-reticulum-resident kinase. *Nature* **397**, 271-274 (1999).
102. Haze, K., Yoshida, H., Yanagi, H., Yura, T. & Mori, K. Mammalian transcription factor ATF6 is synthesized as a transmembrane protein and activated by proteolysis in response to endoplasmic reticulum stress. *Mol Biol Cell* **10**, 3787-3799 (1999).
103. Yoshida, H., Matsui, T., Yamamoto, A., Okada, T. & Mori, K. XBP1 mRNA is induced by ATF6 and spliced by IRE1 in response to ER stress to produce a highly active transcription factor. *Cell* **107**, 881-891 (2001).
104. Harding, H.P., Zhang, Y., Bertolotti, A., Zeng, H. & Ron, D. Perk is essential for translational regulation and cell survival during the unfolded protein response. *Mol Cell* **5**, 897-904 (2000).
105. Vattam, K.M. & Wek, R.C. Reinitiation involving upstream ORFs regulates ATF4 mRNA translation in mammalian cells. *Proc Natl Acad Sci U S A* **101**, 11269-11274 (2004).
106. McCracken, A.A. & Brodsky, J.L. Assembly of ER-associated protein degradation in vitro: dependence on cytosol, calnexin, and ATP. *J Cell Biol* **132**, 291-298 (1996).
107. Vembar, S.S. & Brodsky, J.L. One step at a time: endoplasmic reticulum-associated degradation. *Nat Rev Mol Cell Biol* **9**, 944-957 (2008).
108. Malhotra, J.D. & Kaufman, R.J. Endoplasmic reticulum stress and oxidative stress: a vicious cycle or a double-edged sword? *Antioxid Redox Signal* **9**, 2277-2293 (2007).
109. Bailey, D. & O'Hare, P. Transmembrane bZIP transcription factors in ER stress signaling and the unfolded protein response. *Antioxid Redox Signal* **9**, 2305-2321 (2007).
110. Ron, D. & Walter, P. Signal integration in the endoplasmic reticulum unfolded protein response. *Nat Rev Mol Cell Biol*

- Biol* **8**, 519-529 (2007).
111. Horton, J.D., Goldstein, J.L. & Brown, M.S. SREBPs: activators of the complete program of cholesterol and fatty acid synthesis in the liver. *J Clin Invest* **109**, 1125-1131 (2002).
 112. Brown, M.S., Ye, J., Rawson, R.B. & Goldstein, J.L. Regulated intramembrane proteolysis: a control mechanism conserved from bacteria to humans. *Cell* **100**, 391-398 (2000).
 113. Hua, X., *et al.* SREBP-2, a second basic-helix-loop-helix-leucine zipper protein that stimulates transcription by binding to a sterol regulatory element. *Proc Natl Acad Sci U S A* **90**, 11603-11607 (1993).
 114. Yokoyama, C., *et al.* SREBP-1, a basic-helix-loop-helix-leucine zipper protein that controls transcription of the low density lipoprotein receptor gene. *Cell* **75**, 187-197 (1993).
 115. Rawson, R.B., DeBose-Boyd, R., Goldstein, J.L. & Brown, M.S. Failure to cleave sterol regulatory element-binding proteins (SREBPs) causes cholesterol auxotrophy in Chinese hamster ovary cells with genetic absence of SREBP cleavage-activating protein. *J Biol Chem* **274**, 28549-28556 (1999).
 116. Yang, T., *et al.* Crucial step in cholesterol homeostasis: sterols promote binding of SCAP to INSIG-1, a membrane protein that facilitates retention of SREBPs in ER. *Cell* **110**, 489-500 (2002).
 117. Martinon, F. & Glimcher, L.H. Regulation of innate immunity by signaling pathways emerging from the endoplasmic reticulum. *Curr Opin Immunol* **23**, 35-40 (2011).
 118. Iwakoshi, N.N., *et al.* Plasma cell differentiation and the unfolded protein response intersect at the transcription factor XBP-1. *Nat Immunol* **4**, 321-329 (2003).
 119. Reimold, A.M., *et al.* Plasma cell differentiation requires the transcription factor XBP-1. *Nature* **412**, 300-307 (2001).
 120. Iwakoshi, N.N., Pypaert, M. & Glimcher, L.H. The transcription factor XBP-1 is essential for the development and survival of dendritic cells. *J Exp Med* **204**, 2267-2275 (2007).
 121. Martinon, F., Chen, X., Lee, A.H. & Glimcher, L.H. TLR activation of the transcription factor XBP1 regulates innate immune responses in macrophages. *Nat Immunol* **11**, 411-418 (2010).
 122. Zhang, K., *et al.* Endoplasmic reticulum stress activates cleavage of CREBH to induce a systemic inflammatory response. *Cell* **124**, 587-599 (2006).
 123. Granados, D.P., *et al.* ER stress affects processing of MHC class I-associated peptides. *BMC Immunol* **10**, 10 (2009).
 124. Kaser, A. & Blumberg, R.S. Endoplasmic reticulum stress in the intestinal epithelium and inflammatory bowel disease. *Semin Immunol* **21**, 156-163 (2009).
 125. Todd, D.J., Lee, A.H. & Glimcher, L.H. The endoplasmic reticulum stress response in immunity and autoimmunity. *Nat Rev Immunol* **8**, 663-674 (2008).
 126. Engel, A. & Barton, G.M. Unfolding new roles for XBP1 in immunity. *Nat Immunol* **11**, 365-367 (2010).

CHAPTER 2

OS9 interacts with DC-STAMP and modulates its intracellular localization in response to TLR ligation

**Jansen BJ*, Eleveld-Trancikova D*, Sanecka A,
van Hout-Kuijer MA, Hendriks IA, Looman MW,
Leusen JH, Adema GJ**

* equally contributed to this study

Molecular Immunology (2009), 46(505-515)

Abstract

Dendritic cell-specific transmembrane protein (DC-STAMP) has been first identified as an EST in a cDNA library of human monocyte-derived dendritic cells (DCs). DC-STAMP is a multimembrane spanning protein that has been implicated in skewing haematopoietic differentiation of bone marrow cells towards the myeloid lineage, and in cell fusion during osteoclastogenesis and giant cell formation. To gain molecular insight in how DC-STAMP exerts its function, DC-STAMP interacting proteins were identified in a yeast-2-hybrid analysis. Herein, we report that amplified in osteosarcoma 9 (OS9) physically interacts with DC-STAMP, and that both proteins co-localize in the endoplasmic reticulum in various cell lines, including immature DC. OS9 has previously been implicated in ER-to-Golgi transport and transcription factor turnover. Interestingly, we now demonstrate that toll-like receptor (TLR)-induced maturation of DC leads to the translocation of DC-STAMP from the ER to the Golgi while OS9 localization is unaffected. Applying TLR-expressing CHO cells we could confirm ER-to-Golgi translocation of DC-STAMP following TLR stimulation and demonstrated that the DC-STAMP/OS9 interaction is involved in this process. Collectively, the data indicate that OS9 is critically involved in the modulation of ER-to-Golgi transport of DC-STAMP in response to TLR triggering, suggesting a novel role for OS9 in myeloid differentiation and cell fusion.

Introduction

Dendritic cells play a pivotal role in the initiation of innate and adaptive immune responses. Immature DCs capture foreign antigens in peripheral tissues and migrate to the T-cell areas of secondary lymphoid organs where they present these antigens to T- and B-cells. The capture of antigens in the steady state allows DCs to control immunotolerance towards self^{1,2}. Antigen uptake in the context of inflammation or infection results in DC maturation. In the presence of inflammatory cytokines and through binding of so-called pathogen-associated molecular pattern (PAMP) to one or more paralogues of the toll-like receptor family, DC mature and acquire the capacity to induce potent immunity. They initiate both innate and adaptive immune responses^{3,4}. As a consequence, DC have gained considerable interest as vaccine adjuvants and are currently exploited in the treatment of cancer after loading DC with tumor-cell derived antigens^{5,6}.

Although much is now known about the cellular nature of DC, molecular insight in its function, although mounting, is fragmentary at best. In order to gain more insight into this aspect of DCs, we and others have analyzed DC at the molecular level. One of the genes identified was DC-STAMP, which appears to be preferentially expressed by myeloid DC⁷⁻¹⁰. Others have reported the induction of DC-STAMP expression in macrophages stimulated with interleukin 4 (IL-4)¹¹, as well as its expression in osteoclasts¹². DC-STAMP has 4 to 7 transmembrane regions, and its gene localizes to chromosome 8q23⁹. In monocyte-derived DC and HEK293 cells, DC-STAMP localizes to the endoplasmic reticulum⁸. Biological roles for DC-STAMP are only recently emerging. We previously reported that DC-STAMP inhibits granulopoiesis, but promotes myeloid differentiation in murine bone marrow cells transduced with a retroviral construct expressing DC-STAMP fused to GFP⁷. Also, there is evidence for a role of DC-STAMP in osteoclastogenesis, as DC-STAMP expression appears to facilitate osteoclast differentiation in a murine macrophage RAW cell line that is otherwise incapable of differentiating into osteoclasts¹³. These findings were further corroborated in homozygous DC-STAMP knock-out mice, as these mice have mild osteopetrosis and display debilitating defects in the formation of multinuclear osteoclasts and giant multinucleated cells in response to foreign bodies, showing that DC-STAMP is required for cell fusion. However, the molecular mechanism by which DC-STAMP exerts its effect in osteoclasts and DC remains unknown¹⁴.

In order to identify interacting partners of DC-STAMP, we have constructed a prey cDNA library of mature and immature DCs, and used the cytoplasmic tail of

DC-STAMP as a bait in a yeast-2-hybrid screening. Here we report the identification of amplified in osteosarcoma 9 (OS9) as an interacting partner of DC-STAMP. The interaction of the two proteins is confirmed biochemically and by their colocalization in various cell types, including DC. Previous studies have implicated a role for OS9 in ER-to-Golgi transport^{15,16}. Interestingly, we now demonstrate that DC-STAMP enters the secretory pathway upon TLR stimulation in DC transduced with an adenovirus expressing DC-STAMP and CHO cells stably expressing TLR. The localization of OS9 in CHO cells and DC is not affected by maturation stimuli. Mutational analysis of DC-STAMP and OS9 suggest a critical role of the OS9/DC-STAMP interaction in the ER-to-Golgi transport of DC-STAMP.

Materials and methods

Plasmids, adenoviral vectors and cloning

Plasmids pGADGH and pGBT9 were used for yeast-2-hybrid analysis, and pER-DsRed, which contains the ER-targeting sequence of calreticulin fused to DsRed, was used for co-localization studies (all from Clontech, Mountain View, CA). The plasmids and adenoviral plasmids encoding DC-STAMP fused to the GFP protein have been described elsewhere⁸. The plasmid encoding DC-STAMP fused to a heamagglutinin (HA) tag was created by replacing the EGFP moiety of the pEGFP-N3 backbone with an HA tag. Human OS9 and its splice variant were amplified with specific primers (Sigma Genosystems, St. Louis, MO) from cDNA derived from human immature DC. Their coding sequences were cloned in frame into the pECFP-N1 vector (Clontech, Mountain View, CA). Carboxy-terminally HA-tagged constructs were generated by replacing the ECFP moiety an HA tag. Primer sequences and sequences of the oligonucleotide encoding the HA tag are available upon request. All generated constructs were verified for integrity and correct insertion by means of sequencing at the sequencing facility at the Department of Human Genetics, Radboud University Nijmegen Medical Centre. For the generation of OS9-GST fusion proteins in bacteria for the immunization of rabbits, the cDNA sequence corresponding to the C-terminal 80 amino acids of OS9 were inserted in frame with the C-terminus of GST in pGEX-1, and transformed and propagated in *Escherichia coli* DH5 α cells. For the production of GST-OS9 fusion proteins, the pGEX-1-OS9 construct was transformed in *E. coli* BL21. Generally, plasmid DNA was isolated from *E. coli* DH5 α or DH10 β bacteria using either the Endofree Plasmid Maxi Kit (Qiagen, Venlo, the Netherlands), or the HiSpeed Plasmid Maxi Kit (Qiagen, Venlo, the Netherlands). The cDNA library used in the yeast-2-hybrid analysis was purified by means of cesium chloride equilibrium centrifugation, essentially as described elsewhere¹⁷.

Yeast-2-hybrid analysis

Total RNA for the construction of a prey library was isolated from both immature and mature DC using TriZOL (Invitrogen, Carlsbad, CA), treated with DNase I, and mRNA was isolated

with the Oligotex mRNA midi kit (Qiagen, Venlo, the Netherlands). Messenger RNA was converted to cDNA with the Superscript kit (Invitrogen, Carlsbad, CA) and used to generate a prey library in pGADGH. The bait, corresponding to amino acids 403–470 of the cytoplasmic tail of DC-STAMP, was cloned into pGBT9. The library was amplified in *E. coli* (strain DH10 β , Invitrogen, Carlsbad, CA).

The yeast strain YGH1¹⁸ was used in order to screen the library for interactants with the carboxyterminal tail of DC-STAMP. The bait was transformed in to competent yeast as described elsewhere¹⁹. The cDNA library was then transformed into a clone containing the bait using a high-efficiency transformation protocol²⁰. Yeast culture and the analysis of interactions was carried out as described elsewhere^{21,22}.

Cell lines, cell culture, transfection and adenoviral transduction

Human embryonic kidney (HEK) 293 cells were cultured in Dulbecco's modified Eagle medium (DMEM) containing 4500 mg/l D-glucose, sodium pyruvate and GlutaMAX (Invitrogen, Carlsbad, CA), supplemented with 10% heat-inactivated fetal calf serum (FCS), 0.1 mM MEM non-essential amino acids and 100 units/ml Antibiotic-Antimycotic (Invitrogen, Carlsbad, CA) at 37°C under 5% CO₂. For transfections, cells were plated at a density of 5*10⁶ cells/75 cm², and incubated overnight to allow the cells to adhere. The next day, cells were transfected with a total of 10 μ g of DNA using Lipofectamine (Invitrogen, Carlsbad, CA), according to the manufacturer's directions.

Chinese hamster ovary cell stably expressing human TLR2 or TLR4 were cultured as described before²³. Both CD25 reporter expression after TLR stimulation as well as CD14 and TLR expression were assessed by means of fluorescence-activated cell-sorting (FACS) analysis as described before²³. The following TLR ligands were used in the indicated concentration: LPS (Sigma-Aldrich, St. Louis, MO), 100 ng/ml; Pam3Cys (Sigma-Aldrich, St. Louis, MO), 10 μ g/ml; PGN, 10 μ g/ml; and zymosan (kind gifts of dr. Mihai Netea, Department of Internal Medicine, Radboud University Nijmegen Medical Centre), 10 particles/cell.

Human monocyte-derived DC were generated using GM-CSF and IL-4, and their purity and maturation were assessed by means of FACS analysis as described previously²⁴. Adenovirus transduction of DC was carried out as described before⁸.

RNA isolation and reverse-transcriptase polymerase reaction

Total RNA for reverse-transcription polymerase reaction (RT-PCR) was isolated from cells using TriZOL (Invitrogen, Carlsbad, CA). RNA concentration was determined spectrophotometrically, and quality was assessed by means of conventional agarose gel electrophoresis. Reverse transcription using random hexamers was essentially done as described elsewhere²⁵. Approximately 5 ng of cDNA was used as input in subsequent RT-PCRs. In order to identify the 2 isoforms of OS9, the following primers were used: 5'-TGGAGGAAAAACAGAGTCCAGAGC-3' (forward) and 5'-CCTCATCAGTCAGCCAACGTGC-3' (reverse). Reactions were set up with Amplitaq Taq DNA polymerase kit (Applied Biosystems, Foster City, CA). The following PCR program was used: 5 min 95°C, and then 30 sec 95°C, 45 sec 57.5°C and 30 sec 72°C for 35 cycles, and thereafter 5 min 72°C. PCR products were assessed by conventional agarose gel

electrophoresis.

Co-immunoprecipitation of OS9 and DC-STAMP

The monoclonal antibody used for immunoprecipitation experiments (anti-HA, clone 12CA5, mouse IgG2b) as well as normal rabbit serum, were covalently coupled to Protein G sepharose Fast Flow beads (GE Healthsciences Bio-Sciences, Uppsala, Sweden) using dimethyl pimelimidate dihydrochloride (Sigma–Aldrich, St. Louis, MO) in 0.2 M triethanolamine (pH 8.3) as a protein cross-linker. Right before use, the antibody-protein G sepharose complexes were washed extensively with lysis buffer. Bare protein G beads and beads coupled to rabbit IgGs were subsequently used to preclear lysates in order to diminish unspecific binding of proteins to 12CA5 in the following steps.

For co-immunoprecipitations, HEK293 cells were co-transfected with constructs encoding GFP, DC-STAMP-GFP and OS9-HA or their mutants as described above, and after 48 h lysed in 1.5 ml modified radioimmunoprecipitation (RIPA) buffer (50 mM Tris/HCl pH 7.5, 1% (w/v) Triton X-100, 5 mM EDTA, 150 mM NaCl, 0.5% (w/v) sodium deoxycholate, 0.1% (w/v) sodium dodecyl sulfate, 1 mM phenylmethylsulfonyl fluoride (PMSF), 2 µg/ml aprotinin and 2 µg/ml leupeptin). Insoluble material was removed by centrifugation. After preclear with bare beads and beads coupled to rabbit IgG, the immunoprecipitation was performed with beads coupled to 12CA5. All steps were performed at 4°C. Supernatant was saved and stored at –80°C and beads were washed 4 times with RIPA buffer before being transferred to a clean 1.5 ml tube for a final wash. Beads were stored at –80°C until further processing.

Polyacrylamide gel electrophoresis and Western blotting

Lysates of DC were prepared in SDS lysis buffer as described elsewhere²⁵. For polyacrylamide gel electrophoresis (PAGE), reducing sample buffer (62.5 mM Tris/HCl pH 6.8, 25% (v/v) glycerol, 2% (w/v) sodium dodecyl sulfate, 0.01% (w/v) bromophenol blue, 5% (v/v) β-mercaptoethanol) was added 1:1 to a lysate equivalent to ~50,000 cells. As DC-STAMP-GFP tends to aggregate during heating, samples were not boiled before being loaded onto gel. Samples were subjected to polyacrylamide gel electrophoresis using the MiniProtean system (BioRad, Hercules, CA) and further processed for Western blot analysis. After blocking, membranes were incubated with a mixture of two primary antibodies against either GFP (clones 7.1 and 13.1, Roche Applied Science, Almere, the Netherlands), the HA tag (rat monoclonal 3F10; Sigma–Aldrich, St. Louis, MO) or purified rabbit polyclonal IgGs against OS9. After washing, membranes were incubated with a matching horseradish peroxidase-conjugated secondary antibody (DAKO, Glostrup, Denmark). Immunoreactive bands were visualized using the ECL kit (GE Healthsciences Bio-Sciences, Uppsala, Sweden). Afterwards, membranes were stripped in 0.2 M glycine/1% (w/v) sodium dodecyl sulfate, pH 2.5, blocked and reprobed with a mouse monoclonal against β-Actin (1:20,000; Sigma–Aldrich, St. Louis, MO), and processed as described above.

Production of anti-OS9 antibodies

GST-OS9 fusion protein was produced in BL21 *E. coli* bacteria and purified using glutathion sepharose beads essentially using standard protocols²⁵. The immunization of rabbits was ap-

proved by the institutional Ethics Committee for Animal Experimentation and in accordance with local and national guidelines. Rabbits were immunized 8 times with purified GST-OS9. The first intracutaneous immunization was performed with complete Freund's adjuvant, and subsequent subcutaneous immunizations were performed with incomplete Freund's adjuvant. When sera could detect transiently expressed OS9 in HEK293 lysates in a Western blot assay, rabbits were sacrificed and their whole blood collected. Polyclonal rabbit IgG were isolated from serum by depleting antibacterial and anti-GST IgG with CNBr-activated sepharose beads (GE Healthsciences Bio-Sciences, Uppsala, Sweden) coated with bacterial GST lysate, essentially as described by the manufacturer. Polyclonal anti-OS9 IgG were then isolated using Fast Flow Protein G beads, eluted with 900 μ l 200 mM glycine pH 2.5, 150 mM NaCl, 1 mM EDTA and neutralized in 100 μ l 1M Tris pH 8.0. The antibody concentration was measured using the BCA kit (Pierce, Rockford, IL), and positive fractions were stored at 4°C.

Immunofluorescence staining and microscopy

Dendritic cells or HEK293 cells were seeded onto slides coated with 25 μ g/ml fibronectin, and cells were fixed with 1% paraformaldehyde in PBS, permeabilized with ice-cold methanol, washed with PBS, blocked and stained with antibodies either against protein disulfide isomerase, an ER marker (PDI; Affinity Bioreagents, Golden, CO), ER-Golgi intermediate compartment 53 (ERGIC53; kind gift of dr. J. Fransen, Department of Cell Biology, Nijmegen Centre for Molecular Life Sciences), or polyclonal anti-OS9 antibodies. Antibodies were used as recommended by the various manufacturers. Fluorescently labeled secondary antibodies were obtained from Molecular Probes (Eugene, OR), and cells were mounted in Vectashield (Vector Labs, Burlingame, CA). Transfected CHO/TLR cells were seeded onto glass cover slips coated with fibronectin, fixed with 4% paraformaldehyde in PBS, permeabilized with 0.1% Triton, blocked and stained with antibodies against HA (rat monoclonal 3F10) to detect HA-tagged OS9 or OS9 Δ C, a rabbit anti-Sec23 polyclonal (Santa Cruz Biotechnology, Santa Cruz, CA) a marker for the ER exit sites, or a mouse monoclonal against GM130 (BD Biosciences, San Jose, CA), a marker for the cis-Golgi. The ER was visualized using a construct encoding ER-DsRed (Clontech, Mountain View, CA). Alexa647-labeled secondary antibodies against either rat or mouse IgG were used to visualize OS9 variants or GM130, respectively, whereas Sec23 was visualized with secondary anti-rabbit antibodies labeled with Alexa568 (Molecular Probes, Eugene, OR). Cells were mounted using Mowiol (Calbiochem, San Diego, CA) and further processed as described above. Confocal laser scanning microscopy (CLSM) was carried out with a BioRad MRC1024 confocal laser microscope at the Microscopic Imaging Facility of the Department of Cell Biology, Nijmegen Centre for Molecular Life Sciences, Radboud University Nijmegen Medical Centre, Nijmegen, the Netherlands.

Results

OS9 interacts with the cytoplasmic tail of DC-STAMP

To identify DC-STAMP binding partners, a yeast-2-hybrid analysis was performed. The predicted cytoplasmic carboxy-terminal tail of DC-STAMP, corresponding to amino acids 403–470, was used to screen a prey cDNA library derived from a mixture of immature and mature DC²⁶. As shown in Table 1, of the 58 positive colonies identified, 8 colonies (14 %) contained a sequence derived from human OS9. Further sequence analysis revealed that both OS9 isoform 1 (6 clones) and an alternative splice variant of OS9 (2 clones) were present amongst the positive clones.

Table 1. Overview of the Y-2-H results with the cytoplasmic tail of DC-STAMP

Day	No. of colonies	Positive colonies in 1st screening	Positive colonies containing OS-9 in 2nd screening
5	14	5	3
8	74	31	5*
11	126	22	2*

* Includes 1 clone of an OS-9 splice variant

To confirm the interaction of DC-STAMP with OS9, co-immunoprecipitation experiments were performed in HEK293 cells following transient transfection with OS9 and DC-STAMP. As no suitable antibodies are available for DC-STAMP, GFP-tagged DC-STAMP and HA-tagged OS9 were used instead. We note that the presence of a GFP moiety at the carboxy terminus of the DC-STAMP bait protein did not influence the OS9 interaction in the yeast-2-hybrid analysis (data not shown). As shown in Fig. 1A (middle pictures), both OS9-HA and DC-STAMP-GFP were readily detected in the total lysates following transfection. In addition, OS9-HA was efficiently precipitated at stringent conditions (RIPA buffer containing 1% Triton X-100, 0.1% SDS and 0.5% sodium deoxycholate; see Fig. 1A, upper left picture). Western blot analysis demonstrated that DC-STAMP-GFP, but not control GFP, co-precipitated with OS9-HA (Fig. 1A; lane 6, upper right picture). We note that also in the reciprocal experiment OS9-HA co-immunoprecipitated with DC-STAMP-GFP but not GFP (data not shown). These results corroborate our findings in the yeast-2-hybrid assay and indicate that DC-STAMP can indeed interact with OS9 at stringent conditions.

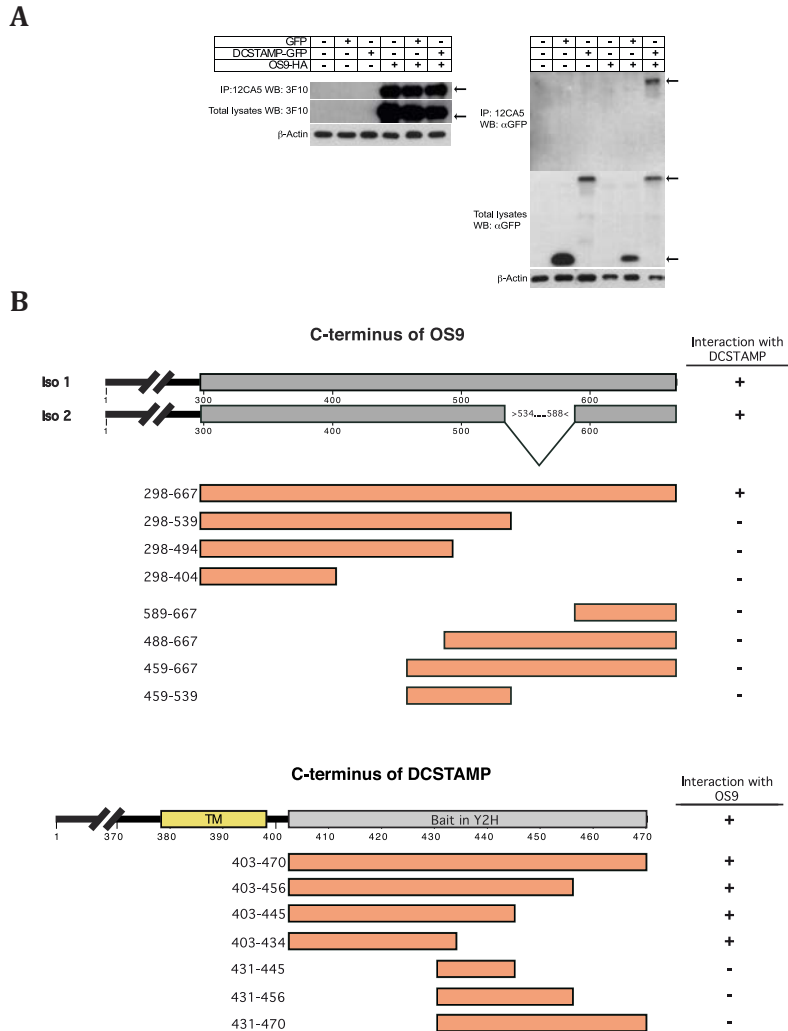


Figure 1. DC-STAMP and OS9 interact with each other. **A)** Co-immunoprecipitation of DC-STAMP and OS9 in HEK293 cells. DC-STAMP and OS9 were co-expressed as fusion proteins to GFP and HA, respectively, and immunoprecipitated with mouse monoclonal 12CA5 (against the HA tag). Total lysates and immunoprecipitations were subjected to Western blotting, and proteins were detected using antibodies specific for their tags (see Materials and methods for details). As controls, cells transfected with pEGFP-N3 were taken along, as well as single transfections with plasmids encoding either DC-STAMP-GFP or OS9-HA. Arrows indicate the products of expected size. β -Actin was stained and visualized as a normalization control. The data are representative of three experiments. **B)** Various bait constructs (prepared in a pGBT9 backbone), containing deletion mutants of the carboxyterminal tail of DC-STAMP, were prepared and screened in a yeast-2-hybrid assay with the carboxyterminal 370 amino acids of OS9 (upper block). Also, various deletion mutants of OS9 (prepared in a pGADGH backbone) were screened in a yeast-2-hybrid assay against the full-length carboxyterminal tail of DC-STAMP (lower block). Legend: + interaction, - no interaction.

Next, we set out to define the OS9/DC-STAMP interacting domains in further detail by Y-2-H analysis. All OS9 clones that were found to interact with the cytoplasmic tail of DC-STAMP match the carboxy-terminal half of OS9 (amino acids 298–667) (Fig. 1B, upper box, grey bars). Analysis of additional OS9 deletion mutants (Fig. 1B, upper part) did not yield a smaller OS9 domain able to interact with the cytoplasmic tail of DC-STAMP, suggesting that the complete C-terminal half is required for proper binding. As OS9 isoform 2 (amino acids 290–612) does interact with the cytoplasmic tail of DC-STAMP in the Y-2-H assays (Fig. 1B, upper part) as well as in IP experiments (data not shown) the amino acids 534–588 that are absent in OS9 isoform 2 are not essential for interaction with DC-STAMP (Fig. 1B, upper part). To further define the parts in the cytoplasmic tail of DC-STAMP that are responsible for the interaction with OS9, we created a series of deletion mutants in the carboxy-terminal tail of DC-STAMP. Subsequent Y-2-H studies revealed that the smallest part in the carboxyterminal part of DC-STAMP that is still able to interact with OS9 contained amino acids 403–434 (Fig. 1B, lower part). Thus, the cytoplasmic tail of DC-STAMP is able to bind to amino acids 298–667 of OS9 through a stretch of 31 amino acids in its carboxy-terminal tail, just proximal to the C-terminal transmembrane domain. It should be noted, however, that additional IP experiments with a DC-STAMP carboxy-terminal deletion mutant revealed that this deletion mutant is still able to interact with OS9, suggesting that OS9 interacts through multiple interfaces with other parts of DC-STAMP that are exposed to the cytosol (see below and supplementary Fig. S1).

OS9 is expressed in immature and mature DC

To assess the expression of OS9 and the OS9 splice variants at the mRNA and protein levels in DC, immature and LPS-matured monocyte-derived DC were generated and analyzed by RT-PCR and Western blotting. As a positive control, various clones identified in the yeast-2-hybrid screening were included for comparison. RT-PCR on cDNA derived from immature and mature DC shows that full-length OS9 and isoform 2 are indeed expressed (Fig. 2A). We were unable to detect OS9 isoform 3 (data not shown).

To investigate OS9 expression at the protein level, a polyclonal rabbit antiserum was raised against the carboxy-terminal 80 amino acids which are present in all known isoforms of OS9. Immature DC were generated with IL-4 and GM-CSF, and further matured with the TLR ligand LPS for 4, 8, 12 and 48 h, and protein samples were prepared for each time point. Successful maturation of DC was confirmed by the upregulation of the co-stimulatory molecules CD80 and CD83, which are considered a hallmark of DC maturation (see Supplementary data, Fig. S2). As shown in Fig. 2B,

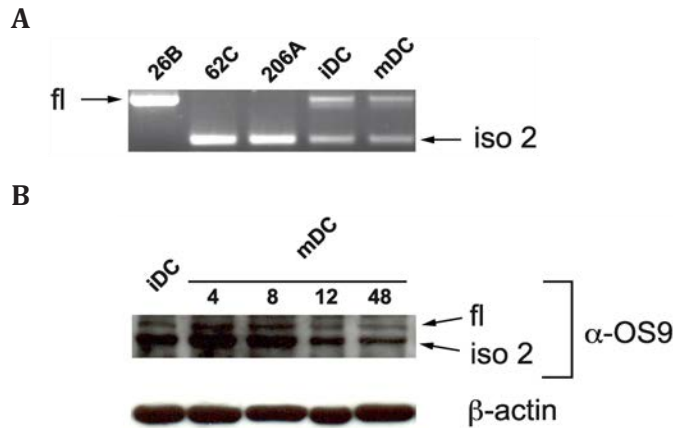


Figure 2. OS9 is expressed in dendritic cells. A) Both full-length OS9 and its isoform 2 are expressed in immature (iDC) and mature DC (mDC) at the mRNA level. Positive controls: 26B, a yeast-2-hybrid clone picked up in the screen containing full-length OS9; 62C and 206A, yeast-2-hybrid clones containing OS9 isoform 2. B) Western blot analysis of OS9 expression in immature and maturing DC. A polyclonal rabbit serum, raised against the carboxyterminal 80 amino acids of human full-length OS9, was used to detect the both the full-length protein and isoform 2. A staining for β -Actin was performed as a normalization control.

both full-length OS9 and isoform 2 were readily detected on Western blots in immature DC. LPS-induced DC maturation results in a transient increase in both OS9 isoforms at 4 and 8 h after which OS9 protein levels drop in fully mature DC to a slightly lower level as observed in immature DC. The predicted OS9 isoform 2 is expressed at higher levels than full-length OS9 throughout DC maturation.

OS9 localizes to the endoplasmic reticulum in immature and mature DC

Previously, we reported that DC-STAMP localizes to the ER in immature DC. Interestingly, mammalian OS9 is a cytosolic protein that has also been shown to strongly associate with the cytosolic side of the ER in different cell lines¹⁵. In order to analyze the subcellular localization of OS9 in DC, immature and mature DC were stained with polyclonal rabbit IgG directed against human OS9 and either a monoclonal against the ER marker PDI (protein disulfide isomerase) or the ER-Golgi intermediate compartment protein ERGIC53. HEK293 cells transfected with OS9 protein fused to CFP were included for comparison. As shown in Fig. 3A, endogenous OS9 in immature DC predominantly colocalizes with the ER marker PDI, but not with ERGIC53 (second and third rows of pictures). The ER localization of OS9 is not affected by maturation of DC by LPS (Fig. 3A, fourth row of pictures). We note that

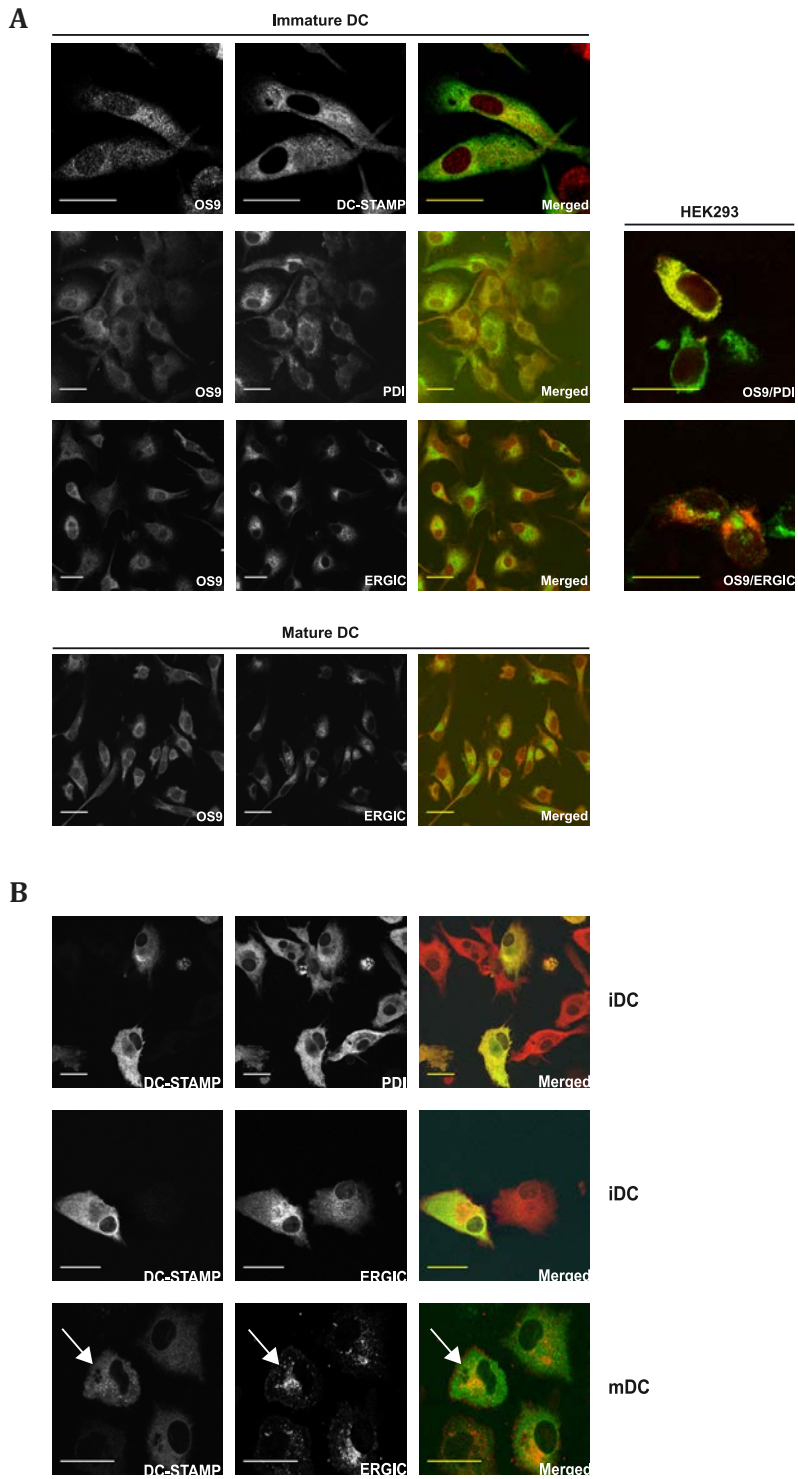


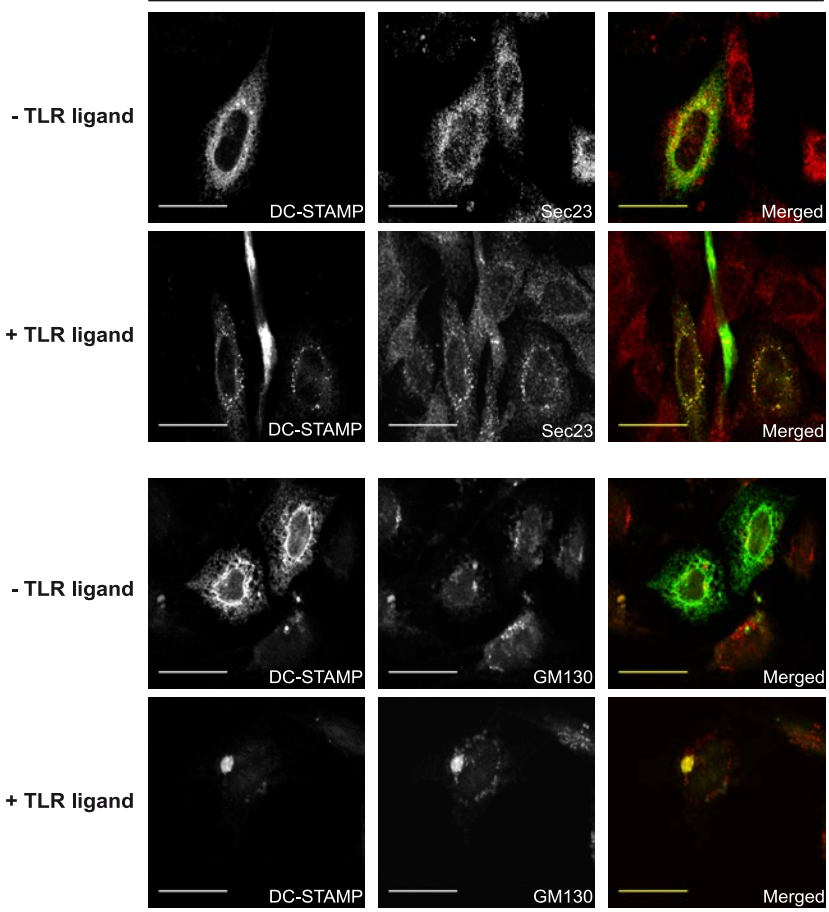
Figure 3. OS9 resides in the ER in DC, regardless of DC maturation status, whereas DC-STAMP translocates to the intermediate compartment. **A)** Immature monocyte-derived DC were fixed and stained with the rabbit polyclonal serum against OS9 (pseudocolored red), as well as a mouse monoclonal against either ER marker PDI (three left pictures, second row; in green), or the intermediate compartment marker ERGIC53 (three left pictures, third row; in green) and mounted and analyzed by means of CLSM. Also, immature DC were transduced with adenovirus expressing DC-STAMP-GFP (in green), fixed and stained to detect endogenous OS9 (in red; upper row of pictures). As a control, HEK293 cells were transiently transfected with a construct encoding OS9-CFP and stained with an anti-GFP antibody (pseudocolored red) and colocalization was assessed with the ER marker PDI and the intermediate compartment marker ERGIC53 (both in green: outermost right column). OS9 does not translocate to the intermediate compartment upon maturation of DC. Immature DC were matured for 48 h with LPS and stained with the polyclonal serum against OS9 (pseudocolored red) and the monoclonal antibody for ERGIC53 (in green; fourth row of pictures) **B)** DC-STAMP-GFP translocates to the intermediate compartment between ER and Golgi in DC. Immature DC were transduced with adenovirus encoding DC-STAMP-GFP, matured for 48 h and processed for CLSM, and colocalization of DC-STAMP (in green) was assessed in immature DC with ER marker PDI (upper row of pictures; in red) and in both immature (middle row of pictures) and mature DC (lower row of pictures) with intermediate compartment marker ERGIC53 (in red). The arrow indicates typical co-localization of DC-STAMP with ERGIC only seen in mature DC. Scale bars: 20 μm .

some cytoplasmic staining is also seen with the anti-OS9 serum, which is in line with previous biochemical data¹⁵. Furthermore, the staining observed in DC essentially mimicked the distribution in OS9-CFP-transfected 293 cells (Fig. 3A, outermost right column).

Since co-localization studies of OS9 and endogenous DC-STAMP in DC are hampered by the absence of suitable antibodies against DC-STAMP, DC were transduced with an adenoviral construct encoding DC-STAMP-GFP⁸ and stained with the polyclonal anti-OS9 serum. As shown in Fig. 3A (upper row of pictures), DC-STAMP-GFP shows a distribution reminiscent of the ER, and clearly co-localizes with endogenous OS9 in the ER of immature DC. Interestingly, while DC-STAMP-GFP almost exclusively colocalized with OS9 and the ER marker PDI in immature DC (Fig. 3B, upper row of pictures), DC-STAMP-GFP localization appears to shift to the intermediate compartment in mature DC. After DC maturation the localization of DC-STAMP-GFP appeared much more heterogeneous. In approximately 20–35% of the mature DC, DC-STAMP-GFP was present in small speckles that showed a clear colocalization with ERGIC53 near the nucleus (Fig. 3B, lower row of pictures indicated by an arrow). The observed diversity in DC-STAMP staining may reflect the transient nature of the relocalization, the heterogeneity in the cell population, or both. Little or no colocalization of DC-STAMP-GFP with the intermediate compartment marker ERGIC53 is observed in immature DC (Fig. 3B, middle row

A

CHO/TLR



- TLR ligand

+ TLR ligand

- TLR ligand

+ TLR ligand

B

CHO/TLR

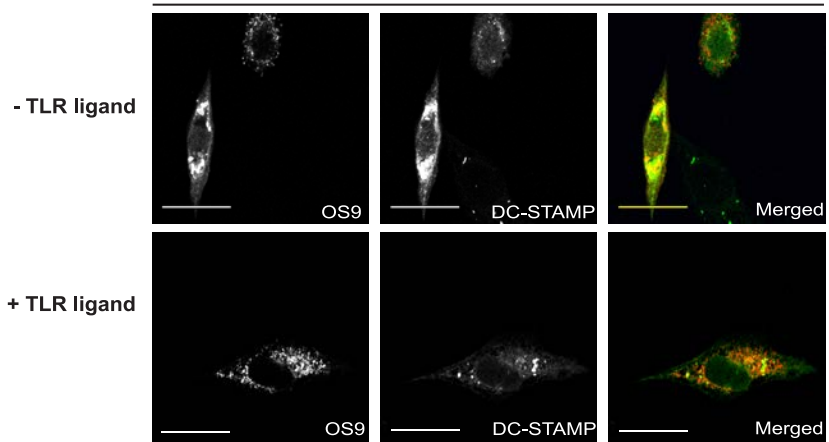


Figure 4. DC-STAMP translocates to the secretory pathway in the CHO/TLR model, irrespective of human OS9. **A)** Upon TLR stimulation, DC-STAMP-GFP colocalizes with Sec23 and GM130. DC-STAMP-GFP was expressed in CHO/TLR cells, plated onto glass cover slips, and not stimulated (first and third row of pictures) or stimulated for 1 h (second row of pictures) or 6 h (fourth row of pictures). Cells were fixed and stained with polyclonal rabbit IgG against Sec23, a marker for ER exit sites (upper two rows of pictures) or with a mouse monoclonal against GM130, a marker for the cis-Golgi (lower two rows of pictures) and cells were mounted and analyzed by means of CLSM. **B)** DC-STAMP and OS9 do not colocalize after TLR stimulation. CHO/TLR cells were transfected with constructs encoding DC-STAMP-GFP (green) and OS9-HA, and either not stimulated (upper row of pictures) or stimulated for 6 h (lower row of pictures). OS9 was visualized using rat monoclonal 3F10 against the HA tag (in red) and cells were mounted and analyzed by means of CLSM. Scale bars: 20 μ m.

of pictures). Thus, while OS9 localization is largely unaffected by TLR stimulation of DC, DC-STAMP relocates to the intermediate compartment out of the ER in a significant proportion of the mature DC.

DC-STAMP is redistributed in a CHO/TLR model system upon TLR stimulation

Co-localization studies in primary DC are difficult and are further hampered by the dynamic nature of the components in the secretory pathway (i.e. the ER, ER exit sites and Golgi) during maturation. Therefore, we set up a model system using CHO cells co-expressing either TLR2 or TLR4 and CD14 to analyze DC-STAMP relocalization in further detail²³. These CHO cells also express human CD25 under control of an NF κ B promoter, allowing to monitor successful TLR stimulation by CD25 upregulation (Fig. S3). CHO/TLR cells transfected with DC-STAMP-GFP were stimulated or left unstimulated and stained with antibodies against Sec23, a marker for ER exit sites. CLSM analysis revealed that DC-STAMP-GFP rapidly (within 1 h) translocated to the ER exit sites after TLR stimulation, as evidenced by the occurrence of a punctate DC-STAMP-GFP pattern that exclusively colocalized with Sec23 (Fig. 4A, upper two rows). Moreover, when cells were stimulated for 6 h, DC-STAMP-GFP appeared in a clear bright spot adjacent to the nucleus, where it completely colocalized with the cis-Golgi marker GM130 (Fig. 4A, two lower rows). Identical co-localization data (Fig. 4B) were obtained after LPS exposure when full length human OS9 was co-transfected in CHO/TLR/DC-STAMP-GFP cells, suggesting that the endogenous Chinese hamster OS9 homologue is sufficient to drive human DC-STAMP transport. It should be noted that, when co-expressed with the human OS9 splice variant as identified in the yeast-2-hybrid analysis, DC-STAMP-GFP was still able to translocate to the secretory pathway (data not shown). Collectively, these data demonstrate that after TLR stimulation DC-STAMP relocates from the ER via

the intermediate compartment to the Golgi in the CHO model system, similar to the findings in TLR-stimulated human DC.

The OS9/DC-STAMP interaction affects DC-STAMP redistribution

To investigate the importance of the DC-STAMP/OS9 interaction in DC-STAMP relocation, a GFP-tagged DC-STAMP deletion mutant was constructed in which amino acids 403–434 in the cytoplasmic carboxyterminus that are known to interact with OS9 are lacking (supplementary Fig. S4). As noted before, DC-STAMP interacts with OS9 through multiple interfaces outside its cytoplasmic tail. Both wild-type and mutant GFP-tagged DC-STAMP were transfected into CHO/TLR cells, together with a construct encoding the ER-targeting signal of calreticulin to the fluorescent protein DsRed in order to visualize the ER. Interestingly, whereas full-length DC-STAMP-GFP showed complete co-localization with ER-DsRed in steady-state conditions, it moves out of the ER upon TLR ligation (compare upper and third row of pictures, Fig. 5A). The DC-STAMP-GFP mutant lacking the minimal carboxyterminal OS9 binding domain failed to show this redistribution after stimulation in CHO/TLR cells, but instead displayed an ER-like distribution as evidenced by the overlap of expression with ER-resident ER-DsRed (compare second and last row of pictures, Fig. 5A). These data imply that OS9 is required for the relocation of DC-STAMP.

To further confirm that OS9 is indeed required for the relocation of DC-STAMP, we constructed a human OS9-HA deletion mutant lacking the complete C-terminal domain (OS9 Δ C, supplementary Fig. S4), which is known to interact with the cytoplasmic tail of DC-STAMP and thus may affect TLR-dependent DC-STAMP relocation. We note, however, that also this OS9 Δ C mutant is still able to interact with full length DC-STAMP (data not shown), strengthening the finding that OS9 and DC-STAMP interact through multiple domains. Furthermore, this mutant still localizes to the ER¹⁵. Consistent with earlier experiments, DC-STAMP readily displays the typical punctate pattern in response to the TLR stimulus in CHO/TLR cells in the presence of full-length OS9 (Fig. 5B, compare first and third row of pictures). In contrast, in the presence of OS9 Δ C DC-STAMP stays in the ER (compare second and last row of pictures, Fig. 5B). These data indicate that OS9 Δ C effectively acts as a dominant-negative mutant for the redistribution of DC-STAMP following TLR triggering. Moreover, these data collectively provide evidence for a role for OS9 in the redistribution of DC-STAMP upon TLR stimulation.

Discussion

This study was carried out to gain insight in the molecular environment of DC-STAMP, a protein involved in myeloid differentiation and giant cell formation. By means of yeast-2-hybrid analysis and co-immunoprecipitation assays, we identified OS9 as a bona fide DC-STAMP-interacting protein (Figs. 1 and 2). Furthermore, endogenous OS9 co-localizes with DC-STAMP in the ER of immature DC and in OS9 transfected HEK293 cells (Fig. 3). Intriguingly, upon TLR stimulation DC-STAMP, but not OS9 relocalized from the ER to the intermediate/Golgi compartment in OS9-dependent manner in DC and TLR expressing CHO cells (Figs. 4 and 5).

OS9 is a broadly expressed protein consisting of 3 different isoforms. Here we show that DC express OS9 isoforms 1 and 2 and that the expression levels of both isoforms are modulated upon TLR induced DC maturation. Within immature DC, OS9 predominantly co-localized with the ER resident protein PDI, and upon maturation displayed similar intracellular distribution, as its expression did not overlap with the intermediate compartment marker ERGIC53. Functionally, OS9 has been implicated in ER-to-Golgi transport of the membrane protease meprin A beta (MEP1B). Our data now demonstrate the involvement of OS9 in the transport of DC-STAMP out of the ER upon DC maturation. Using CHO cells expressing TLR2 or -4 it was confirmed that DC-STAMP relocalizes to the cis-Golgi in the presence of full-length OS9 (Fig. 5) and OS9 isoform 2 (data not shown), and this process is inhibited by OS9 Δ C. Interestingly, the region in cytoplasmic tail of DC-STAMP that binds to OS9 also appears to be required for its transport (Fig. 5). Studies by Litovchick et al.¹⁵ showed that MEP1B transport requires full-length OS9 isoform 1 but that, in contrast to DC-STAMP transport, this process is inhibited by OS9 isoform 2. Furthermore, MEP1B transport depends on the motif (Y/F)C(X/XX)(R/K)(R/K)(R/K) in its cytoplasmic tail. Mutant MEP1B, lacking this motif, cannot be transported from the ER to the Golgi²⁷, and does not bind OS9. Although a DC-STAMP mutant lacking the cytoplasmic OS9-interacting domain is also unable to translocate, it does not contain a motif resembling the one present in MEP1B. Contrary to MEP1B, which is a type I transmembrane protein, DC-STAMP has at least 4 transmembrane domains and our data show that DC-STAMP interacts with OS9 through multiple interfaces. Another important difference between MEP1B and DC-STAMP is that the latter does not go to the plasma membrane, whereas MEP1B does, which may reflect differences in (required) binding motifs. Collectively, these data suggests that OS9 binds to more transmembrane proteins than the 25 predicted so far¹⁵ and serves as a multitarget adapter for transport of proteins from the ER-to-Golgi. How exactly OS9 regulates ER-

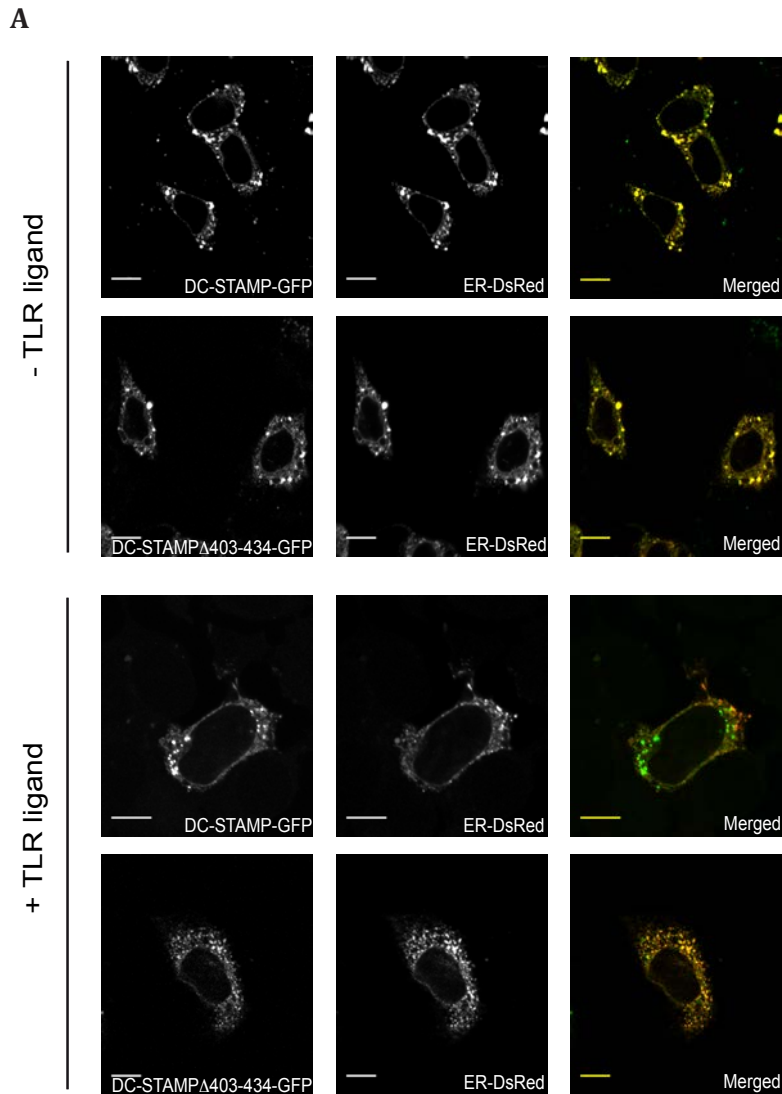
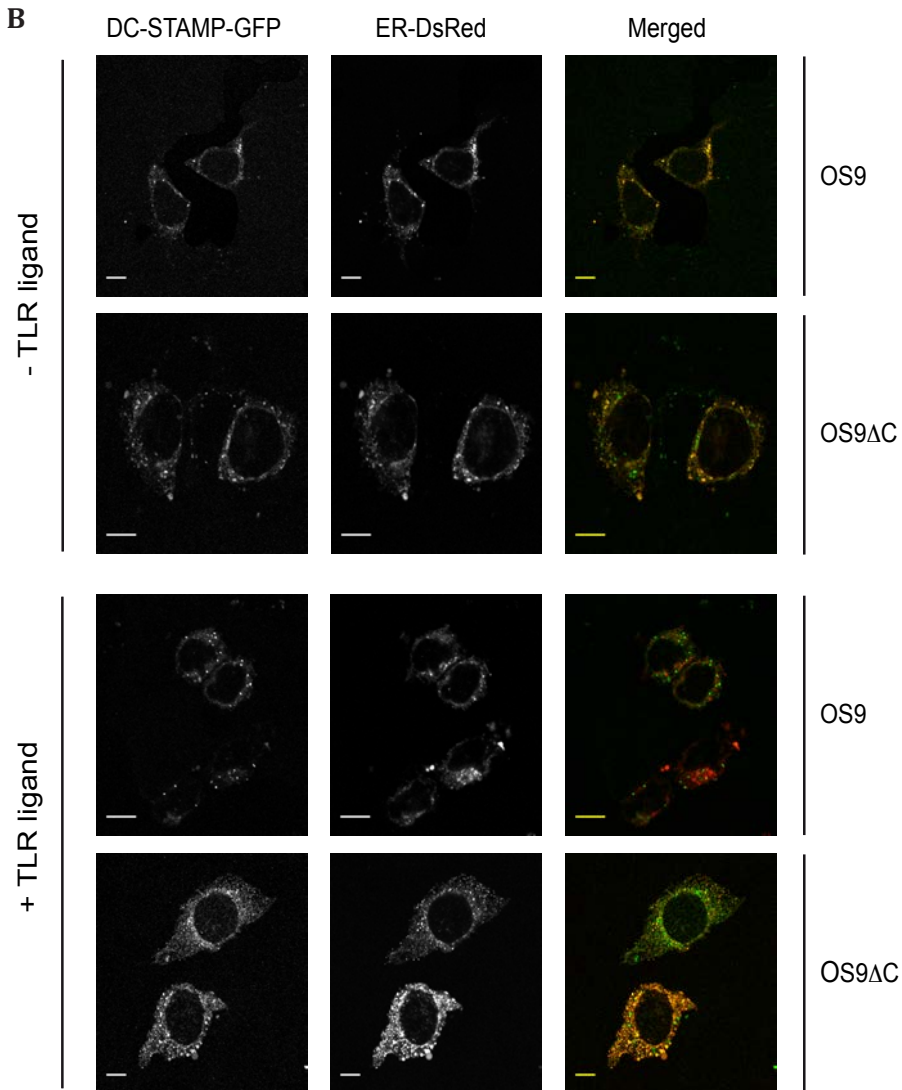


Figure 5. The OS9/DC-STAMP interaction affects DC-STAMP redistribution. A) CHO/TLR cells were transfected with constructs encoding DC-STAMP-GFP and ER-DsRed (first and third row of pictures), or a construct encoding deletion mutant DC-STAMP Δ 403–434-GFP, which lacks the minimal carboxyterminal OS9-interacting domain (second and fourth row of pictures). Cells were either not stimulated (upper two rows of pictures) or stimulated with a TLR ligand for 6 h (lower two rows of pictures), fixed, mounted and the DC-STAMP redistribution (in green) was assessed by means of CLSM. B) Co-transfections in CHO/TLR cells were performed with constructs encoding DC-STAMP-GFP and either OS9-HA (first and third



row of pictures) or OS9ΔC-HA (second and fourth row of pictures), which lacks the DC-STAMP-interacting domain as determined by yeast-2-hybrid analysis. Cells were either not stimulated (upper two rows of pictures) or stimulated with a TLR ligand for 6 h (lower two rows of pictures), fixed, mounted and the DC-STAMP redistribution (in green) was assessed by means of CLSM. In all pictures, the red color represents ER-DsRed. Scale bars: 10 μm.

to-Golgi transport of DC-STAMP or MEP1B remains unclear. In the case of MEP1B, OS9 has been suggested to reside at the interface of ER and the secretory pathway based on Western blot analysis¹⁵. We were unable, however, to show that OS9 colocalizes with the transitional ER/COPII sites (data not shown), where cargo is concentrated for transport to the Golgi. Instead, DC-STAMP colocalization with Sec23-positive ER exit sites was readily observed following TLR activation. It is tempting to speculate that the OS9/DC-STAMP pathway fulfills a role in ER-to-Golgi transport during DC maturation. During DC maturation, many different transmembrane proteins, such as cytokines, cytokine receptors, chemokines and MHC1-antigen complexes need to be transported to the surface of the cell. Whether or not the DC-STAMP/OS9 pathway is directly involved in the increased transport during DC maturation remains to be determined.

Besides its role in ER-to-Golgi transport, OS9 has been reported to play role in the regulation of proteasome-mediated degradation of the transcription factor *hypoxia-inducible factor 1 alpha* (HIF1 α) and the *vanilloid transient receptor potential protein 4* (TRPV4). HIF1 α is involved in the genetic response to hypoxia²⁸. Interestingly, immune cells are often exposed to low oxygen tensions, which markedly affect their cellular metabolism²⁹. OS9 is an essential component of a multiprotein complex that regulates HIF-1alpha levels through proteasomal degradation in an O₂-dependent manner. Recent studies have also implicated OS9 in the clearance of misfolded protein conformers³⁰ and of mutated α 1-antitrypsin from the ER³¹. Moreover, OS9 is involved in the maturation of TRPV4 by preventing the polyubiquitination of TRPV4 monomers and, importantly, impedes TRPV4 transport to the plasma membrane³². It should be noted that the levels of DC-STAMP, based on immunofluorescence data, go down dramatically after TLR stimulation (see Figs. 3, 4 and 5). Although we have not in detail explored the degradation of DC-STAMP in the presence of OS9 upon TLR stimulation, preliminary biochemical data suggest that, besides promoting DC-STAMP relocalization, OS9 may also be involved in the degradation of DC-STAMP (data not shown). In steady-state conditions, OS9 interacts with DC-STAMP in the ER and may act as a chaperone there, possibly regulating the expression of DC-STAMP proteins and/or the disposal of their misfolded derivatives, whereas upon TLR stimulation their interaction may lead to rapid overall clearance of excess DC-STAMP in the ER. However, further experiments are needed to uncover the precise mechanism behind this process.

Since DC-STAMP has been implicated in both osteoclastogenesis, where it appears to be required for cell fusion, as well as the development of myeloid cells from bone

marrow-derived hematopoietic stem cells, it is tempting to speculate that the OS9/DC-STAMP pathway plays a role in both processes. Still little is known regarding the role of DC-STAMP in DC activation and function. The finding that the DC-STAMP/OS9 pathway is responsive to TLR-triggering implies a role for inflammatory stimuli in its activation. Further research is needed to clarify the role of this novel pathway in immune signaling and inflammatory protein transport in DC.

Acknowledgements

We gratefully acknowledge Dr. Jack Fransen, Department of Cell Biology, NCMLS, Radboud University Nijmegen Medical Centre, for providing the antibody against ERGIC53, and Angeliq Lemckert and Menzo Havenga, Crucell NV, Leiden, the Netherlands, for providing the adenoviral DC-STAMP-GFP construct. Furthermore, we would like to thank Dr. Richard Janssen, BioFocus DPI BV, Leiden, the Netherlands, for helpful discussion. This work was financially supported by grant 912-02-34 and VICI grant 918-66-615 (awarded to G.J.A.) from the Netherlands Organization for Scientific Research (NWO).

References

1. Banchereau, J. & Steinman, R.M. Dendritic cells and the control of immunity. *Nature* **392**, 245-252 (1998).
2. Mellman, I. & Steinman, R.M. Dendritic cells: specialized and regulated antigen processing machines. *Cell* **106**, 255-258 (2001).
3. Akira, S. & Takeda, K. Toll-like receptor signalling. *Nat Rev Immunol* **4**, 499-511 (2004).
4. Janeway, C.A., Jr. & Medzhitov, R. Innate immune recognition. *Annu Rev Immunol* **20**, 197-216 (2002).
5. Figdor, C.G., de Vries, I.J., Lesterhuis, W.J. & Melief, C.J. Dendritic cell immunotherapy: mapping the way. *Nat Med* **10**, 475-480 (2004).
6. Schreurs, M.W., Eggert, A.A., Punt, C.J., Figdor, C.G. & Adema, G.J. Dendritic cell-based vaccines: from mouse models to clinical cancer immunotherapy. *Crit Rev Oncog* **11**, 1-17 (2000).
7. Eleveld-Trancikova, D., et al. The DC-derived protein DC-STAMP influences differentiation of myeloid cells. *Leukemia* **22**, 455-459 (2008).
8. Eleveld-Trancikova, D., et al. The dendritic cell-derived protein DC-STAMP is highly conserved and localizes to the endoplasmic reticulum. *J Leukoc Biol* **77**, 337-343 (2005).
9. Hartgers, F.C., et al. Genomic organization, chromosomal localization, and 5' upstream region of the human DC-STAMP gene. *Immunogenetics* **53**, 145-149 (2001).
10. Hartgers, F.C., et al. DC-STAMP, a novel multimembrane-spanning molecule preferentially expressed by dendritic cells. *Eur J Immunol* **30**, 3585-3590 (2000).
11. Staeger, H., Brauchlin, A., Schoedon, G. & Schaffner, A. Two novel genes FIND and LIND differentially expressed in deactivated and Listeria-infected human macrophages. *Immunogenetics* **53**, 105-113 (2001).
12. Nomiya, H., et al. Identification of genes differentially expressed in osteoclast-like cells. *J Interferon Cytokine Res* **25**, 227-231 (2005).
13. Kukita, T., et al. RANKL-induced DC-STAMP is essential for osteoclastogenesis. *J Exp Med* **200**, 941-946 (2004).
14. Yagi, M., et al. DC-STAMP is essential for cell-cell fusion in osteoclasts and foreign body giant cells. *J Exp Med* **202**, 345-351 (2005).
15. Litovchick, L., Friedmann, E. & Shaltiel, S. A selective interaction between OS-9 and the carboxyl-terminal tail of meprin beta. *J Biol Chem* **277**, 34413-34423 (2002).
16. Friedmann, E., Salzberg, Y., Weinberger, A., Shaltiel, S. & Gerst, J.E. YOS9, the putative yeast homolog of a gene amplified in osteosarcomas, is involved in the endoplasmic reticulum (ER)-Golgi transport of GPI-anchored proteins. *J Biol Chem* **277**, 35274-35281 (2002).
17. Maniatis, T., Fritsch, E.F. & Sambrook, J. *Molecular cloning: a laboratory manual*, (Cold Spring Harbor Laboratory, Cold Spring Harbor, N.Y., 1982).
18. Hannon, G.J., Demetrick, D. & Beach, D. Isolation of the Rb-related p130 through its interaction with CDK2 and cyclins. *Genes Dev* **7**, 2378-2391 (1993).
19. Klebe, R.J., Harriss, J.V., Sharp, Z.D. & Douglas, M.G. A general method for polyethylene-glycol-induced genetic transformation of bacteria and yeast. *Gene* **25**, 333-341 (1983).
20. Gietz, R.D. & Woods, R.A. Transformation of yeast by lithium acetate/single-stranded carrier DNA/polyethylene glycol method. *Methods Enzymol* **350**, 87-96 (2002).
21. Beekman, J.M., Bakema, J.E., van de Winkel, J.G. & Leusen, J.H. Direct interaction between FcγRI (CD64) and periplakin controls receptor endocytosis and ligand binding capacity. *Proceedings of the National Academy of Sciences of the United States of America* **101**, 10392-10397 (2004).
22. Beekman, J.M., et al. Modulation of FcγRI (CD64) ligand binding by blocking peptides of periplakin. *J Biol Chem* **279**, 33875-33881 (2004).
23. Yoshimura, A., et al. Cutting edge: recognition of Gram-positive bacterial cell wall components by the innate immune system occurs via Toll-like receptor 2. *J Immunol* **163**, 1-5 (1999).
24. de Vries, I.J., et al. Phenotypical and functional characterization of clinical grade dendritic cells. *J Immunother* **25**, 429-438 (2002).
25. Ausubel, F.M. *Current protocols in molecular biology*, (Greene Publishing Associates ; J. Wiley, order fulfillment, Brooklyn, N. Y. Media, Pa., 1987).
26. Triantis, V., et al. Identification and characterization of DC-SCRIPT, a novel dendritic cell-expressed member of the zinc finger family of transcriptional regulators. *J Immunol* **176**, 1081-1089 (2006).

27. Litovchick, L., Chestukhin, A. & Shaltiel, S. The carboxyl-terminal tail of kinase splitting membranal proteinase/meprin beta is involved in its intracellular trafficking. *J Biol Chem* **273**, 29043-29051 (1998).
28. Baek, J.H., et al. OS-9 interacts with hypoxia-inducible factor 1alpha and prolyl hydroxylases to promote oxygen-dependent degradation of HIF-1alpha. *Mol Cell* **17**, 503-512 (2005).
29. Sitkovsky, M. & Lukashev, D. Regulation of immune cells by local-tissue oxygen tension: HIF1 alpha and adenosine receptors. *Nat Rev Immunol* **5**, 712-721 (2005).
30. Bernasconi, R., Pertel, T., Luban, J. & Molinari, M. A dual task for the Xbp1-responsive OS-9 variants in the mammalian ER: Inhibiting secretion of misfolded protein conformers and enhancing their disposal. *J Biol Chem* **283**, 16446-16454 (2008).
31. Christianson, J.C., Shaler, T.A., Tyler, R.E. & Kopito, R.R. OS-9 and GRP94 deliver mutant alpha1-antitrypsin to the Hrd1-SEL1L ubiquitin ligase complex for ERAD. *Nature cell biology* **10**, 272-282 (2008).
32. Wang, Y., et al. OS-9 regulates the transit and polyubiquitination of TRPV4 in the endoplasmic reticulum. *J Biol Chem* **282**, 36561-36570 (2007).

Supplementary figures

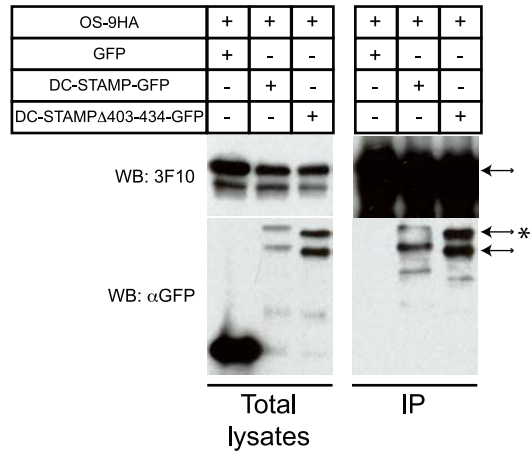


Figure S1. The DC-STAMP Δ 403-434 mutant also co-immunoprecipitates with OS9. DC-STAMP Δ 403-434 and OS9 were co-expressed in HEK293 cells as fusion proteins to GFP and HA, respectively, and immunoprecipitated with mouse monoclonal 12CA5 (against the HA tag). Total lysates and immunoprecipitations were subjected to Western blotting, and proteins were detected using antibodies specific for their tags (see Materials and methods for details). The arrows indicate expected products. The arrow with asteriks indicates DC-STAMP protein which is post-translationally modified.

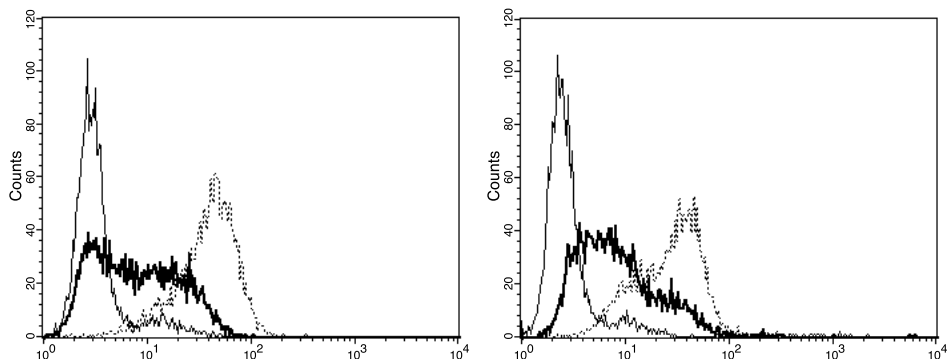


Figure S2. Example of successfully matured DC. Surface expression of the maturation markers CD80 and CD83 was assessed by means of FACS before and after stimulation of DC with LPS. Legend: thin line, isotype control; thick line, immature DC; dotted line, DC matured for 48 h with LPS.

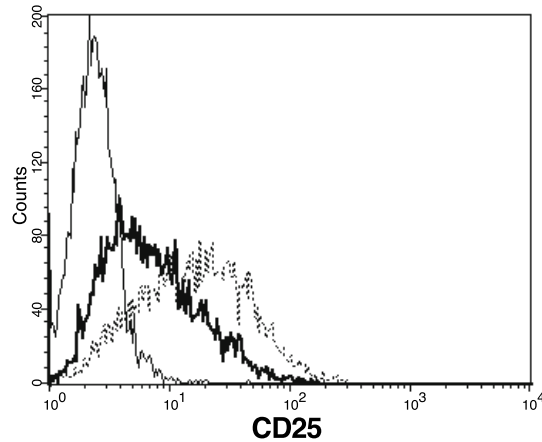


Figure S3. CHO cells stably expressing a TLR were stimulated with TLR ligand and $\text{NF}\kappa\text{B}$ -driven surface expression of reporter CD25 was assessed by means of FACS. Legend: thin line, isotype control; thick line, unstimulated cells; dotted line, cells stimulated with ligand for 7 h.

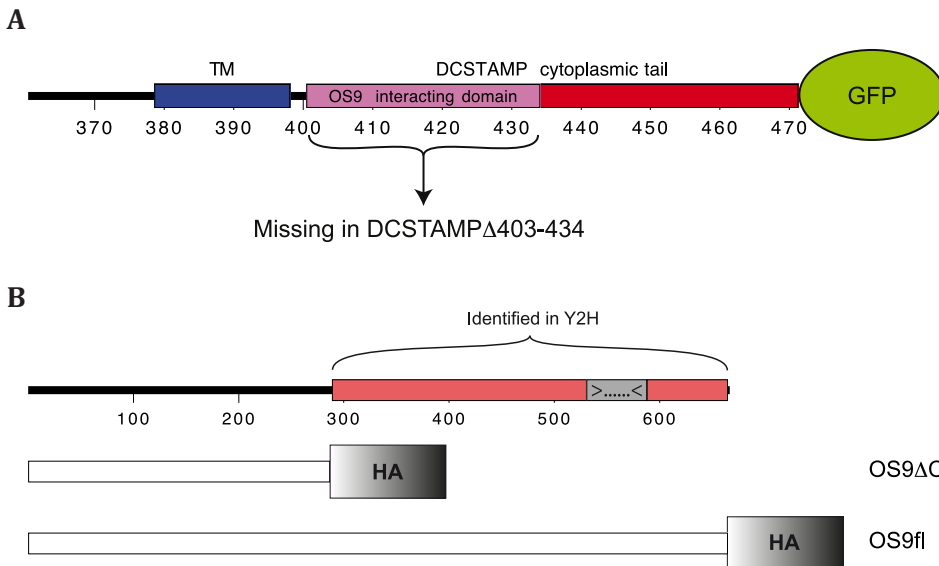


Figure S4. Maps of the mutants used in this study. **A)** A schematic representation of the carboxyterminus of a DC-STAMP mutant lacking the minimal OS9 binding domain as determined by yeast-2-hybrid analysis, corresponding to amino acids 403–434. The mutant is fused to GFP. **B)** Schematic overview of the OS9 variants used in this study. OS9fl: OS9 isoform 1; OS9 Δ C: OS9 deletion mutant lacking the part identified to interact with DC-STAMP in the yeast-2-hybrid screen. Both full-length and mutant OS9 were fused to an HA moiety.

CHAPTER 3

**DC-STAMP interacts with
ER-resident transcription factor
LUMAN which becomes activated
during DC maturation**

**Eleveld-Trancikova D, Sanecka A,
van Hout-Kuijjer MA, Looman MW, Hendriks IA,
Jansen BJ, Adema GJ**

Molecular Immunology (2010), 47(1963-1973)

Abstract

Dendritic cells (DC) are the professional antigen-presenting cells (APC) which efficiently prime the immune response or induce tolerance. We recently identified Dendritic Cell Specific TrAnsMembrane Protein (DC-STAMP), a novel 470 amino acid protein preferentially expressed by dendritic cells. Previously we demonstrated that DC-STAMP re-localizes towards the Golgi upon DC maturation. To identify proteins that interact with DC-STAMP, a yeast-2-hybrid analysis was performed. Here, we report a physically interacting partner of DC-STAMP in the endoplasmic reticulum (ER), called LUMAN (also known as CREB3 or LZIP). LUMAN was previously described as an ER-resident transcription factor with unknown function. It is activated in a process called regulated intramembrane proteolysis (RIP), which involves translocation to the Golgi and subsequent proteolytic cleavage. The proteolytically activated form of the protein then translocates to the nucleus. Our data indicate that DC-STAMP plays an important role in the modulation of LUMAN activation. Moreover, we demonstrate that LUMAN is endogenously expressed by DC and becomes activated by RIP upon DC maturation induced by various different stimuli. These data define LUMAN/DC-STAMP as a novel regulatory circuit in DC.

Introduction

Dendritic cells (DC) are the professional antigen-presenting cells of the immune system. They instruct and control B and T lymphocytes, but also activate natural killer (NK) cells and can produce large amounts of interferon, thus providing a link between the adaptive and innate immune system. Inflammatory mediators and Toll-like-receptors (TLR) promote DC activation/maturation resulting in DC, well-equipped to initiate adaptive immunity^{1,2}. In the presence of immune inhibitory signals, however, immature or semi-mature DCs induce immune tolerance via the induction of suppressive regulatory T cells (Treg)^{3,4}. How these external signals translate into the genetic programming of the DC is largely unknown. This genetic reprogramming process takes place in a relative short time frame (from several minutes to 24 h) and does not require cell division. Multiple transcription factors, notably NF κ B, are already present in an inactive state in immature DC⁵. The external signals that DC receive determine the activation of pathways to these “ready to go” transcription factors ensuring a rapid, well-controlled response by the DC.

To fully exploit DC in a clinical setting, a molecular understanding of DC immunobiology is essential. Several novel molecules preferentially expressed by DC have been isolated and functionally characterized. We have identified a novel DC-specific transmembrane protein DC-STAMP that is tightly regulated during DC activation^{6,7}. DC-STAMP is a multimembrane spanning protein localizing to the endoplasmic reticulum (ER)⁸. It was implicated in myeloid lineage differentiation⁹, in osteoclast fusion¹⁰ and very recently in the maintenance of immune tolerance through DC¹¹. The function of DC-STAMP at the molecular level is unknown. A yeast-2-hybrid analysis was performed to discover its interacting proteins. Previously, we identified and characterized OS9 as a *bona fide* DC-STAMP binding partner associated with the ER¹². We showed that upon DC maturation DC-STAMP translocates to the Golgi apparatus and this re-localization is influenced by OS9. A second interacting partner of DC-STAMP identified by yeast-2-hybrid screening was LUMAN.

LUMAN (Gene Symbol: CREB3; also known as LZIP) is a basic leucine zipper transcription factor of the CREB/ATF gene family. It was first identified as a counterpart of the herpes simplex virus transcriptional activator VP16 that binds to the host cell factor (HCF) binding protein¹³. Although LUMAN is ubiquitously expressed at the mRNA level, endogenous LUMAN protein has been found only in the trigeminal ganglionic neurons and recently also in monocytes^{14,15}. In ganglionic neurons, and in transfected cell lines, LUMAN is found primarily associated with the

ER¹⁴. Raggio *et al.* (2002) showed that LUMAN undergoes a proteolytic processing event known as regulated intramembrane proteolysis (RIP)¹⁶, a process of rapid protein activation without a need for cell division. Regulated intramembrane proteolysis (RIP) was first described for sterol regulatory element-binding proteins (SREBP) and later for activating transcription factor 6 (ATF6), two well-characterized ER-associated bZIP transcription factors^{17,18}. In the steady state, transcription factors reside in ER, but upon the stimulation (depletion of sterols for SREBP, ER stress for ATF6), these transcription factors leave the ER and proceed to the Golgi where they are subsequently cleaved by two specific proteases releasing the cytoplasmic aminoterminal part of the transcription factor. This active form of the transcription factor translocates to the nucleus to drive transcription of target genes^{17,18}. LUMAN is a type II transmembrane protein and like ATF6, all known functional domains involved in transcription are located in the aminoterminal region and hence, on the cytoplasmic side of the ER membrane¹⁶. The relocalization to different compartments can be mimicked using Brefeldin A (BfA), a chemical agent able to fuse the ER and Golgi and thereby making Golgi-resident proteases accessible without an additional stimulus^{16,19}.

In this study we characterized LUMAN as a binding partner of DC-STAMP in dendritic cells. We demonstrate that LUMAN is expressed at the protein level in DCs. Furthermore, for the first time we show LUMAN activation upon DC maturation, as it is proteolytically activated and translocates to the nucleus. Moreover, we show that the physical interaction between DC-STAMP and LUMAN influences proteolysis of LUMAN upon BfA treatment. Our data strongly suggest that activation of LUMAN is controlled by DC-STAMP, which implicates a novel pathway in modulation of DC activation.

Materials and methods

Plasmids, adenoviral vectors and cloning

The adenoviral constructs encoding DC-STAMP fused to a GFP tag and plasmids encoding DC-STAMP fused to an HA tag were described elsewhere⁸. The plasmid encoding DC-STAMP fused to the RFP protein was created by replacing the EGFP moiety of the pEGFP-N3 backbone with RFP. Human cDNA of LUMAN was amplified with specific primers and cloned in frame into the pEYFP-C1 vector (Clontech, Mountain View, CA) and FLAG-pcDNA3 vector (kind gift of R.A.J. Janssen, Galadeno, Leiden, the Netherlands). To create the LUMAN-IRES-GFP plasmid, the IRES consensus sequence was inserted upstream of the GFP moiety of pEGFP-N3 (Clontech, Mountain View, CA), whereas the coding sequence of LUMAN, including the stop codon, was cloned upstream of IRES-GFP. The coding sequences of LUMAN dp (aa 1–144) and LUMAN dn (aa145–372) were cloned in frame into the pECFP-N1 vector (Clontech, Mountain View, CA). The OS9-HA construct was described previously¹². All constructs were verified for integrity and correct insertion by means of sequencing at the sequencing facility at the Department of Human Genetics, Radboud University Nijmegen Medical Centre. For the generation of LUMAN-GST fusion proteins in bacteria for the immunization of rabbits, the cDNA sequence corresponding to the aminoterminal 151 amino acids of LUMAN was inserted in frame with the carboxyterminus of GST in pRP265 (derivative vector from pGEX-2T; kind gift of F. N. van Leeuwen, UMCN Nijmegen) Generally, plasmid DNA was isolated from *E. coli* DH5 α or DH10 β bacteria using the Endofree Plasmid Maxi Kit (Qiagen, Venlo, the Netherlands).

Yeast-2-hybrid analysis

Plasmids pGADGH and pGBT9 were used for yeast-2-hybrid analysis (Clontech, Mountain View, CA). The cDNA library used in the yeast-2-hybrid analysis was constructed as described previously¹². The bait, corresponding to amino acids 403–470 of the cytoplasmic tail of DC-STAMP, was cloned into pGBT9. The library was amplified in *E. coli* (strain DH10 β , Invitrogen, Carlsbad, CA) and analysis was performed as described previously¹².

Cell culture, transfections, transductions and generation of human DC

Human embryonic kidney HEK293 cells were cultured in DMEM (GibcoBRL Life Technologies), supplemented with 10% heat-inactivated FCS (GibcoBRL Life Technologies); 10 nM HEPES pH7.7 (Boehringer Mannheim GmbH, Germany); 0.1 mM MEM non essential amino acids and 100 units/ml Antibiotic-Antimycotic (both GibcoBRL Life Technologies) at 37°C in 5% CO₂. HEK293 cells were transfected with LipofectAMINE (GibcoBRL Life Technologies) as described elsewhere⁸.

HL60 and THP1 cell lines were cultured in RPMI1640 (GibcoBRL Life Technologies), supplemented with 10% heat-inactivated FCS (GibcoBRL Life Technologies) and 100 units/ml Antibiotic-Antimycotic (both GibcoBRL Life Technologies) at 37°C in 5% CO₂. Hep3B cells were maintained in DMEM (GibcoBRL Life Technologies), supplemented with 10% heat-inactivated FCS (GibcoBRL Life Technologies) and 100 units/ml Antibiotic-Antimycotic (both GibcoBRL Life Technologies) at 37°C in 5% CO₂.

Chinese hamster ovary cells (CHO) and CHO cells stably transfected with the TLR2 or TLR4

(CHO/TLR) were cultured as described before²⁰. This clonal line has been co-transfected with CD14 and an NF κ B-dependent reporter plasmid that drives the expression of surface CD25 Ag in response to TLR activation. CHO cells were transfected with LipofectAMINE (GibcoBRL Life Technologies) as described elsewhere¹².

Human monocyte-derived DC were generated using GM-CSF and IL-4, and their purity and maturation were assessed by means of FACS analysis as described previously²¹⁻²⁴. Adenotransduction of DC was performed as described elsewhere⁸.

RNA isolation and quantitative PCR

Total RNA for RT-PCR was isolated from cells using TriZOL (Invitrogen, Carlsbad, CA). RNA concentration was determined spectrophotometrically, and quality was assessed by means of conventional agarose gel electrophoresis. Reverse transcription using random hexamers was essentially done as described elsewhere²⁵.

Relative mRNA levels were determined using the ABI PRISM 7000 Sequence Detection System and SYBR Green Reagent (Applied Biosystems). Copy DNA was synthesized from 2.0 μ g of total RNA using Moloney murine leukemia virus reverse transcriptase (MMLV-RT; Invitrogen Corp.). A quantitative PCR reaction mix contained 1 x SYBR Green Master Mix, 300 nM of each forward and reverse primer, and 25 ng cDNA in a total volume of 25 μ l. The following primers were used: hLUMAN forward (5'-ACCCAGATGACTCCACAGCAT-3'), hLUMAN reverse (5'-GAATAAGCCCCTCTTCTCCAA-3'), hDC-STAMP forward (5'TTCAGTGGATTTATGGCCTTGC-3'), hDC-STAMP reverse (5'-GCTGTCAATTTAGCTGTGCCTC-3'), hPBGD (porphobilinogen deaminase) forward (5'-GGCAATGCGGCTGCAA-3'), hPBGD reverse (5'-GGGTACCCACGCGAATCAC-3') (all from Sigma-Aldrich St. Louis, MO). Mean relative mRNA expression from 3 replicate measurements was calculated using ABI PRISM 7000 SDS software (version 1.0; Applied Biosystems). Expression per sample was normalized to the Ct value of PBGD, and then normalized to the expression in monocytes, which was set to 1.

Production of anti-LUMAN antibodies

GST-LUMAN fusion protein was produced in BL21 *E. coli* bacteria and purified using glutathion sepharose beads essentially using standard protocols²⁵. The institutional Ethics Committee approved the immunization of rabbits for Animal Experimentation and in accordance with local and national guidelines. Rabbits were immunized 4 times with purified GST-LUMAN. The first intracutaneous immunization was performed with complete Freund's adjuvant, and subsequent subcutaneous immunizations were performed with incomplete Freund's adjuvant. When sera could detect transiently expressed LUMAN in HEK293 lysates in a Western blot assay, rabbits were sacrificed and all their blood collected. Polyclonal rabbit IgG was isolated from serum by depleting antibacterial and anti-GST IgG with CNBr-activated sepharose beads (GE Healthsciences Bio-Sciences, Uppsala, Sweden) coated with bacterial GST lysate, essentially as described by the manufacturer. Polyclonal anti-LUMAN IgG was then isolated using Fast Flow Protein G beads, eluted with 900 μ l 200 mM glycine pH 2.5; 150 mM NaCl, 1 mM EDTA and neutralized in 100 μ l 1M Tris pH 8.0. The antibody concentration was measured using the BCA kit (Pierce, Rockford, IL), and positive fractions were stored at 4°C.

Protein analysis and immunoprecipitation

Lysates were prepared in SDS lysis buffer as described elsewhere²⁵. For PAGE gel electrophoresis, reducing sample buffer (62.5 mM Tris/HCl pH 6.8, 25% (v/v) glycerol, 2% (w/v) sodium dodecyl sulfate, 0.01% (w/v) bromophenol blue, 5% (v/v) β-mercaptoethanol) was added 1:1 to a lysate equivalent to ~200 000 cells. Samples were subjected to polyacrylamide gel electrophoresis using the MiniProtean system (BioRad, Hercules, CA) and further processed for Western blot analysis. After blocking, membranes were incubated with one of the following antibodies: mouse anti-GFP (0.04 μg/ml; a mixture of mouse monoclonals, 7.1 and 13.1; Roche Applied Science, Almere, the Netherlands), mouse anti-FLAG (5 μg/ml; Sigma-Aldrich; St. Louis, MO), rat anti-HA (3F10; Roche Applied Science BV, Almere, the Netherlands), rabbit anti-LUMAN (1:100), or mouse anti β-actin (1:10 000; Sigma-Aldrich, St. Louis, MO). The membranes were washed and incubated with a secondary HRP conjugated goat anti-mouse IgG (H+L) Ab (0.4 μg/ml, DAKO, Glostrup, Denmark) or swine anti-rabbit Ab (0.4 μg/ml, Dako, Glostrup, Denmark). Immunoreactive bands were visualized using the ECL kit (GE Healthsciences Bio-Sciences, Uppsala, Sweden) on Kodak Scientific Imaging Films. If necessary, membranes were stripped in 0.2 M glycine/1% (w/v) sodium dodecyl sulfate, pH 2.5, blocked, re-probed and processed as described above. When indicated, the goat anti-rabbit AlexaFluor 680 (0.1 mg/ml; Molecular Probes, Eugene, OR) and goat anti-mouse IRDye800CW (0.1 μg/ml; LI-COR Biosciences, Lincoln, NE) were used as a secondary antibody followed by analysis with the LI-COR Odyssey (LI-COR Biosciences, Lincoln, NE; 169 μm resolution, 3–7 sensitivity). Integrated intensities were analyzed using Excel (Microsoft Corp., Redmond, WA).

In the case of immunoprecipitations, HEK293 cells were transiently transfected GFP, DC-STAMP-GFP and FLAG-LUMAN as described above, and after 48 h lysed for ~1 h in 1.5 ml lysis buffer containing 50 mM HEPES pH 8.0, 5 mM, MgCl₂, 150 mM NaCl, 1 mM PMSF, 20 mg/ml aprotinin, 10 mg/ml leupeptin and 1% Brij-97. Insoluble material was removed by centrifugation. After pre-clear with bare beads and beads coupled to rabbit IgG, the immunoprecipitation was performed with beads coupled to GFP (rabbit polyclonal; a kind gift of dr FJM Kupveld, UMCN Nijmegen). All steps were performed at 4°C. Supernatant was saved and stored at –80°C and beads were washed 4 times with lysis buffer before being transferred to a clean 1.5 ml tube for a final wash. Beads were stored at –80°C until further processing.

IF staining and Confocal laser scanning microscopy

For immunofluorescent staining, HEK293 cells were seeded on 8-chamber slides (NUNC) coated with fibronectin (20 μg/ml, Roche Applied Science BV, Almere, the Netherlands). Immature and mature DC were seeded on glass coverslips coated with poly-L-lysine (100 μg/ml Sigma-Aldrich; St. Louis, MO). Where indicated, cells were treated with BFA (10 mg/ml, Sigma-Aldrich; St. Louis, MO) for a maximum of 6 h. Furthermore, cells were fixed with 1% PFA for 15 minutes, permeabilized by methanol (–20°C; 1 min), and blocked with 3% BSA (Calbiochem, San Diego, CA) in PBS. The following antibodies were used: mouse anti-PDI (Protein Disulfide Isomerase, 1:100; MA3-019, ABR); rabbit anti-LUMAN (1:100). As isotype controls purified IgG2a (Becton Dickinson) or pre-bleed non immune serum of the immu-

nized rabbit were used. As secondary antibodies, Texas Red-conjugated goat anti-mouse IgG, (5 µg/ml; H+L, Molecular Probes; Eugene, OR), Alexa488-, Alexa568- or Alexa 647-conjugated goat anti-mouse IgG and goat anti-rabbit IgG (Invitrogen Corp.) were used where appropriate. Slides were mounted with Vectashield or Vectashield-PI (Vector Laboratories, Burlingame, CA) and analysed by CLSM using Biorad MRC1024 or Olympus FV100 at the Microscopic Imaging Facility of the Department of Cell Biology, Nijmegen Centre for Molecular Life Sciences, Radboud University Nijmegen Medical Centre, Nijmegen, the Netherlands. The data were analyzed using Olympus FV1000 and ImageJ software.

Results

LUMAN is a binding partner of DC-STAMP

To gain insight in the molecular pathway involving DC-STAMP, a yeast-2-hybrid screening was performed to identify DC-STAMP-interacting proteins. As DC-STAMP is preferentially expressed in DC, we first constructed a yeast-2-hybrid library of a mixture of cDNAs isolated from immature and mature DC with a complexity of 10^6 independent clones. This library was screened using the 74 amino-acid carboxyterminal cytoplasmic tail of DC-STAMP as bait. Ten out of 58 clones represented one single gene, LUMAN (CREB3, LZIP)²⁶. LUMAN is a 372 amino acids long protein that belongs to the CREB/ATF family of transcription factors. As shown in Fig. 1A (and schematically in Fig. 3A), two independent clones of different lengths specifically interacted with the DC-STAMP bait. No interaction was observed with the empty bait vector.

To confirm the specific binding of LUMAN to DC-STAMP, HEK293 cells were transfected with cDNAs encoding DC-STAMP-GFP and FLAG-LUMAN fusion proteins. Cells co-transfected with FLAG-LUMAN and GFP served as a control. Western blot analysis of total lysates showed that DC-STAMP-GFP, GFP and FLAG-LUMAN are expressed in single and double transfectants (Fig. 1B). DC-STAMP-GFP and GFP were both efficiently immunoprecipitated from total lysates using a mixture of 2 monoclonal GFP antibodies. Subsequent Western blot analysis revealed that Flag-LUMAN is specifically present in the DC-STAMP-GFP immunoprecipitated fraction. No LUMAN was co-immunoprecipitated with GFP alone (Fig. 1B). Moreover, the observation that LUMAN is not only co-immunoprecipitated with DC-STAMP, but also with the previously identified DC-STAMP-interacting protein OS9, further substantiates these findings (Fig. S1). They also suggest that DC-STAMP, LUMAN and OS9 are part of the same complex.

Previously we described that DC-STAMP localizes to the endoplasmic reticulum⁸. Raggio *et al.* reported ER-localization of LUMAN in transfected COS cells¹⁶. To confirm and extend these findings, HEK293 cells were transfected with DC-STAMP-RFP and YFP-LUMAN constructs and stained for the ER-resident protein PDI. As shown in Supplementary Fig. S2A, both DC-STAMP-RFP and YFP-LUMAN show clear co-localization with PDI. In addition, a clear co-localization of DC-STAMP-RFP and YFP-LUMAN is observed upon their co-expression in cell lines of different origin (HEK293 and CHO; Fig. 2). Since co-localization studies of LUMAN and endogenous

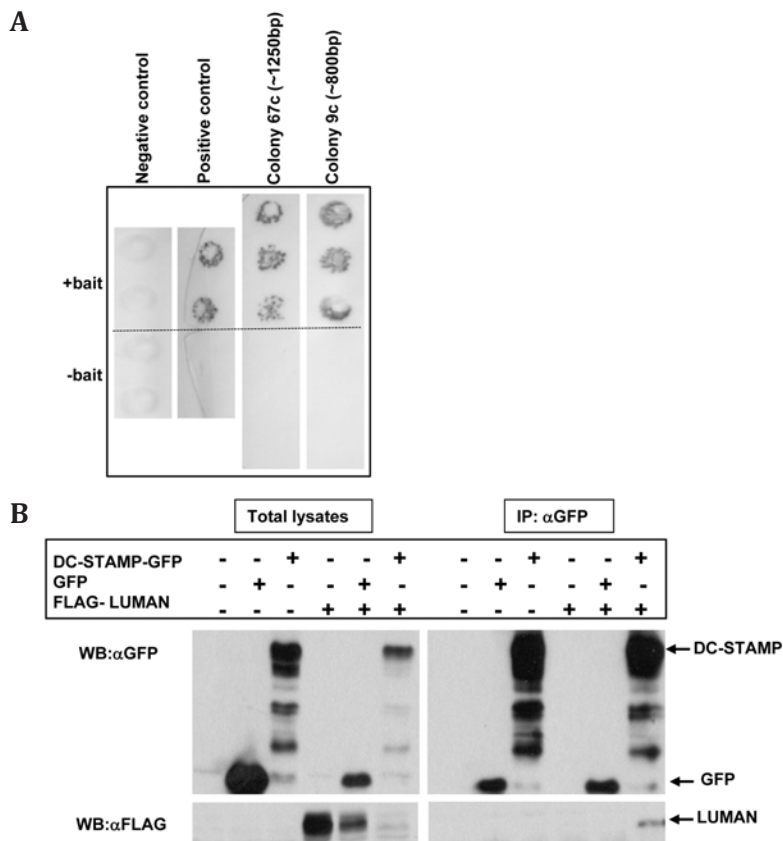


Figure 1. LUMAN is a DC-STAMP-interacting protein. **A)** Two LUMAN clones of different length interact with the DC-STAMP bait in a Y-2-H analysis. A cDNA library of immature and mature DC was screened with the cytoplasmic tail of DC-STAMP as bait. **B)** LUMAN co-immunoprecipitates with DC-STAMP in HEK293 cells. HEK293 cells were transfected with constructs encoding DC-STAMP-GFP or GFP and FLAG-LUMAN, where GFP served as a control. The immunoprecipitation was performed using the polyclonal rabbit αGFP antibody, whereas GFP was visualized with a mixture of mouse monoclonal antibodies. To visualize LUMAN, Western blots were stained with αFLAG antibody. As reference total lysates were included.

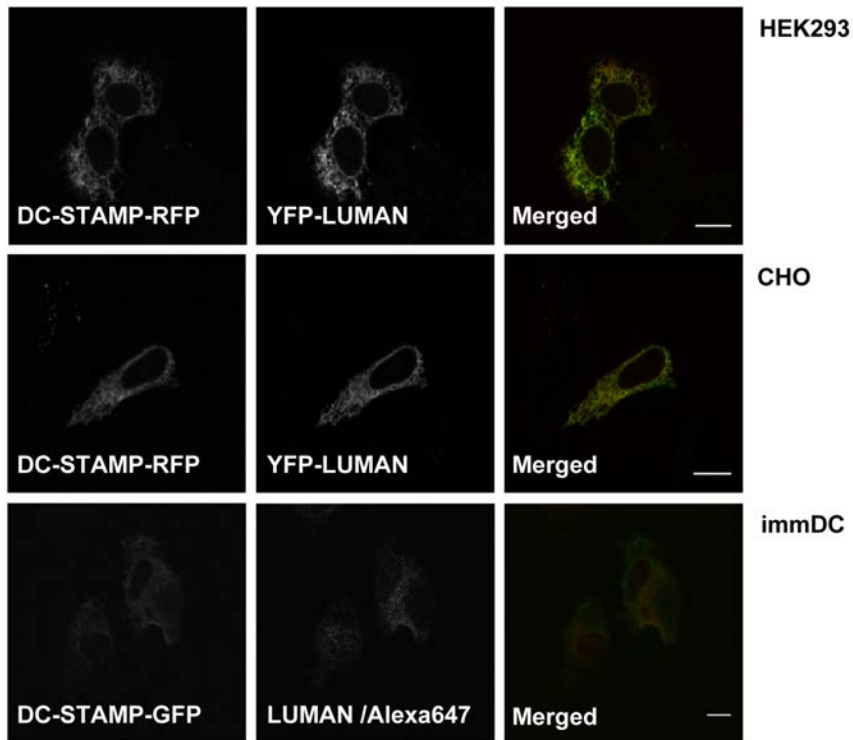


Figure 2. Co-localization of DC-STAMP and LUMAN. Two different cell lines (HEK293 and CHO) were co-transfected with DC-STAMP-RFP and YFP-LUMAN and co-localization was analyzed by CLSM. Immature DC were transduced with an adenoviral construct encoding DC-STAMP-GFP and stained with the polyclonal anti-LUMAN serum. Scale bar: 10 μ m.

DC-STAMP in DC are hampered by the absence of suitable antibodies against DC-STAMP, DC were transduced with an adenoviral construct encoding DC-STAMP-GFP⁸ and stained with the polyclonal anti-LUMAN serum. As shown in Fig. 2 (lower row of pictures), in immature DC DC-STAMP-GFP shows a distribution reminiscent of the ER, as does endogenous LUMAN. Collectively, these observations fully support the yeast-2-hybrid data and provide evidence that DC-STAMP and LUMAN are binding partners that are present in the ER compartment of the cell.

Mapping of the binding regions

To identify the minimal part of LUMAN that is able to bind to DC-STAMP, a series of LUMAN deletion mutants was made and tested in the yeast-2-hybrid assay. The longest LUMAN clone interacting with DC-STAMP identified in the initial screen spans amino acids 62–372 (Fig. 3A). The minimal amino-acid sequence of

LUMAN needed for binding to the cytoplasmic tail of DC-STAMP is located between amino acid 98 and 276. This region of LUMAN contains the DNA binding domain, the leucine zipper motif and extends approximately 30 amino acids beyond the



Figure 3. Mapping of the interaction domains of DC-STAMP and LUMAN by means of yeast-2-hybrid analysis. **A)** Mapping of the binding site in LUMAN using different deletion mutants cloned in the prey vector. The minimal region in LUMAN needed for the interaction with the DC-STAMP cytoplasmic tail spans amino acids 98–276. Both originally identified clones (9c and 67c) contain this region. **B)** Mapping of the binding site in DC-STAMP by means of yeast-2-hybrid analysis. The minimal region of DC-STAMP which interacts with LUMAN spans amino acids 430–456 of the cytoplasmic tail of DC-STAMP. Note that a GFP tag at the C-terminus of DC-STAMP has no influence on the interaction with LUMAN.

transmembrane domain¹⁴. Based on this we conclude that cytosolic part of LUMAN interacts physically with the cytosolic carboxyterminus of DC-STAMP. Intriguingly, the luminal part of LUMAN is also necessary, possibly establishing conformational requirements for this interaction.

To map the DC-STAMP binding site, a series of DC-STAMP cytoplasmic-tail deletion mutants was generated and tested in the yeast-2-hybrid system as well. The minimal sequence that is required for LUMAN binding comprises amino acids 430–456 of the DC-STAMP cytoplasmic tail (Fig. 3B). We note that fusion of GFP to the C-terminus of the cytoplasmic-tail did not affect the interaction in the yeast-2-hybrid experiments (Fig. 3B). The observed binding to amino acids 430–456 was as efficient as the entire DC-STAMP cytoplasmic bait. Interestingly, the membrane proximal amino acids 403–434 in the cytoplasmic tail of DC-STAMP do not appear to contribute to LUMAN binding. These are exactly the 30 amino acids that have previously been identified as the binding site for the DC-STAMP interacting protein OS9 (Fig. 3B and ¹²). Collectively, these data show that LUMAN binds to the carboxyterminal part of DC-STAMP proximal to but not overlapping with the OS9 binding site in DC-STAMP. Furthermore, our data indicate that the amino acid sequence of LUMAN required for binding to DC-STAMP involves the central part of the sequence including its transmembrane region.

Elevated LUMAN protein expression in DC

Next, we determined LUMAN mRNA levels during DC differentiation and maturation by quantitative RT-PCR. A panel of cell lines and freshly isolated leukocyte subsets were included as controls and DC-STAMP mRNA levels were analyzed in parallel. As shown in Fig. 4A LUMAN mRNA is expressed at approximately the same level in all cell lines, freshly isolated leukocytes, and different stages of DC differentiation/maturation. These data are in line with previous studies demonstrating that LUMAN mRNA is ubiquitously expressed in a wide variety of different cell types²⁶. In contrast, DC-STAMP mRNA is essentially absent in the cell lines, monocytes and lymphocytes (Fig. 4B). Upon differentiation of monocytes towards immature DC DC-STAMP mRNA levels are increased 500-fold and are strongly down-regulated upon DC maturation (Figure 4B and ⁶). These data demonstrate that LUMAN mRNA is ubiquitously expressed in DC as well as other cell lines examined. Immature DC are unique in that they express high levels of the DC-STAMP mRNA as well as its binding partners LUMAN (Fig. 4) and OS9¹².

Although LUMAN mRNA is ubiquitously expressed, endogenous LUMAN protein has so far only been found in trigeminal ganglionic neurons and monocytes using

immunohistochemistry^{14,15}. To assess LUMAN protein expression in DC, a rabbit polyclonal antibody was raised against the aminoterminal 220 amino acids of LUMAN. The anti-LUMAN antibodies specifically detected a doublet of 65 kDa and 60 kDa in HEK293 cells transfected with a LUMAN-IRES-GFP construct. The size of

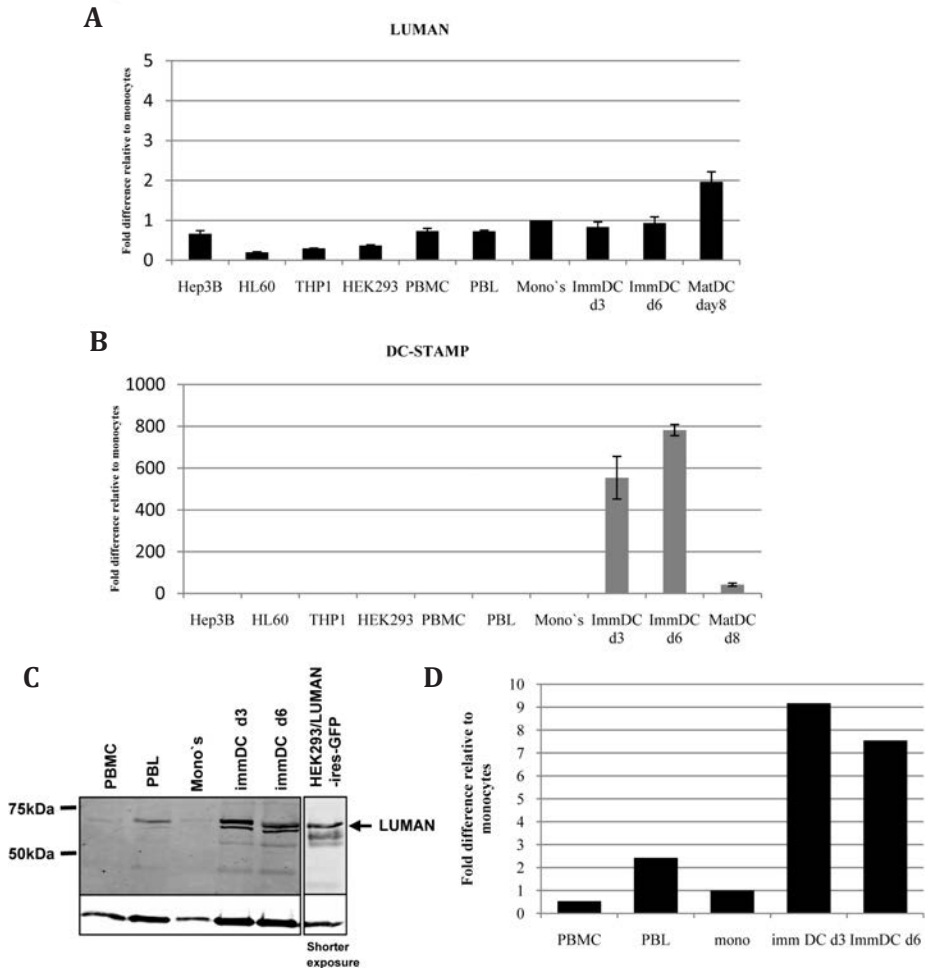


Figure 4. Expression of LUMAN at the mRNA and protein level. Messenger RNA levels of LUMAN **A)** and DC-STAMP **B)** in different human cell lines, freshly isolated leukocytes and DC during differentiation. The expression in monocytes is set to 1. **C)** Protein expression of LUMAN during DC differentiation analyzed by Western blot analysis using a rabbit polyclonal antibody against the aminoterminal part of LUMAN. HEK293 cells transfected with a LUMAN-IRES-GFP construct were included as a control. Due to overexpression of the transfected protein a shorter exposure of the last lane of the Western blot is shown. **D)** Quantitative analysis of LUMAN expression in various cell types. Integrated intensity of full length LUMAN was normalized to the integrated intensity of β -actin in each lane.

these protein bands nicely fit previously published data on size of LUMAN protein in transfected COS cell line, with the lower band representing the non-glycosylated form of LUMAN¹⁶. Next, total cell lysates from PBMC, PBL, monocytes, and days 3 and 6 immature monocyte-derived DC were subjected to Western blot analysis and data were quantified relative to β -actin. As shown in Fig. 4C, LUMAN is expressed in freshly isolated PBMC, PBL and monocytes at low levels. Day 3 monocyte-derived DC express 8-fold higher levels of LUMAN relative to monocytes and this increased expression is sustained in day 6 immature DC (Fig. 4C and D). The larger product of the endogenous LUMAN doublet has the same molecular weight as observed in LUMAN-transfected 293 cells and likely represents glycosylated LUMAN protein. The electrophoretic mobility of the smaller protein is somewhat higher in the transfected cells than in DC, which may be a reflection of cell type-specific glycosylation differences. We conclude that although LUMAN mRNA is expressed to similar extent in different immune as well as non-immune cells, LUMAN protein expression is increased up to 8-fold in immature DC relative to monocytes.

LUMAN undergoes RIP and nuclear translocation upon DC maturation

The transcription factor LUMAN is a type II transmembrane protein that localizes to the ER. LUMAN has been shown to translocate from the ER to the Golgi where it undergoes a proteolytic processing event known as Regulated Intramembrane Proteolysis (RIP)¹⁶. As a result, the aminoterminal part of LUMAN carrying the transcription factor moiety is released from the carboxyterminal part and translocates to the nucleus. The physiological signals that activate RIP of LUMAN are not known. RIP can be mimicked by Brefeldin A (BfA), an agent inducing fusion of the ER and Golgi compartments¹⁹. To study the localization of endogenously expressed LUMAN in DC, immature DC were cultured in the presence or absence of BfA, stained with the polyclonal anti-LUMAN antibody, and analyzed by CLSM. HEK293 cells transfected with FLAG-LUMAN were included as a control. As shown in Fig. 5A, staining of immature DC with the polyclonal LUMAN serum resulted in a cytoplasmic staining pattern, similar to the ER staining pattern in the FLAG-LUMAN expressing control cells. Double staining of immature DC for LUMAN and the ER marker PDI confirmed the ER localization of LUMAN in immature DC (Fig. S2A; upper row). LUMAN staining of BfA treated immature DC or FLAG-LUMAN transfected control cells resulted in a clear shift in the localization of LUMAN from the cytoplasm to the nucleus. The nuclear localization of LUMAN was confirmed by co-staining of the BfA-treated immature DC with the nuclear marker PI. These data

strongly suggest that the machinery responsible for RIP of LUMAN is present and can be activated in DC.

Previously, we showed that in DC-STAMP-GFP-transduced immature DC, DC-STAMP localizes to the ER⁸ and translocates towards the Golgi compartment upon DC maturation using the TLR4 ligand LPS¹². Unfortunately, co-localization studies of LUMAN and DC-STAMP in DC are hampered by the absence of antibodies against DC-STAMP. To study the localization of LUMAN in DC at different conditions, immature DC and LPS induced mature DC were stained for LUMAN. Strikingly, while in immature DC LUMAN is predominantly present in the ER, in mature DC the endogenous LUMAN protein is mainly localized in the nucleus (Fig. 5B and Fig. S2B, lower row). RIP has been shown to release a 37–40 kDa protein consisting of the aminoterminal part of LUMAN that is able to enter the nucleus¹⁶. To determine whether the nuclear localization observed for LUMAN in mature DC is accompanied by RIP, Western blot analysis was performed on immature and mature DC. As shown in Fig. 5B, a protein of 37–40 kDa reactive with the anti-LUMAN serum is present in mature but not immature DC and coincides with its nuclear localization. These data indicate that LPS induced DC maturation results in RIP of LUMAN, resulting in the accumulation of the aminoterminal part of LUMAN in the nucleus of mature DC.

To assess the kinetics of LUMAN activation a time course experiment was performed using BfA and LPS stimulations of DC. As a control HEK293 cells were transfected with LUMAN-IRES-GFP construct and stimulated with BfA for 6 h, which resulted in a 37 kDa product reactive with anti-LUMAN serum. Interestingly, in DCs the cleaved aminoterminal part of LUMAN protein with a size of 40 kDa appears from 16 h on after LPS stimulation (Fig. 5C). Additionally, the weak product of 37 kDa is visible as a result of BfA treatment of DC after 8 hours (Fig. 5C, indicated by asterisk). We conclude that RIP of LUMAN is a late event upon the LPS-induced DC maturation and is more efficient than BfA treatment. Moreover, activation of LUMAN can be a general event since the 40 kDa product of LUMAN was observed upon different types of stimulation usually leading only to immune activation (Fig. 5D and Fig. S3).

The presence of DC-STAMP inhibits proteolysis of LUMAN

The data so far show that DC are unique among LUMAN expressing cells in that they co-express its interacting partner DC-STAMP. To elucidate the role of DC-STAMP in this complex process, we determined whether the presence or absence of DC-STAMP affects BfA induced RIP of LUMAN in a CHO cell line model described previously¹². Cells were transfected with YFP-LUMAN and either DC-STAMP-HA or a control construct encoding Dectin1-HA. Twenty-four hours after transfection

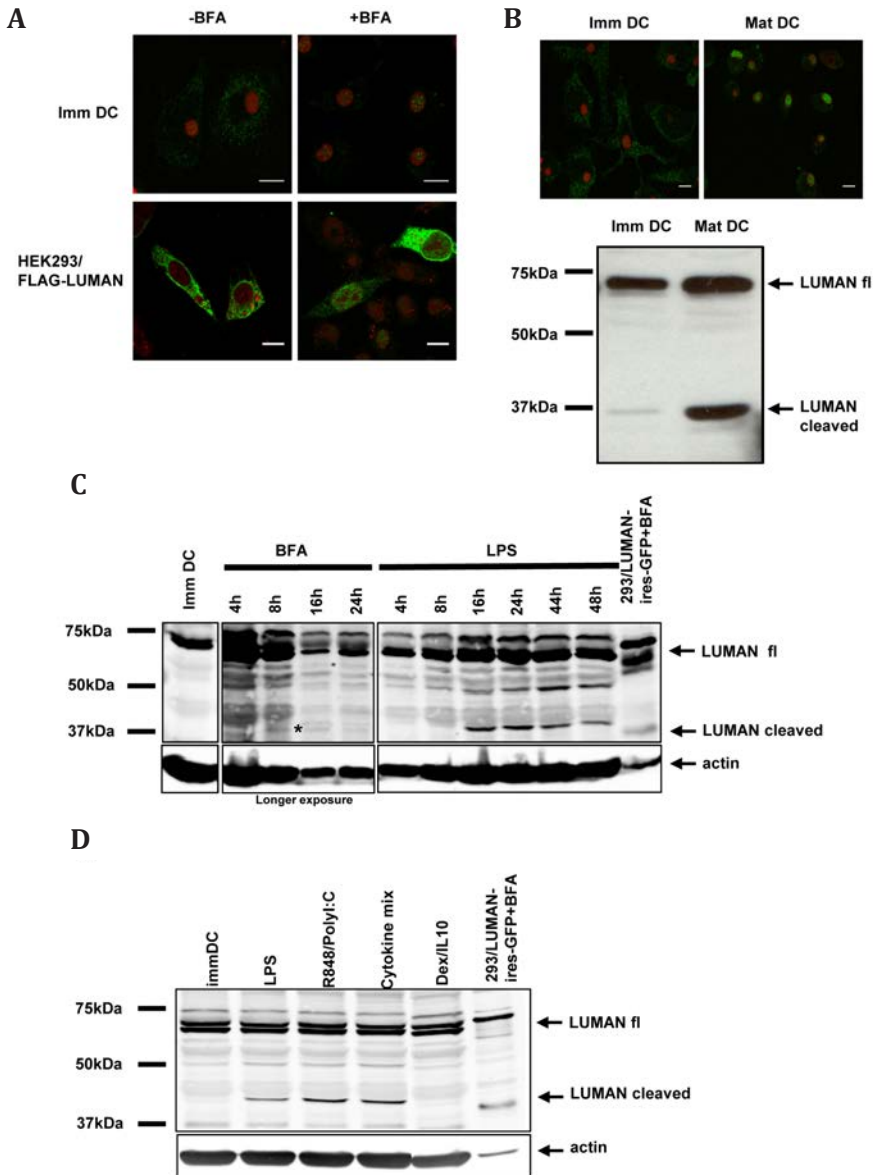


Figure 5. RIP activation of LUMAN. **A**) Analysis of LUMAN expression in untreated (left column) and Bfa-treated (right column, 6 h) immature DC and HEK293 cells transfected with FLAG-LUMAN. LUMAN is visualized using the polyclonal antibody against its aminoterminal part, followed by a secondary antibody coupled to Alexa488 (green). Nuclei are stained with PI (red). Scale bar: 10 μ m. **B**) Endogenous expression of LUMAN in immature and mature DC analyzed by CLSM (upper row) and Western blot (lower picture). In both cases the staining was performed using the polyclonal antibody against the aminoterminal part of LUMAN followed by secondary antibody coupled to Alexa488 (green) for CLSM or to HRP and visualized by ECL for Western blot. Nuclei are stained with PI (red). Scale bar: 10 μ m. **C**) Kinetics of LUMAN activation assessed by Western blot. Immature DC were treated with BFA (10 μ g/ml) or stimulated with LPS (1 μ g/

ml) and subjected to Western blot analysis. LUMAN was visualized using a secondary antibody coupled to Alexa680 and analyzed with Odyssey software. HEK293/ LUMAN-IRES-GFP transfected cells treated with BFA for 6 h were included as a control. β -actin was used as a loading control. Due to lower expression of the cleaved product of LUMAN in BFA-treated samples the corresponding part of the Western blot is shown after longer exposure. **D)** LUMAN activation in differently matured DC. DC were matured by LPS (1 $\mu\text{g/ml}$), mix of TLR7/8 and TLR3 ligands (R848 0.4 $\mu\text{g/ml}$, Poly I:C 20 $\mu\text{g/ml}$), cytokine mix (IL1 β , IL6, TNF α and PGE2; all 1 $\mu\text{g/ml}$), and mix of IL10 and Dexamethasone (100 U/ml; and 10^{-6} M, respectively) and subjected to Western blot analysis. Western blot analysis after 24 h of stimulation is shown. LUMAN was visualized as described above. HEK293/LUMAN-IRES-GFP transfected cells treated with BFA for 6 h were taken along as a control. β -actin was used as a loading control.

transfected cells were stimulated for 6 h with BFA or left untreated, lysed and subjected to Western blotting and quantitative protein analysis (Fig. 6A and B). It appeared that DC-STAMP-HA, Dectin1-HA and YFP-LUMAN were expressed in the transfected cells (Fig. 6A and unpublished results). As expected, addition of BFA specifically induced the proteolytic activation of LUMAN (approximately 70 kDa, including YFP, Fig. 6A). Strikingly, the ratio between cleaved and uncleaved LUMAN following BFA treatment in the presence of DC-STAMP was significantly impaired as compared to Dectin-1 (Fig. 6B). The inhibitory effect of DC-STAMP on BFA-dependent LUMAN activation was confirmed in multiple independent experiments and shown to be independent of the type of tags on either DC-STAMP or LUMAN (unpublished results). Collectively, these data indicate that, in the absence of additional stimuli, BFA induced RIP of LUMAN is downregulated by DC-STAMP.

Discussion

This study was carried out to gain insight in the molecular function of DC-STAMP, a protein involved in myeloid differentiation and giant cell formation. By means of yeast-2-hybrid analysis and co-immunoprecipitation assays, we identified LUMAN as a *bona fide* DC-STAMP-interacting protein (Figs. 1 and 2). The LUMAN-interacting domain in DC-STAMP does not overlap with that of OS9, another binding partner of DC-STAMP. Furthermore, LUMAN co-localizes with DC-STAMP in the ER of transfected HEK293 and CHO cells (Fig. 3). We also demonstrate endogenous expression of LUMAN protein in dendritic cells (Fig. 4 and 5). LUMAN is localized in the ER in immature DC, like DC-STAMP. Intriguingly, upon DC maturation, LUMAN re-localizes to the nucleus, presumably to activate or repress transcription of target genes. Moreover, by co-transfecting DC-STAMP and LUMAN into a model cell line

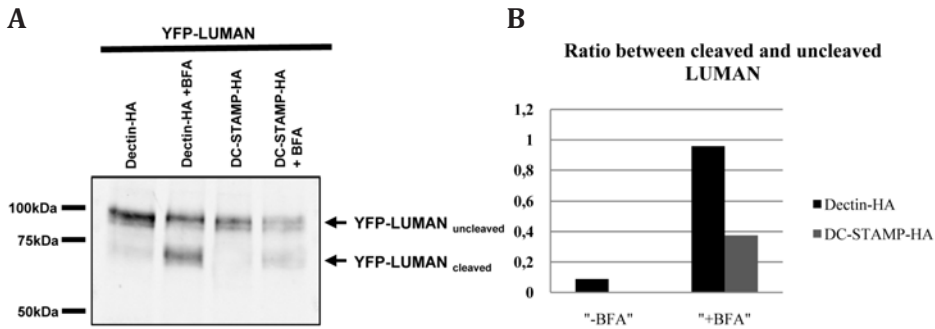


Figure 6. DC-STAMP modulates the ability of BFA to cause RIP of LUMAN. **A)** CHO/TLR cells were transfected with YFP-LUMAN together with DC-STAMP-HA or Dectin-HA as a control. 24 h after transfection, cells were or were not stimulated with Bfa for 6 h and subjected to Western blot analysis. LUMAN was visualized by staining with a mixture of two monoclonal α GFP antibodies. **B)** Quantitative analysis of LUMAN cleavage was performed using Odyssey software. The graph represents the ratio between the cleaved and uncleaved form of LUMAN.

modulation of Bfa-mediated activation of LUMAN by DC-STAMP is demonstrated (Fig. 6).

The yeast-2-hybrid approach demonstrated that the newly discovered interactors LUMAN and OS9 each bind to different regions within the cytoplasmic tail of DC-STAMP (Fig. 3). When mapping of the binding sites of LUMAN we observed an interesting phenomenon: the interaction with DC-STAMP requires both cytoplasmic and luminal sequences. As the cytoplasmic tail of DC-STAMP was used as bait, we hypothesize that the interaction takes place at the cytoplasmic side of the ER, and that the luminal domain of LUMAN is needed to ensure a proper conformation at the cytoplasmic side of the ER. We cannot exclude the possibility that LUMAN and DC-STAMP also interact through their luminal domains inside the ER, and further research is needed to address that possibility.

LUMAN is ubiquitously expressed at the mRNA level but at the protein level it was observed only in the trigeminal ganglionic neurons and monocytes^{14,15}. Our result confirms the ubiquitous mRNA levels of LUMAN (Fig. 4). Additionally, we clearly show its protein expression in DC, which was almost 10 times higher than in monocytes. In some of the experiments we observed two (iso)forms of LUMAN, where the larger protein likely represents a glycosylated form of full-length LUMAN, as reported by Raggo *et al.*¹⁶. Strikingly, for the first time we were able to detect the transcriptionally active aminoterminal part of endogenous LUMAN in mature DC (Fig. 5). Based on the kinetics of LUMAN activation it is reasonable to assume

that LUMAN serves in a feedback control mechanism, as the activation of LUMAN is a late event during DC maturation (Fig. 5C). This notion is further supported by the reported role of its interacting partner DC-STAMP in DC activation and function, as a recent study by Sawatani indicates its possible role in the maintenance of immune self-tolerance¹¹.

Most of our experiments were conducted using LPS, a TLR4 ligand, as a maturation stimulus. It is, however, interesting to note that two different “maturation cocktails” currently used to mature DC in clinical vaccination studies^{21,22} resulted in the same proteolytically cleaved LUMAN protein (Fig. 5D). Strikingly, stimulation leading towards a tolerogenic phenotype did not result in LUMAN activation (Fig. 5D) suggesting a specific pathway in DC primed towards immunity. An additional 50 kDa product in mature DC was observed, which seemed to be more pronounced at later time points than the 40 kDa product. An interesting possibility is that LUMAN may undergo SUMOylation, which would add approximately 10 kDa to the protein, in line with the observed size. This is further supported by bioinformatics analysis (unpublished results), which revealed three possible SUMOylation sites in the nuclear, aminoterminal part of LUMAN.

There is some controversy regarding the localization of endogenous LUMAN. It has been reported that LUMAN is primarily associated with the ER in the trigeminal ganglionic neurons and in transfected cell lines¹⁴, whereas other studies show that LUMAN is expressed in the cytoplasm with partial cell membrane localization in monocytes¹⁵. Our data support ER localization of LUMAN protein in different cell lines and endogenously in immature DC (Figs. 2 and 5 and S2). Brefeldin A treatment, known to facilitate re-localization of activated LUMAN to the nucleus, indeed resulted in nuclear localization of LUMAN in a transfected cell line as well as in immature DC. Interestingly, upon DC maturation the endogenous, aminoterminal part of LUMAN clearly localizes to the nucleus, confirming the presence of the machinery in DC needed to proteolytically activate LUMAN (Fig. 5). These observations fully corroborate the data obtained by Western blot analysis.

Since DC are primary cells, manipulation of these cells using molecular techniques is often difficult. Most notably, DC-manipulation often has an impact on DC function and induces maturation which is one of the processes we now show are important in relation to DC-STAMP/LUMAN. We therefore used a cell line model in which DC-STAMP is not endogenously expressed and which allows easy modulation of its expression by standard transfection technologies. CHO cells were used to investigate whether DC-STAMP plays a role in the activation of LUMAN. The quantification of Western

blot analysis clearly shows that co-transfection of DC-STAMP negatively influences the BfA-induced cleavage of LUMAN in CHO cells (Fig. 6). The overexpression of DC-STAMP in DCs had the same effect on BfA-induced LUMAN activation as in the transfected cell line, but to a lesser extent (unpublished results). The negative effect of DC-STAMP on BfA-induced cleavage of LUMAN observed in Fig. 6 may explain the data presented in Fig. 5C, where a time course analysis of BfA stimulation resulted in a very weak proteolytic product of 37 kDa in comparison to a larger cleaved product of LUMAN (40 kDa) upon LPS stimulation. The differences in size of cleaved Luman observed may be the result of a phosphorylation event and suggests that in DC the natural route of LUMAN activation via LPS is not identical to BfA-treatment that has so far been used to induce LUMAN translocation. Additionally, since DC-STAMP is preferentially expressed by DC, there may be a specific role for the LUMAN/DC-STAMP pathway in the context of DC, since we were not able to clearly show LPS-mediated activation of LUMAN in the CHO/TLR model.

Our data indicate a physical interaction of DC-STAMP and LUMAN (Figs. 1–3). Moreover, in or at the ER membrane DC-STAMP significantly influenced the BfA-mediated cleavage of LUMAN. Interestingly, less full-length LUMAN protein was present in co-transfections with DC-STAMP, which suggests an additional effect of DC-STAMP on stability of LUMAN (Figs. 1B and 6). In this respect it is important to note that another DC-STAMP-interacting partner, OS9, is known to play a role in the regulation of proteasome-mediated degradation of the transcription factor *hypoxia-inducible factor 1 alpha* (HIF1 α) and the *vanilloid transient receptor potential protein 4* (TRPV4)^{27,28}. Our immunoprecipitation data (Fig. S1) show also physical interaction between OS9 and LUMAN, and OS9 may be important in the regulation of the stability or turnover of this transcription factor, however this needs further analysis.

As has been reported before, LUMAN can undergo RIP¹⁶, a process of rapid activation of ER-resident transcription factors by means of transport to and proteolytic cleavage in the Golgi. To reach the Golgi, an accessory protein is needed which serves as a sensor of the environmental changes of initiating the RIP or a transporter. For LUMAN, no natural triggers were known so far. Also, no ER-resident, interacting proteins have been reported. Here, we demonstrate for the first time the activation of endogenous LUMAN upon DC maturation. Based on similarities between the SREBP/SCAP model²⁹ and LUMAN/DC-STAMP, a following model is proposed: in immature DC, DC-STAMP interacts with LUMAN and OS9 in the ER (Fig. 7A). Upon DC maturation, the DC-STAMP/LUMAN complex is released from

the ER (Fig. 7B; step 1) and the complex translocates to Golgi. LUMAN is activated by proteolytic cleavage and its aminoterminal part re-locates to the nucleus (Fig. 7B; step 2). This model implies that DC-STAMP fulfills a role as a transport protein, much akin to the role of SCAP in SREBP activation, however we have not established a role as a sensor. Although not clear at this stage, OS9 may serve at the same time as a regulator of turnover as well as transport of the DC-STAMP/LUMAN complex transport in the ER¹². It is likely that both OS9 and DC-STAMP play an important role

3

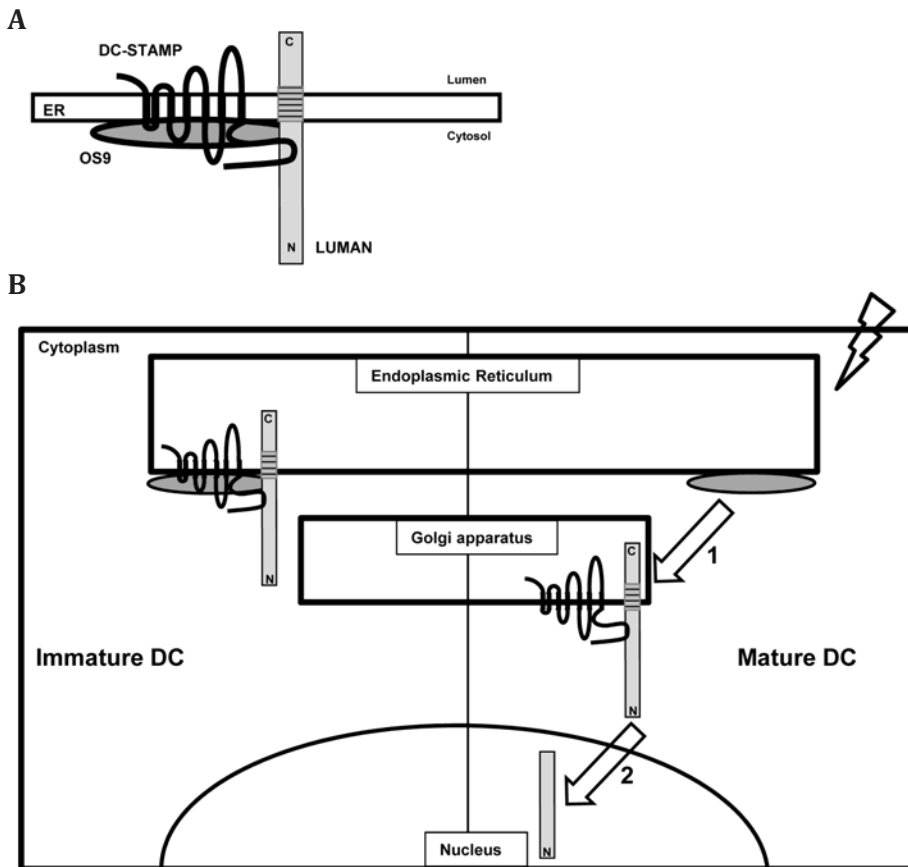


Figure 7. Model of DC-STAMP/LUMAN/OS-9 pathway. A) Schematic representation of DC-STAMP, LUMAN and OS9 complex in the ER. DC-STAMP, LUMAN and OS9 interact with each other at the cytosolic site of the ER. B) In steady-state conditions in immature DC the DC-STAMP/LUMAN/OS9 complex reside in the ER (left). Upon DC maturation, OS9 does not alter its localization, but the DC-STAMP/LUMAN complex translocates to the Golgi (right; step 1), where LUMAN is subsequently cleaved and its aminoterminal region is liberated, which then relocates to the nucleus (right; step 2).

in LUMAN function as both DC-STAMP and OS9 physically interact with LUMAN (Fig. S1).

As LUMAN plays a role in an ER stress response pathway³⁰ a survey of public microarray data in the Gene Expression Omnibus (<http://www.ncbi.nlm.nih.gov/geo/>) has been performed and did not reveal differential expression of known LUMAN targets in activated DC, strongly suggesting that is involved in a different, novel pathway in DC.

Intriguingly, DC-STAMP has been also implicated in osteoclastogenesis, where it was suggested to localize to the cell membrane in osteoclasts¹⁰. It is very well possible that DC-STAMP localization is cell-type dependent. It is tempting to speculate that the LUMAN/DC-STAMP/OS9 pathway plays a role in both DC maturation and osteoclastogenesis. Here, we have provided evidence for a new pathway involving DC-STAMP, LUMAN and OS9 in response to innate immune signaling in DC. Ongoing and future research will clarify the role of this complex in DC immunobiology, and lead to a better understanding of the molecular wiring of these cells, hopefully to the benefit of their clinical use.

Acknowledgements

This work was financially supported by grant 912-02-34 and VICI grant 918-66-615 (awarded to G.J.A.) from the Netherlands Organization for Scientific Research (NWO). We gratefully acknowledge Angelique Lemckert and Menzo Havenga, Crucell NV, Leiden, the Netherlands, for providing the adenoviruses bearing the DC-STAMP-GFP construct. We thank Jeanette Leusen, UMCU, Utrecht, the Netherlands, for helping to set up the yeast-2-hybrid analysis. Furthermore we would like to thank Richard Janssen, Galadeno, Leiden, the Netherlands, for providing the FLAG-pCDN3 vector and for helpful discussion. We thank Ruurd Torensma and Jolanda de Vries, NCMLS, RUNMC Nijmegen, the Netherlands, for critical reading of the manuscript.

References

1. Banchereau, J. & Steinman, R.M. Dendritic cells and the control of immunity. *Nature* **392**, 245-252 (1998).
2. Akira, S. & Takeda, K. Toll-like receptor signalling. *Nat Rev Immunol* **4**, 499-511 (2004).
3. Mellman, I. & Steinman, R.M. Dendritic cells: specialized and regulated antigen processing machines. *Cell* **106**, 255-258 (2001).
4. Janeway, C.A., Jr. & Medzhitov, R. Innate immune recognition. *Annu Rev Immunol* **20**, 197-216 (2002).
5. Hayden, M.S. & Ghosh, S. Shared principles in NF-kappaB signaling. *Cell* **132**, 344-362 (2008).
6. Hartgers, F.C., *et al.* DC-STAMP, a novel multimembrane-spanning molecule preferentially expressed by dendritic cells. *Eur J Immunol* **30**, 3585-3590 (2000).
7. Hartgers, F.C., *et al.* Genomic organization, chromosomal localization, and 5' upstream region of the human DC-STAMP gene. *Immunogenetics* **53**, 145-149 (2001).
8. Eleveld-Trancikova, D., *et al.* The dendritic cell-derived protein DC-STAMP is highly conserved and localizes to the endoplasmic reticulum. *J Leukoc Biol* **77**, 337-343 (2005).
9. Eleveld-Trancikova, D., *et al.* The DC-derived protein DC-STAMP influences differentiation of myeloid cells. *Leukemia* **22**, 455-459 (2008).
10. Yagi, M., *et al.* DC-STAMP is essential for cell-cell fusion in osteoclasts and foreign body giant cells. *J Exp Med* **202**, 345-351 (2005).
11. Sawatani, Y., *et al.* The role of DC-STAMP in maintenance of immune tolerance through regulation of dendritic cell function. *Int Immunol* **20**, 1259-1268 (2008).
12. Jansen, B.J., *et al.* OS9 interacts with DC-STAMP and modulates its intracellular localization in response to TLR ligation. *Mol Immunol* **46**, 505-515 (2009).
13. Freiman, R.N. & Herr, W. Viral mimicry: common mode of association with HCF by VP16 and the cellular protein LZIP. *Genes Dev* **11**, 3122-3127 (1997).
14. Lu, R. & Misra, V. Potential role for luman, the cellular homologue of herpes simplex virus VP16 (alpha gene trans-inducing factor), in herpesvirus latency. *J Virol* **74**, 934-943 (2000).
15. Ko, J., *et al.* Human LZIP binds to CCR1 and differentially affects the chemotactic activities of CCR1-dependent chemokines. *Faseb J* **18**, 890-892 (2004).
16. Raggio, C., *et al.* Luman, the cellular counterpart of herpes simplex virus VP16, is processed by regulated intramembrane proteolysis. *Mol Cell Biol* **22**, 5639-5649 (2002).
17. Brown, M.S. & Goldstein, J.L. The SREBP pathway: regulation of cholesterol metabolism by proteolysis of a membrane-bound transcription factor. *Cell* **89**, 331-340 (1997).
18. Wang, Y., *et al.* Activation of ATF6 and an ATF6 DNA binding site by the endoplasmic reticulum stress response. *J Biol Chem* **275**, 27013-27020 (2000).
19. De Lemos-Chiarandini, C., *et al.* A Golgi-related structure remains after the brefeldin A-induced formation of an ER-Golgi hybrid compartment. *Eur J Cell Biol* **58**, 187-201 (1992).
20. Yoshimura, A., *et al.* Cutting edge: recognition of Gram-positive bacterial cell wall components by the innate immune system occurs via Toll-like receptor 2. *J Immunol* **163**, 1-5 (1999).
21. Boullart, A.C., *et al.* Maturation of monocyte-derived dendritic cells with Toll-like receptor 3 and 7/8 ligands combined with prostaglandin E2 results in high interleukin-12 production and cell migration. *Cancer Immunol Immunother* **57**, 1589-1597 (2008).
22. de Vries, I.J., Adema, G.J., Punt, C.J. & Figdor, C.G. Phenotypical and functional characterization of clinical-grade dendritic cells. *Methods Mol Med* **109**, 113-126 (2005).
23. de Vries, I.J., *et al.* Maturation of dendritic cells is a prerequisite for inducing immune responses in advanced melanoma patients. *Clin Cancer Res* **9**, 5091-5100 (2003).
24. de Vries, I.J., *et al.* Phenotypical and functional characterization of clinical grade dendritic cells. *J Immunother* **25**, 429-438 (2002).
25. Ausubel, F.M. *Current protocols in molecular biology*, (Greene Publishing Associates; J. Wiley, order fulfillment, Brooklyn, N. Y. Media, Pa., 1987).
26. Lu, R., Yang, P., O'Hare, P. & Misra, V. Luman, a new member of the CREB/ATF family, binds to herpes simplex virus VP16-associated host cellular factor. *Mol Cell Biol* **17**, 5117-5126 (1997).
27. Baek, J.H., *et al.* OS-9 interacts with hypoxia-inducible factor 1alpha and prolyl hydroxylases to promote oxygen-dependent degradation of HIF-1alpha. *Mol Cell* **17**, 503-512 (2005).

-
28. Wang, Y, *et al.* OS-9 regulates the transit and polyubiquitination of TRPV4 in the endoplasmic reticulum. *J Biol Chem* (2007).
 29. Horton, J.D., Goldstein, J.L. & Brown, M.S. SREBPs: activators of the complete program of cholesterol and fatty acid synthesis in the liver. *J Clin Invest* **109**, 1125-1131 (2002).
 30. Liang, G, *et al.* Luman/CREB3 induces transcription of the endoplasmic reticulum (ER) stress response protein Herp through an ER stress response element. *Mol Cell Biol* **26**, 7999-8010 (2006).

Supplementary figures

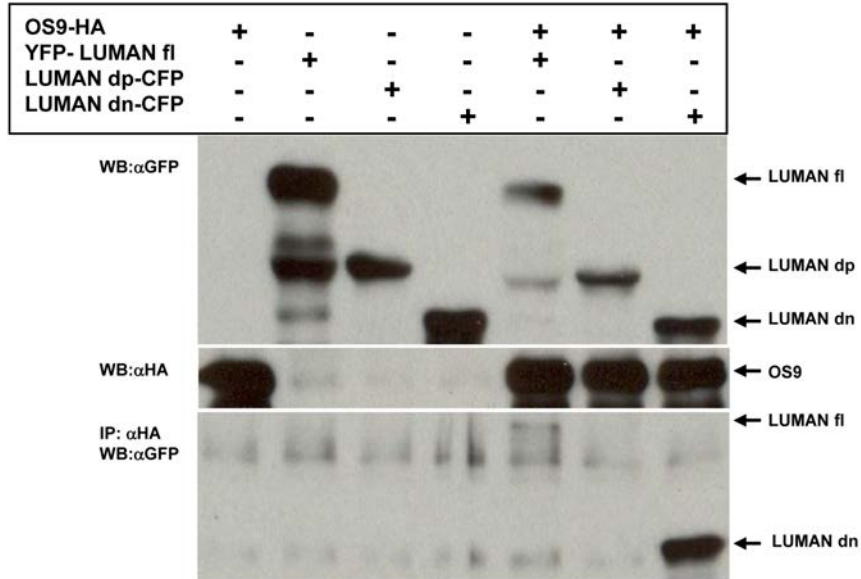


Figure S1. LUMAN co-immunoprecipitates with OS9 in HEK293 cells. HEK293 cells were transfected with OS9-HA and LUMAN and different deletion mutants: LUMAN full-length (fl), dominant-positive (dp; amino acids 1–220), and dominant negative (dn amino acids 145–372) fused to YFP or CFP in a double transfection. The immunoprecipitation was performed using the mouse αHA (12CA5) monoclonal antibody. Only the fl and dn mutant of LUMAN are able to interact with OS9. To visualize LUMAN, Western blots were stained with a mixture of two αGFP monoclonal antibodies. OS9-HA was visualized using the rat αHA monoclonal 3F10.

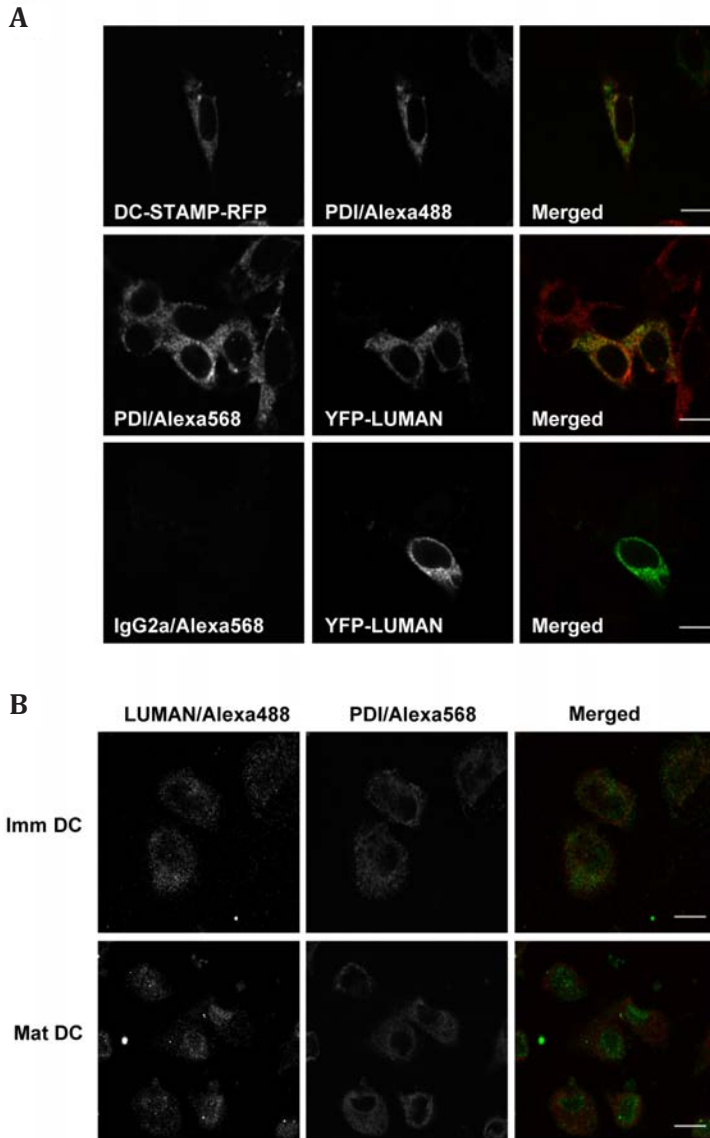


Figure S2. Localization of LUMAN and DC-STAMP in transfectants and in DC. **A)** ER localization of DC-STAMP-RFP and YFP-LUMAN in HEK293 transfectants. HEK293 cells were transfected with constructs encoding DC-STAMP-RFP or YFP-LUMAN, and stained with α PDI antibody to visualize ER and analyzed by CLSM. IgG2a was used as a negative control. Scale bar: 10 μ m. **B)** Endogenous expression of LUMAN in immature (upper row) and mature DC (lower row) co-stained with an ER marker PDI, followed by a secondary antibody conjugated to Alexa568 (red). LUMAN is visualized by the polyclonal antibody against the aminoterminal part of LUMAN, followed by secondary antibody coupled to Alexa488 (green). Scale bar: 10 μ m.

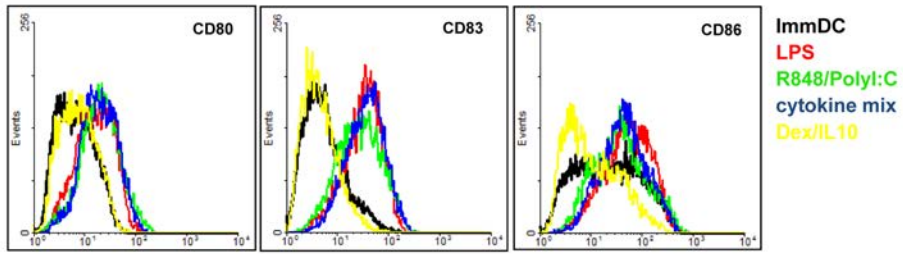


Figure S3. Expression of DC markers after different stimulation. Surface expression of the maturation markers CD80, CD83 and CD86 was assessed by means of FACS before and after different stimulation as used in the Fig. 5D.

CHAPTER 4

DC-STAMP knock-down deregulates cytokine production and T-cell stimulatory capacity of LPS-matured dendritic cells

**Sanecka A, Ansems M, Prosser AC, Warner K,
Danielski K, den Brok MH, Jansen BJ,
Eleveld-Trancikova D, Adema GJ**

BMC Immunology (2011), 12:57

Abstract

Dendritic cells (DCs) are the highly specialized antigen presenting cells of the immune system that play a key role in regulating immune responses. DCs can efficiently initiate immune responses or induce tolerance. Due to this dual function, DCs are studied in the context of immunotherapy for both cancer and autoimmune diseases. Characterization of DC-specific genes, leading to better understanding of DC immunobiology, will help to guide their use in clinical settings. We previously identified DC-STAMP, a multi-membrane spanning protein preferentially expressed by DCs. DC-STAMP resides in the endoplasmic reticulum (ER) of immature DCs and translocates towards the Golgi compartment upon maturation. In this study we knocked down DC-STAMP in mouse bone marrow-derived DCs (mBMDCs) to determine its function. We demonstrate that DC-STAMP knock-down mBMDCs secrete less IL-6, IL-12, TNF- α and IL-10 while IL-1 production is enhanced. Moreover, LPS-matured DC-STAMP knock-down mBMDCs show impaired T cell activation potential and induction of Th1 responses in an alloreaction. We show that DC-STAMP plays an important role in cytokine production by mBMDCs following LPS exposure. Our results reveal a novel function of DC-STAMP in regulating DC-initiated immune responses.

Introduction

Dendritic cells (DCs) are professional antigen presenting cells (APC) that play a central role in innate and adaptive immunity. DCs, armed with a wide range of receptors that sense danger signals and scavenge antigens in the surrounding environment, constantly scan our body. Antigen uptake in the presence of inflammation and danger signals results in DC maturation. In this active state DCs are able to efficiently induce immune responses¹. On the other hand, in the absence of danger signals DCs regulate tolerance to self-antigens in order to prevent autoimmunity.

During maturation DCs upregulate costimulatory molecules such as CD40, CD80 and CD86 as well as MHC class II, which allows for effective antigen presentation to naïve T cells. Furthermore, mature DCs produce and secrete proinflammatory cytokines and chemokines to attract and activate innate effector cells as well as to direct the development of specific T helper (Th) subsets². High levels of IL-12 will induce differentiation of naïve CD4⁺ T cells into Th1 cells while blocking the development of the Th2 lineage³. To prime Th2 responses IL-4 produced by Th2 cells themselves, NKT cells, eosinophils or basophils is needed^{4,5}. Additionally, IL-1 has a positive influence on expansion of the murine Th2 cells⁶. The murine Th17 T-cell subset efficiently develops in the presence of the proinflammatory cytokines IL-6 and TGF- β ⁷.

Due to their immunoregulatory capacities DCs are a promising tool for immunotherapy. Indeed, DC-based therapies are currently being used for treatment of cancer, autoimmune diseases and the prevention of transplant rejection⁸⁻¹². Detailed understanding of molecular aspects of DC immunobiology is crucial for optimal application of DCs in immunotherapy. Characterization of genes like DC-SIGN¹³, DC-CK1¹⁴ and DC-SCRIPT¹⁵⁻¹⁷ has already resulted in many novel findings regarding the molecular basis of DC function.

Recently, we reported on the isolation and characterization of a novel molecule named DC-STAMP, both in human and mouse DCs^{18,19}. DC-STAMP was shown to be a multi-membrane spanning protein preferentially expressed by myeloid DCs¹⁸, macrophages²⁰ and osteoclasts²¹. In immature DCs, DC-STAMP localizes to the endoplasmic reticulum²² and upon DC maturation translocates towards the Golgi compartment, which is most likely facilitated by its interacting partner OS9²³, a protein that has previously been implicated in ER-to-Golgi transport^{24,25}. Interestingly, DC-STAMP also interacts with the ER-resident transcription factor LUMAN²⁶.

LUMAN is activated in a process called regulated intramembrane proteolysis (RIP), which involves its translocation to the Golgi compartment, proteolytic cleavage and subsequent nuclear localization²⁷. The immunological and biological processes DC-STAMP is involved in are only recently emerging. Functional studies in DC-STAMP knock-out mice have shown that DC-STAMP is essential for fusion of osteoclasts and foreign body giant cells^{21,28}. Much less is known regarding the role of DC-STAMP in myeloid immune cells. DC-STAMP was shown to inhibit granulocyte development from hematopoietic progenitor cells²⁹, however its expression is not required for proliferation and differentiation of DCs³⁰. Initial data using immature DCs from DC-STAMP knock-out mice have suggested involvement of DC-STAMP in phagocytosis and antigen presentation. As aged DC-STAMP knock-out mice show symptoms of autoimmune diseases, a role of DC-STAMP in maintaining the balance between immunity and tolerance has been proposed³⁰.

In the current study we examined the role of DC-STAMP in immature and TLR-matured DCs. For this purpose, we generated lentiviruses encoding DC-STAMP-specific shRNAs to knock-down DC-STAMP in BMDCs. We found that DC-STAMP knock-down in mature but not immature DCs affects cytokine production, induction of T cell proliferation and Th1 cell activation.

Materials and methods

Cell lines and cell culture

The human embryonic kidney cell line HEK293 was cultured in DMEM (Invitrogen) supplemented with 10% heat-inactivated FCS (Greiner Bio-One), 1% of non-essential amino acids (NEAA) (Invitrogen) and 0.5% antibiotic-antimycotic (Invitrogen). The mouse embryonic fibroblast cell line NIH3T3 was cultured in DMEM supplemented with 5% heat-inactivated FCS, and 0.5% antibiotic-antimycotic. HEK293FT cells (Invitrogen) were cultured in DMEM supplemented with 10% heat-inactivated FCS, 1% NEAA, 0.5% antibiotic-antimycotic, 1% ultra-glutamine (Lonza), and 1 mM sodium pyruvate (Invitrogen). Cells were kept under selection with 500 µg/ml of Geneticin (G418) (Invitrogen).

Generation of bone marrow-derived DCs

Mouse BMDCs were generated from bone marrow progenitor cells, according to the modified protocol of Lutz³¹. Bone marrow cells were flushed from the femurs and tibias of 6- to 8-week-old female C57BL/6 mice (Charles River WIGA GmbH), washed and counted. Cells were plated at a concentration of 4×10^6 cells per 10 cm Petri dish in 13 ml of RPMI-1640 medium (Invitrogen) supplemented with 10% FCS, 1% ultra-glutamine, 28 µM of β-mercaptoethanol (Sigma-Aldrich), 0.5% antibiotic-antimycotic and 20 ng/ml of murine recombinant GM-CSF (PeproTech). After 3 days, 4 ml of fresh medium was added containing fresh GM-CSF to final

concentration of 8.75 ng/ml. At day 6 non-adherent and loosely adherent cells were harvested and used for transduction.

Vectors and validation of RNAi

The construction of murine DC-STAMP-GFP vector was described previously²². Four SureSilencing shRNA plasmids encoding the shRNA sequence targeting murine DC-STAMP: shST1 (5'-gctggaagttcacttgaaact-3'), shST2 (5'-ttgtggctggaagtatgagaatgt-3'), shST3 (5'-tctggatgacacctgtgtt-3'), shST4 (5'-ggttcctctcagtattattct-3') and negative control scrambled shRNA (shScr) (5'-ggaatctcattcgatgcatac-3') plasmid were obtained from SuperArray Bioscience. In order to validate the silencing of mDC-STAMP, HEK293 cells were co-transfected with a plasmid expressing mDC-STAMP-GFP plasmid and a SureSilencing shRNA plasmid encoding either a control shRNA or mDC-STAMP-targeting shRNA using Lipofectamine (Invitrogen) according to the manufacturer's protocol. Forty-eight hours following transfection, mDC-STAMP-GFP protein levels were determined by Western blot.

Western blotting

Cells were lysed in 1% SDS buffer and subjected to Western blot analysis as described previously²². GFP-tagged mDC-STAMP was detected using mouse anti-GFP antibody (Roche). Actin was detected with a mouse anti- β -actin Ab (Sigma-Aldrich). Rabbit anti-mouse-HRP (Dako-Cytomation) was used as a secondary antibody. For detection an ECL Western Blotting Detection Reagents kit (Amersham Bioscience) and BioMax XAR Film (Kodak) were used.

Generation of the lentiviral vector stocks

Using Gateway technology, DNA encoding sequences for short-hairpin RNAs in the BLOCK-iT-U6-RNAi Entry vector were introduced into the pLenti6/BLOCK-iT-DEST vector (Invitrogen), following the manufacturer's protocol. The individual vectors were co-transfected with packaging vectors into the HEK293FT cells according to the manufacturer's instructions. Virus was produced in HEK293FT culture medium supplemented with 82.5 μ g/ml of water-soluble cholesterol (Sigma-Aldrich) and collected from tissue culture supernatant 24 and 48 h after transfection. Cell debris was removed by centrifugation and supernatant containing virus particles was filtered through a 0.45 μ m filter. Aliquots were stored at -80°C until use.

Viral titers were determined by transduction of NIH3T3 cells with serial dilutions of the virus stock in the presence of 10 μ g/ml of polybrene (Sigma-Aldrich). Two days after transduction the cells were cultured under selection with 2 μ g/ml of Blasticidin (Invitrogen) for 12 days. Medium was refreshed every third day. To determine the titer, the number of colonies was determined after crystal violet staining. The titer ranged between 2×10^5 to 13×10^5 transfection units (TU)/ml

Lentiviral knockdown of mDC-STAMP in mBMDCs

Mouse BMDCs were harvested after 6 days of culture and 1.2×10^6 cells were resuspended in 700 μ l of virus supernatant containing 10 μ g/ml of DEAE-dextran (Pharmacia Biotech AB) to facilitate viral infection. Cell-virus suspensions were plated on 12-well tissue culture plates (700 μ l/well) and centrifuged for 90 min at 2200 rpm and 37°C . After centrifugation, virus supernatant was replaced by mBMDC culture medium. The infection procedure was repeated

the following day. As a negative control, mBMDC culture medium with DEAE-dextran was used. The multiplicity of infection (MOI) for silencing of DC-STAMP was matched with the MOI of the scrambled shRNA control in each experiment.

RNA isolation and quantitative real-time PCR (qPCR)

Total RNA was isolated from at least 6×10^5 cells using a Quick-RNA MiniPrep kit (Zymo Research). RNA quantity and purity were determined using a NanoDrop spectrophotometer. Two micrograms of total RNA were treated with DNase-I (Invitrogen) and cDNA was synthesized using random primers and SuperScript Moloney murine leukemia virus reverse transcriptase (II-MMLV) (Invitrogen). Messenger RNA levels for the genes of interest were determined with a Bio-rad CFX96 (Bio-rad) using Fast Start SYBR Green kit (Roche) and primers for one of the following genes: porphobilinogen deaminase (PBGD) (forward: 5'-CCTACCATAC-TACCTCCTGGCTTTAC-3'; reverse: 5'-TTTGGGTGAAAGACAACAGCAT-3'), DC-STAMP (forward: 5'-TTGCCGCTGTGGACTATCTG-3'; reverse: 5'-GAATGCAGCTCGGTTCAAAC-3'), IL-6 (forward: 5'-TGGGAAATCGTGAAATGAG-3'; reverse: 5'-CAAGTGCATCATCGTTGTTC-3'), IL-1 α (forward: 5'-CGAAGACTACAGTTCTGCCATT-3'; reverse: 5'-GACGTTTCAGAGGTTCTCAGAG-3'), IL-1 β (forward 5'-GTGATGAGAATGACCTGTCTTTG-3'; reverse: 5'-GATTTGAAGCTGGATGCTCTC-3'), IL-12p40 (forward 5'-GACACGCCTGAAGAAGATGAC-3'; reverse: 5'-TAGTCCCTTTGGTCCAGTGTG-3'). Data were analyzed with Bio-rad CFX manager version 1.6 (Bio-rad) and checked for correct amplification and dissociation of the products. PBGD served as a reference gene. DC-STAMP and IL-6 levels relative to PBGD were calculated as: $2^{-\Delta\Delta Ct}$.

Cytokine measurements

For cytokine assays, 1×10^5 day 11 mBMDCs were plated per well on 96-well plate in 200 μ l of culture medium. Cells were stimulated with 1 μ g/ml of LPS (E. coli, 0111:B4, Sigma-Aldrich). Supernatants were harvested at the indicated time points and stored at -80°C . Concentrations of IL-12p70 and IL-6 in cell culture supernatants were measured by ELISA (BD Biosciences), according to manufacturer's protocol.

The cytokines and chemokines IL-10, IFN- γ , IL-15, IL-17, IL-1 α , IL-1 β , IL-2, IL-4, IL-5, IL-7, IL-9, IP-10 (CXCL10), KC (CXCL1), MCP-1 (CCL2), MIP-1 α (CCL3), MIP-2 (CXCL2), RANTES (CCL5), TNF- α and VEGF in cell culture supernatants were measured using the mouse cytokine multiplex (Milliplex, Millipore) following the manufacturer's protocol. Data analysis was performed using Bio-Plex Manager software (Bio-Rad Laboratories).

Immunofluorescent staining and Confocal Laser Scanning Microscopy

Immature mBMDCs (day 11) were seeded onto cover slides coated with poly-L-lysine (Sigma-Aldrich) (5×10^5 cells/slide), adhered for 2 hours and fixed with 1% PFA for 15 minutes. Cells were permeabilized with methanol (-20°C ; 1 min) and blocked with 3% BSA (Calbiochem) in 1 x PBS supplemented with 0.1% saponin (Sigma-Aldrich). Rabbit anti-calreticulin (Calbiochem) antibody was used to visualize ER. As an isotype control, purified rabbit IgG (Sigma-Aldrich) was used. As a secondary antibody, goat anti-rabbit-Alexa488 (BD Biosciences) was used. The nucleus was stained with DAPI. Slides were mounted in Mowiol (Calbiochem) and analyzed by CLSM using an Olympus FV1000.

Mixed lymphocyte reactions

Mixed lymphocyte reactions (MLRs) were performed using day 12 C57BL/6 mBMDCs as stimulators. Splenocytes from Balb/c mice (Harlan) depleted for B220-positive cells were used as responders. Negative selection for B220-positive cells was performed to increase T cell numbers in the splenocyte pool. Briefly, splenocytes were stained with an anti-B220-FITC antibody (BioLegend) then incubated with magnetic beads coupled to anti-FITC antibodies and purified with a magnetic bead-based kit (MACS; Miltenyi-Biotec). Cells were labeled with 1 μ M CFSE (Invitrogen) at a concentration of 50 x 10⁶ B220-negative cells/ml for 7 min at 37°C in PBS with 1% FCS. MLR assays were carried out in 96-well round-bottom plates (200 μ l/well) at a ratio of 1:2 or 1:3 (responders to stimulators), for 4 to 5 days in T cell medium (IMDM (Invitrogen) containing 10% FCS, 1% antibiotic-antimycotic, 0.5% ultra-glutamine, 28 μ M of β -mercaptoethanol and 60 IU of human IL-2 (Proleukin; Chiron BV, Amsterdam, the Netherlands). The proliferation rate was assessed by FACS analysis of CFSE dilution.

Flow cytometry

For cell surface labeling, the following anti-mouse antibodies were used (from BD Biosciences, unless stated differently): PE-conjugated anti-CD86 (GL1), anti-CD80 (16-10A1), anti-CD40 (3/23), anti-CD8 α (53-6.7), anti-MHC class II (M5/114.15.2, eBioscience); PerCP-conjugated anti-CD62L (Mel-14, BioLegend); APC-conjugated anti-CD11c (N418, BioLegend); APCcy7-conjugated anti-CD4 (L3T4). Flow cytometry was performed using a CyAn flow cytometer (Beckman Coulter) and analyzed with FlowJo software (TreeStar).

Statistical analysis

Statistical significance was calculated using a two-tailed Student t test (GraphPad Prism version 4.00 software). Data obtained from ELISA and Milliplex experiments were log₂-transformed before statistical analysis. Significance of difference was determined by the p value (*p < 0.05; **p < 0.01; ***p < 0.001).

Results

DC-STAMP silencing in mouse bone marrow-derived DCs

To investigate the role of DC-STAMP in DCs, we performed DC-STAMP knock-down studies in mBMDCs. Hereto, four different DC-STAMP shRNA sequences and a control scrambled shRNA sequence (shScr) were tested for their ability to silence murine DC-STAMP-GFP following co-transfection in HEK293 cells. Silencing was assessed by western blot analysis using antibodies directed against the GFP-moiety of the DC-STAMP-GFP fusion protein (Fig. 1A). The results show that the shRNA sequences shST1 and shST4 were most effective in DC-STAMP silencing whilst the scrambled shRNA had no effect. Therefore, these two DC-STAMP shRNA sequences were chosen for further use in mBMDCs. As mBMDCs are difficult to transfect, we

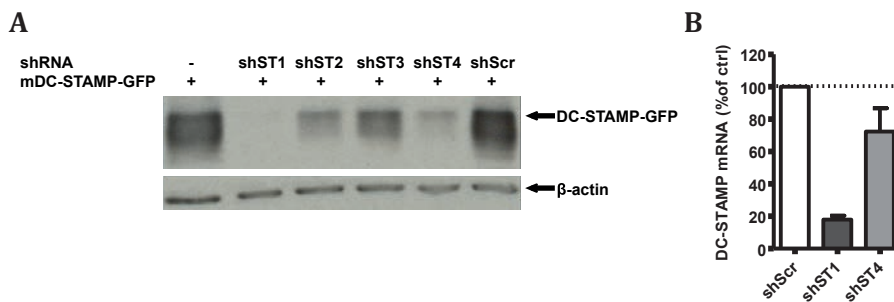


Figure 1. Efficiency of DC-STAMP silencing. **A)** HEK293 cells were co-transfected with mDC-STAMP-GFP plasmid and one of four plasmids expressing different shRNA sequences, designed to silence DC-STAMP, or with plasmid expressing scrambled shRNA. Cells were lysed 48 hours post-transfection and lysates were subjected to Western blot analysis. Blots were stained for GFP and re-probed for β-actin as an internal reference. Data shown are representative of two independent experiments. **B)** Murine BMDCs were transduced with lentivirus expressing shST1 or shST4 to silence DC-STAMP, or shScr as a negative control. Messenger RNA expression of DC-STAMP was assessed by qPCR. Levels of normalized DC-STAMP mRNA expression in cells infected with shST1 and shST4 lentiviruses were related to normalized DC-STAMP mRNA expression in shScr lentivirus infected cells. Data are depicted as mean percentage of control (shScr) ± SEM of three independent experiments.

used lentiviral shRNA delivery to stably produce shRNA from an integrated RNAi cassette and avoid as much as possible the host's defense mechanisms. Assessment of the effect of lentiviral transduction on maturation marker expression and cytokine production at the time of DC stimulation, revealed comparable levels of CD86 and MHC class II expression between non-transduced and mock transduced (shScr) mBMDCs. Additionally, proinflammatory and anti-inflammatory cytokines were not detectable in the supernatants of both non-infected and infected cells (data not shown). Taken together, these results indicate that infected cells did not mature spontaneously.

Bone marrow-derived DCs were infected with lentivirus expressing shST1, shST4 or shScr at day 6 and day 7 of culture. As specific antibodies against mDC-STAMP are not available, silencing of mDC-STAMP in mBMDCs was determined at the mRNA level by quantitative real-time PCR (qPCR). Effective silencing of DC-STAMP mRNA was observed at both day 9 and day 11 of culture (40 and 90 hours after second transduction) (Fig. 1B and data not shown). DCs at day 11 of culture were used for further experiments. In accordance with the results in HEK293 cells, shST1 was more effective in silencing DC-STAMP (70% silencing) as compared to shST4. Collectively, these data show that we are able to effectively silence DC-STAMP mRNA in mBMDCs with two independent shRNAs.

DC-STAMP silencing does not induce phenotypic changes in mBMDCs

First, the effect of DC-STAMP silencing on DC morphology and appearance was determined. Observation of the cells in culture after infection (day 6 and 7) until day 11 of culture did not reveal significant differences in DC morphology of both the non-adherent and loosely adherent cells between DC-STAMP knock-down and control cells (Fig. 2A). As DC-STAMP is a molecule residing in the endoplasmic reticulum, we investigated the ER in DC-STAMP knock-down and control cells in more detail by staining for the ER-residing protein calreticulin. Confocal microscopy analysis of the ER did not show any substantial differences in ER abundance or morphology in the DC-STAMP knock-down cells (Fig. 2B). This confirms results from DC-STAMP deficient mice indicating that DC-STAMP does not affect the appearance of the ER in DCs³⁰.

To evaluate the effects of DC-STAMP silencing on the expression of DC surface molecules flow cytometry analysis was performed. Expression of MHC class I and class II, and the costimulatory molecules, CD80, CD86 and CD40 was analyzed on immature and LPS-matured DC-STAMP knock-down (shST1 and shST4) and control (shScr) mBMDCs. To monitor the effect of viral infection, non-infected cells (no virus) were taken along in this analysis. No significant differences between control (shScr) and DC-STAMP knock-down immature mBMDCs were observed for any of the surface markers analyzed (Fig. 2C and data not shown). Upon LPS stimulation for 24 h, CD80, CD86, and MHC class II expression levels were elevated in both control and DC-STAMP-silenced DCs (Fig. 2C and data not shown). Non-infected and control shRNA (shScr) infected mBMDC did not significantly differ in their response to LPS stimulation, although the upregulation of costimulatory molecules in lentivirus infected cells was somewhat less. Furthermore, no differences in overall morphology or cell death were observed between the DC-STAMP knock-down and control cells following LPS-induced DC maturation. These data show that the phenotype of DC-STAMP knock-down cells does not differ from the control cells and correlates with results obtained from DC-STAMP knock-out mice³⁰. Additionally, our data show that the upregulation of costimulatory molecules following maturation is not affected in DC-STAMP silenced DCs relative to control cells.

LPS-induced cytokine secretion is altered in DC-STAMP knock-down mBMDCs

Upon DC maturation, along with changes in cell surface molecule expression, DCs also begin secreting cytokines and chemokines that play an important role in regulating immune responses. To determine the capacity of DC-STAMP knock-down

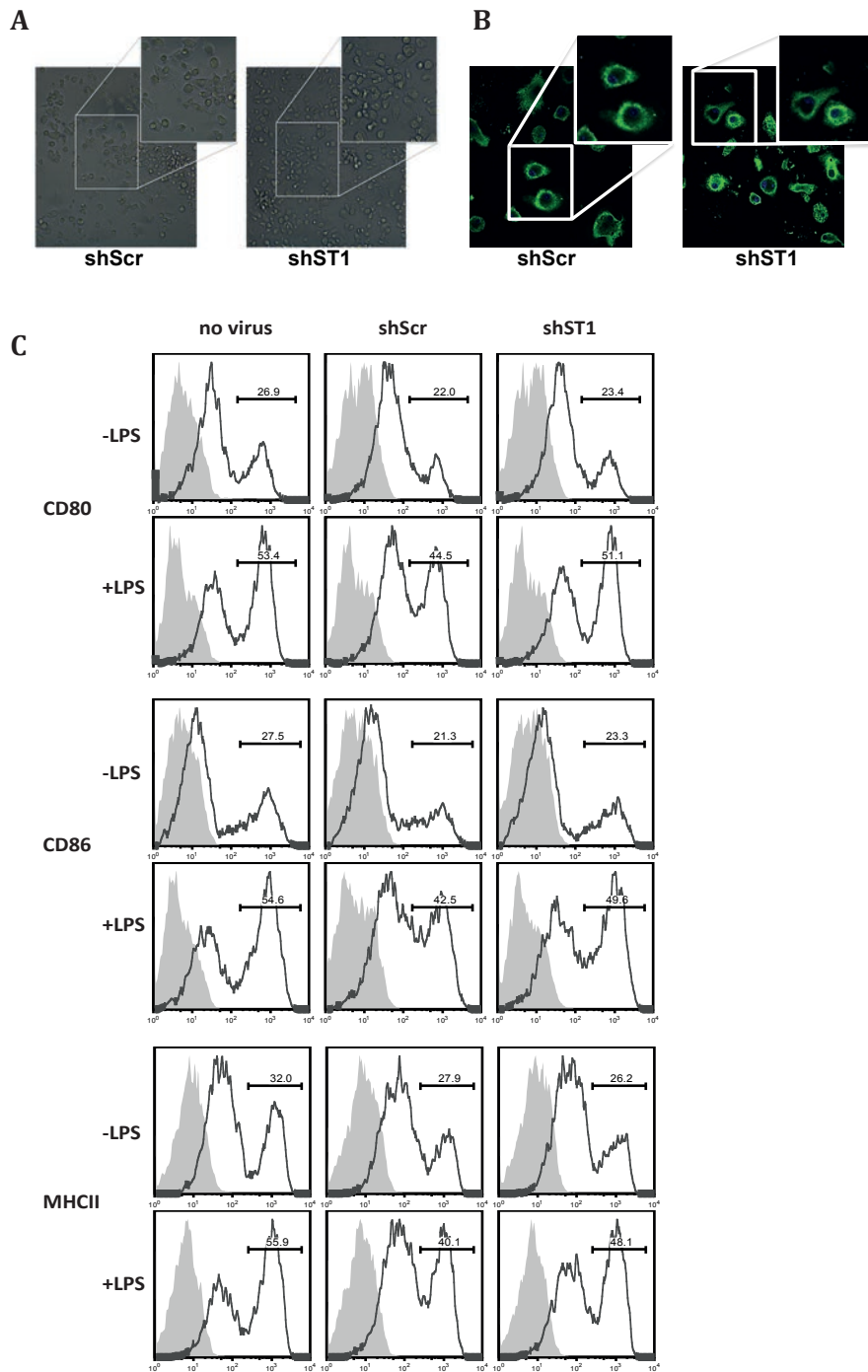


Figure 2. DC-STAMP silencing does not induce phenotypic changes in mBMDCs. Murine BMDCs were infected with shScr and shST1 lentivirus at day 6 and day 7 of culture. **A)** Light field microscopy image of mBMDCs in culture 4 days post-infection. **B)** Lentivirally transduced mBMDCs stained with antibody

against calreticulin (green) to visualize ER and DAPI staining of nucleus (blue) analyzed by CLSM. C) Flow cytometric analysis of CD80, CD86 and MHC class II surface expression in CD11c⁺ immature (-LPS) and LPS-matured (+LPS) non-infected (no virus), shScr and shST1 mBMDCs. Isotype controls are indicated by shaded area. Data shown are representative of two or three independent experiments.

mBMDCs to produce cytokines, cells were either left unstimulated or stimulated with LPS for 6, 16 and 24 h and the production of IL-6 was measured by ELISA. No difference in the cytokine production by the mBMDCs was observed without LPS stimulation, indicating that knock-down of DC-STAMP does not induce spontaneous IL-6 production. In contrast, the amount of IL-6 in supernatants of the DC-STAMP knock-down DCs after LPS stimulation was significantly decreased relative to control mBMDCs at all time points (Fig. 3A). Moreover, this effect was proportional to the level of DC-STAMP silencing. Cells transduced with shST1 produced 50% less of IL-6 than control mBMDCs whilst cells transduced with shST4 produced only 20-30% less. Next, IL-12p70 levels were measured in supernatants of DC-STAMP knock-down and control DCs. No IL-12 was spontaneously induced in immature DC-STAMP knock-down DCs (Fig. 3B). Interestingly, IL-12p70 was readily detected at 16 and 24 h of LPS stimulation, but the levels were significantly lower in DC-STAMP knock-down mBMDCs (shST1) (Fig. 3B). The finding that the level of DC-STAMP down-regulation with the two independent shST1 and shST4 DC-STAMP shRNAs is proportional to the decrease in IL-12 production further demonstrates the relevance of this observation.

To further define the effect of DC-STAMP on cytokine and chemokine production, supernatants of immature and 24 hours LPS-matured mBMDCs transduced with shST1 and shScr were analyzed by Milliplex bead assay. As expected, the predominantly T cell derived cytokines IFN- γ , IL-2, IL-4, IL-5, IL-9, IL-17, as well as IL-7 and IL-15 were not present at detectable levels in the supernatants of mBMDCs irrespective of DC-STAMP silencing and LPS stimulation (data not shown). Expression of the chemokines RANTES, IP-10, KC, MCP-1, MIP-2 as well as growth factor VEGF was readily detected upon LPS stimulation but no significant differences between shST1 and shScr control cells were observed (Fig. 3C and data not shown). In contrast, the proinflammatory chemokine MIP-1 α was expressed by both immature and mature DC and was clearly decreased in the supernatants of both immature and LPS-matured DC-STAMP knock-down DCs (Fig. 3C). Secretion of TNF- α and the anti-inflammatory cytokine IL-10 was also significantly decreased in supernatants of the LPS-matured DC-STAMP knock-down mBMDCs. On the other hand, LPS induction of the proinflammatory cytokine IL-1 α was significantly

increased in DC-STAMP knock-down mBMDCs relative to control DCs at the 24 hour time point. IL-1 β levels were also increased in supernatants of mature DC-STAMP knock-down mBMDCs although the difference did not reach statistical significance (Fig. 3C). Further analysis revealed that the increase in IL-1 α production in LPS-matured DC-STAMP silenced DCs is not present at earlier time points (6 and 16 h) (data not shown).

To address whether the observed deregulation in cytokine production can be explained by an effect of DC-STAMP silencing on cytokine transcription, the levels of the IL-6, IL-12p40, IL-1 α and IL-1 β mRNA were assessed (Fig. 3D). Detected differences in mRNA levels fluctuated between experiments, however the same tendency was observed. IL-6 and IL-12p40 mRNA levels were decreased in DC-STAMP knock-down cells (shST1) (20-75% for IL-6, 20-65% for IL-12p40), while mRNA of IL-1 α and IL-1 β levels were increased (25-48% for IL-1 α and 27-35% for IL-1 β).

Taken together, these results demonstrate that DC-STAMP deficiency results in the deregulation of cytokine production by mBMDCs and suggest the involvement of transcriptional regulation of cytokine genes in this phenomenon.

DC-STAMP deficiency leads to decreased T-cell proliferation

Next, we investigated the capacity of immature and LPS-matured DC-STAMP knock-down and control DCs to stimulate proliferation of CFSE-labeled allogeneic splenocytes depleted for B220 positive cells. The proliferation rate of total CD3⁺ T cells co-cultured with immature mBMDCs did not differ between DC-STAMP knock-down and control cells (Fig. 4A and 4B). In contrast, when the LPS-matured DC-STAMP knock-down mBMDCs were used as stimulators a significantly decreased proliferation rate of total CD3⁺ T cells was observed (Fig. 4A and 4B). In line with this finding, a significantly higher expression of CD62L was still present on CD4⁺ as well as CD8⁺ T cells in the cultures stimulated with the matured DC-STAMP knock-down mBMDCs compared to those stimulated with control DCs (Fig. 4C and 4D). No difference in CD62L expression was observed on the T cells activated by the immature mBMDCs. These data confirm that DC-STAMP knock-down mature mBMDCs have an impaired ability to activate T cells in an allogeneic MLR.

T cells stimulated by activated DCs can differentiate into different directions to promote Th1, Th2 or Th17 type responses. As we observed differences in proliferation rate and activation of T cells of co-cultures stimulated with mature mBMDCs, we analyzed supernatants from these co-cultures for the presence of a number of cytokines and chemokines (Fig. 4E). Strikingly, the levels of IFN- γ , a

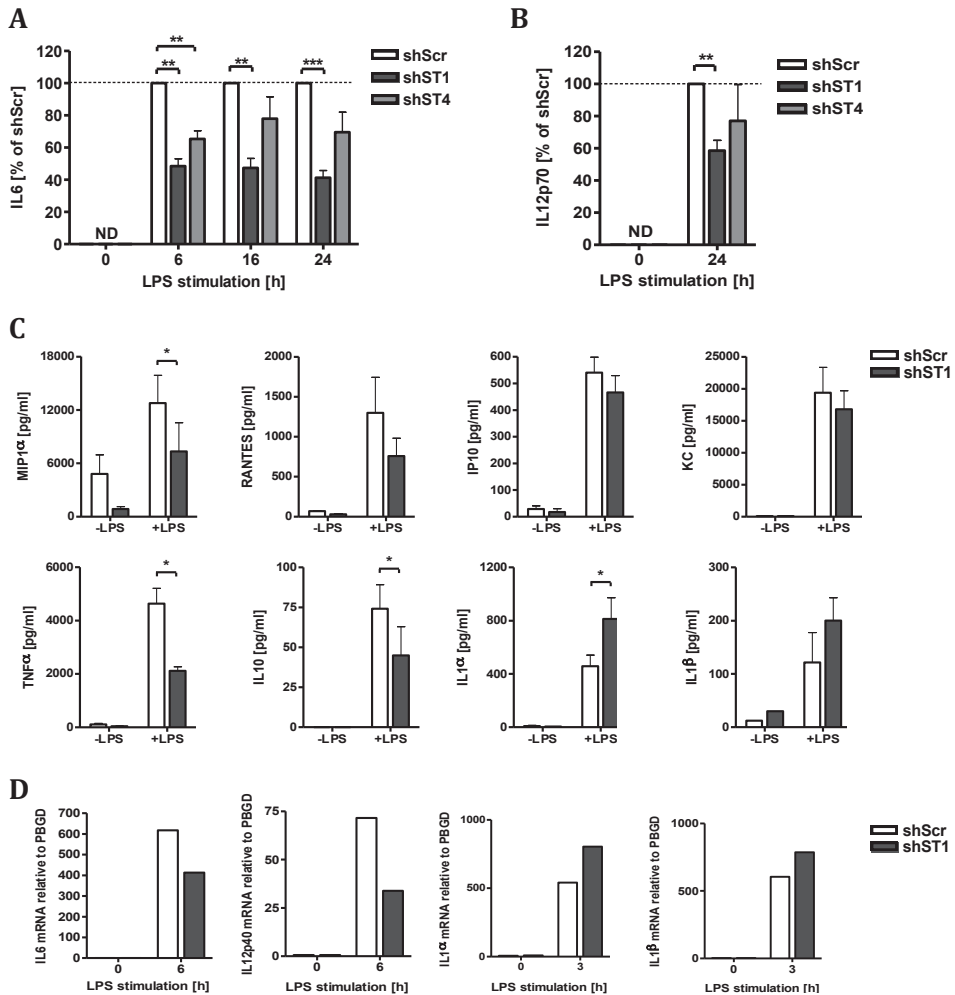


Figure 3. LPS-induced cytokine secretion is altered in DC-STAMP knock-down mBMDCs. Murine BMDCs transduced with shST1, shST4 or shScr were stimulated with 1 μ g/ml of LPS for 6, 16 and 24 hours. **A)** Levels of secreted IL-6 were measured by ELISA. Data are expressed as a percentage of control (shScr). Mean \pm SEM calculated of four independent experiments. Values in all experiments ranged from 5 to 500 ng/ml. **B)** Levels of secreted IL-12 p70 were measured by ELISA. Data shown are representative of three independent experiments and are expressed as a percentage of control (shScr). Mean \pm SEM calculated from triplicates. Values in all experiments ranged from 0.4 to 5 ng/ml. **C)** Levels of secreted cytokines were determined in supernatants 0 and 24 hours after LPS stimulation using Milliplex bead assay. Mean \pm SEM calculated from at least three independent experiments. Two-tailed Student *t* test was performed in A, B and C (ND-not detectable, **p* < 0.05; ***p* < 0.01; ****p* < 0.001). **D)** Total RNA was isolated from shScr and shST1 mBMDCs stimulated with LPS. Messenger RNA expression levels of IL-6, IL-12p40, IL-1 α and IL-1 β were determined by quantitative RT-PCR where PBGD served as an internal reference. Results shown are representative of at least three independent experiments. The differences in mRNA levels between shScr and shST1 in all experiments ranged from 20% to 75% for IL-6, 20-65% for IL-12p40, 25-48% for IL-1 α and 27-35% for IL-1 β .

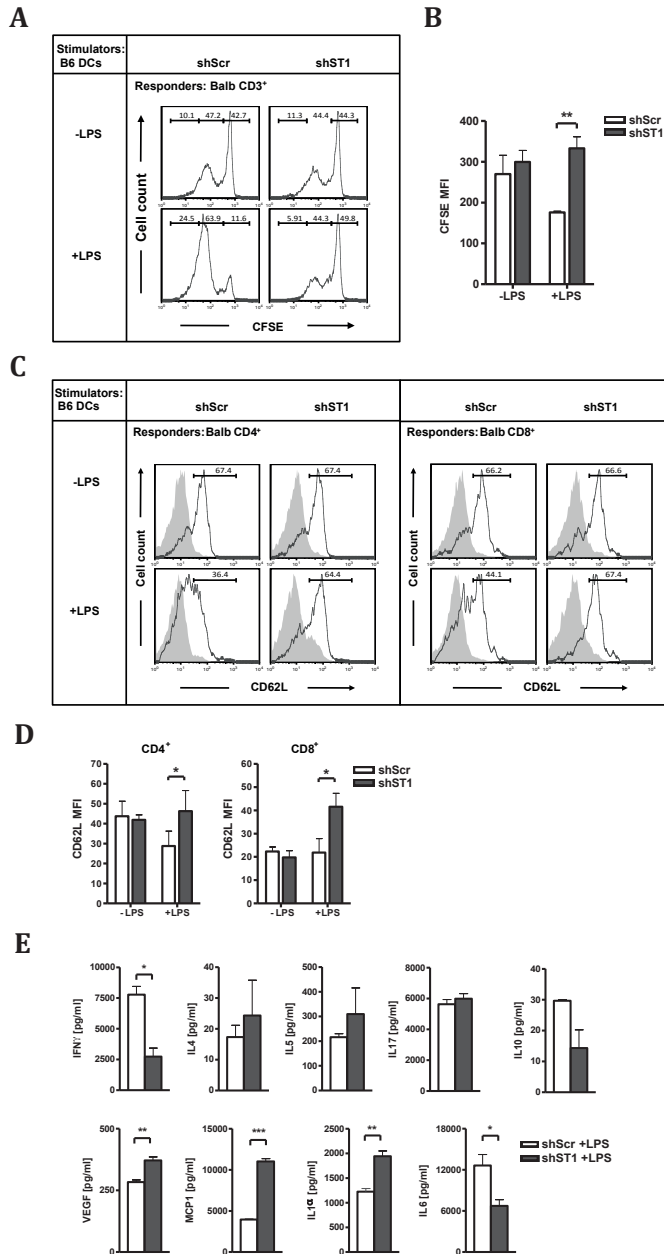


Figure 4. Decreased ability of DC-STAMP knock-down mBMDCs to stimulate T cell proliferation in allogeneic MLR. Splenocytes depleted for B220⁺ cells from Balb/c mice were stained with CFSE and co-cultured with immature (-LPS) or LPS-matured (+LPS) DC-STAMP knock-down (shST1) or control (shScr) mBMDCs from C57BL/6 mice. **A**) FACS data of CFSE dilution in CD3⁺ T cells. **B**) Quantified T-cell proliferation as a mean fluorescent intensity (MFI) of CFSE dilution in CD3⁺ T cells. Mean \pm SEM of four independent experiments are shown. **C**) FACS data of CD62L surface expression in CD3⁺CD4⁺ and CD3⁺CD8⁺

T cells (Balb/c) from co-cultures with DC-STAMP knock-down (shST1) or with control (shScr) mBMDCs (C57BL/6) (black line) compared to isotype control (grey shaded area). Data shown are representative of three independent experiments. **D**) Quantification of CD62L MFI on CD3⁺CD4⁺ and CD3⁺CD8⁺ T cells (Balb/c) from co-cultures with DC-STAMP knock-down mBMDCs (shST1) and shScr mBMDCs (C57BL/6). Data are expressed as mean \pm SEM of three independent experiments. **E**) Supernatants from allogeneic MLR co-cultures with mature mBMDCs were analyzed for indicated cytokines and chemokines by Milliplex bead assay. Data shown are mean \pm SEM from triplicates and are representative of at least three experiments. Two-tailed Student *t* test was performed in B, D and E (ND-not detectable, **p* < 0.05; ***p* < 0.01; ****p* < 0.001).

cytokine produced mainly by CD4⁺ cells of the Th1 phenotype, were significantly reduced in supernatants from co-cultures with DC-STAMP knock-down mature mBMDCs. Cytokines produced by Th2 type cells, IL-4 and IL-5, were present in somewhat higher amount in supernatants of co-cultures with DC-STAMP knock-down mBMDCs although these differences were not statistically significant. No difference in IL-17 levels was observed in the co-cultures with DC-STAMP knock-down and control mBMDCs while IL-10 was decreased without reaching statistical significance. Corresponding to our results obtained from supernatants of mBMDCs cultures, IL-6 expression was decreased and IL-1 α expression was increased in co-cultures with mature DC-STAMP knock-down mBMDCs. The proinflammatory chemokines MCP-1 and VEGF were present in significantly higher quantities in supernatants of co-cultures with DC-STAMP knock-down mBMDCs (Fig. 4E) relative to control DC. Together, these results show that LPS-matured DC-STAMP knock-down mBMDCs are less efficient in stimulating T cell proliferation and initiating IFN- γ producing Th1 cells.

Discussion

DCs are professional antigen-presenting cells that are critically involved in the initiation of the primary immune response¹. Maturation of the DC is important for priming naïve T cells and the generation of appropriate T cell responses. Here we show that silencing of the DC-expressed molecule DC-STAMP results in a distorted cytokine production both on mRNA and protein level in mBMDCs following LPS exposure. The importance of DC-STAMP in mBMDC maturation is further emphasized by the decreased ability of mature but not immature DC-STAMP knock-down DCs to stimulate naïve T cells and to prime Th1 responses.

Studies of DC-STAMP overexpression in murine bone marrow progenitor cells have suggested that DC-STAMP affects granulocyte development from hematopoietic progenitor cells²⁹. On the other hand, analysis of DC-STAMP knock-out mice mBMDCs

shows that DC-STAMP is not necessary for DC proliferation and differentiation³⁰. Little is known about the role of DC-STAMP in the maturation of DCs. DC maturation is a key checkpoint in the initiation of immunity and has important consequences on the quality of the immune response. Our previous studies have shown translocation of DC-STAMP from ER towards the Golgi compartment upon maturation of DCs²³. This differential localization of DC-STAMP in immature and mature DCs may suggest that DC-STAMP exerts an important role during the complex process of maturation. No significant differences in the morphology and the expression of DC-maturation markers between DC-STAMP knock-down and control immature and mature mBMDCs was observed. These data indicate that DC-STAMP silencing does not affect the phenotype of mBMDCs.

Upon TLR ligation, besides co-stimulatory molecule expression, DCs also start to produce a wide range of cytokines and chemokines to attract and stimulate other cells of the immune system¹. Our data show that despite the mature cell surface phenotype, DC-STAMP knock-down mBMDCs exhibit distorted cytokine production upon LPS stimulation (Fig. 3). Further analysis indicated that observed differences in secretion of IL-6, IL-12, IL-1 α and IL-1 β proteins are accompanied by the corresponding changes in mRNA levels (Fig. 3D), suggesting regulation at the transcriptional level. Interestingly, one of the DC-STAMP interacting partners, LUMAN, is a transcription factor that resides in the ER. For its activation LUMAN is translocated towards the Golgi compartment, cleaved and subsequently accumulates in the nucleus²⁷. Previously, we have shown that LUMAN protein in human myeloid DCs becomes translocated to the nucleus following TLR4 ligation in mature DCs²⁶. Others have shown that LUMAN can bind to cAMP response element (CRE) and unfolded protein response element (UPRE) transcription factor binding sites in promoters of target genes³²⁻³⁴. CRE sites are present in promoters of many cytokines, including, IL-2, IL-6, IL-10 and TNF- α ³⁵. It is therefore tempting to speculate that LUMAN is responsible at least in part for the deregulation of cytokine production observed in TLR-matured DC-STAMP knock-down DCs. LUMAN knock-down studies are required to confirm this hypothesis.

We further observed that levels of IL-1 α and IL-1 β were increased in DC-STAMP knock-down mBMDCs. This upregulation of IL-1 family cytokines seems to be contradictory to the observed decrease in IL-6 production as it is well established that IL-1 is able to induce expression of IL-6^{36,37}. The fact that IL-6 is also implicated in inhibition of IL-1 and TNF- α production^{38,39}, however, indicates that the relation between IL-6 and IL-1 α and IL-1 β is more complex. Looking at the mRNA level, IL-6

and IL-1 mRNA production is primarily affected by decreased DC-STAMP expression at early time points. The decrease in IL-6 protein level was observed early on after LPS stimulation, while translation and release of IL-1 α and IL-1 β took much longer. These data suggest that the cytokine profile in DC-STAMP KO DC may be explained by differences in the kinetics in the transcription, translation and release of IL-6 and IL-1 cytokines, and could possibly occur through the involvement of caspase-1/calpain in IL-1 β /IL-1 α release^{40,41}.

Many factors influence the differentiation process of CD4⁺ T cells into Th1, Th2 or Th17 effector cells, including antigen dose, the signal strength through the T cell receptor, and costimulation⁴². Especially cytokines were shown to be key determinants in the outcome of this differentiation²⁻⁷. In our MLR assays we observed negative effect of DC-STAMP silencing on T cell activation by mature DCs. Decreased levels of IFN- γ in these co-cultures, indicate an impaired ability of mature DC-STAMP knock-down mBMDCs to prime Th1 responses. As IL-12 is critically involved in the promotion of Th1 development³, we postulate that this decreased ability to support the development of Th1 lineage is determined by the reduced production of IL-12 by LPS-stimulated DC-STAMP knock-down mBMDCs. This is also supported by the fact that expression of costimulatory molecules was not affected by DC-STAMP knock-down. Impaired stimulation of Th1 responses allows differentiation of Th2 and Th17 subsets. Additionally, IL-1 α and IL-1 β were shown to stimulate Th2 and Th17 responses⁶, as well as induce the release of Th2 cytokines⁴³. The observed increase in IL-4 and IL-5 levels in co-cultures with mature DC-STAMP knock-down mBMDCs could suggest skewing the responses towards Th2 cells, which may be enhanced due to the higher levels of IL-1 cytokines in these co-cultures. Lower number of CD8⁺ T cells alone was observed after co-culture with DC-STAMP knock-down mature mBMDCs, however cells, which were dividing, went through the same number of divisions like the ones in co-culture with control mBMDC (data not shown). We postulate that the decrease in the CD8⁺ T cells proliferation is a result of the reduced CD4⁺ T cells help.

Sawatani *et al.* showed that aged DC-STAMP knock-out mice have symptoms of autoimmune disease and suggested involvement of increased phagocytosis and antigen presentation in onset of autoimmunity³⁰. We did not observe any differences in T cell proliferation between control and DC-STAMP knock-down cells when we used immature DC. This discrepancy between our and Sawatani *et al.* data may be explained by different design of the proliferation assays. We used allogeneic MLR to look at the ability of the DC-STAMP knock-down mBMDCs to stimulate differentiation

of naïve T cells while they looked at antigen-specific (OVA) responses. Decreased levels of proinflammatory cytokines IL-6, IL-12 and TNF- α do not easily explain the symptoms of autoimmune diseases observed in DC-STAMP-deficient mice. On the other hand, diminished production of anti-inflammatory cytokine IL-10 could be dominant over the reduction in proinflammatory cytokines. As IL-10 is crucially involved in preventing excessive immune responses⁴⁴ and plays an important role in development of suppressor T cells^{45,46} decrease in its production could lead to autoimmune disease.

In conclusion we clearly show the importance of DC-STAMP expression in cytokines production by mature mBMDCs. Further studies are necessary to resolve the pathway by which this phenomenon occurs. We postulate that the deregulated cytokines production in DC-STAMP knock-down mBMDCs upon LPS stimulation is responsible for impaired T-cell stimulatory capacity of these cells.

Acknowledgements

This work was supported by Vici grant 918-66-615 (awarded to G.J.A) from The Netherlands Organization for Scientific Research (NWO). We gratefully acknowledge Marije Koenders for help with the Milliplex cytokine bead assay, Jürgen Dieker for providing us with spleens of Balb/c mice, Ben van den Brand for help in optimizing lentivirus production and infection of mBMDCs.

References

1. Banchereau, J. & Steinman, R.M. Dendritic cells and the control of immunity. *Nature* **392**, 245-252 (1998).
2. Mosmann, T.R., Cherwinski, H., Bond, M.W., Giedlin, M.A. & Coffman, R.L. Two types of murine helper T cell clone. I. Definition according to profiles of lymphokine activities and secreted proteins. *J Immunol* **136**, 2348-2357 (1986).
3. Macatonia, S.E., *et al.* Dendritic cells produce IL-12 and direct the development of Th1 cells from naive CD4+ T cells. *J Immunol* **154**, 5071-5079 (1995).
4. Kopf, M., *et al.* Disruption of the murine IL-4 gene blocks Th2 cytokine responses. *Nature* **362**, 245-248 (1993).
5. Le Gros, G., Ben-Sasson, S.Z., Seder, R., Finkelman, F.D. & Paul, W.E. Generation of interleukin 4 (IL-4)-producing cells in vivo and in vitro: IL-2 and IL-4 are required for in vitro generation of IL-4-producing cells. *J Exp Med* **172**, 921-929 (1990).
6. Ben-Sasson, S.Z., *et al.* IL-1 acts directly on CD4 T cells to enhance their antigen-driven expansion and differentiation. *Proc Natl Acad Sci U S A* **106**, 7119-7124 (2009).
7. Bettelli, E., *et al.* Reciprocal developmental pathways for the generation of pathogenic effector TH17 and regulatory T cells. *Nature* **441**, 235-238 (2006).
8. Tacken, P.J. & Figdor, C.G. Targeted antigen delivery and activation of dendritic cells in vivo: Steps towards cost effective vaccines. *Semin Immunol* **23**, 12-20 (2010).
9. Palucka, K., Ueno, H. & Banchereau, J. Recent developments in cancer vaccines. *J Immunol* **186**, 1325-1331 (2010).
10. Natarajan, S. & Thomson, A.W. Tolerogenic dendritic cells and myeloid-derived suppressor cells: potential for regulation and therapy of liver auto- and alloimmunity. *Immunobiology* **215**, 698-703 (2010).
11. Mukherjee, G. & Diloranzo, T.P. The immunotherapeutic potential of dendritic cells in type 1 diabetes. *Clin Exp Immunol* **161**, 197-207 (2010).
12. Ehser, S., *et al.* Suppressive dendritic cells as a tool for controlling allograft rejection in organ transplantation: promises and difficulties. *Hum Immunol* **69**, 165-173 (2008).
13. Geijtenbeek, T.B., *et al.* Identification of DC-SIGN, a novel dendritic cell-specific ICAM-3 receptor that supports primary immune responses. *Cell* **100**, 575-585 (2000).
14. Adema, G.J., *et al.* A dendritic-cell-derived C-C chemokine that preferentially attracts naive T cells. *Nature* **387**, 713-717 (1997).
15. Triantis, V., *et al.* Identification and characterization of DC-SCRIPT, a novel dendritic cell-expressed member of the zinc finger family of transcriptional regulators. *J Immunol* **176**, 1081-1089 (2006).
16. Triantis, V., *et al.* Molecular characterization of the murine homologue of the DC-derived protein DC-SCRIPT. *J Leukoc Biol* **79**, 1083-1091 (2006).
17. Ansems, M., *et al.* DC-SCRIPT: nuclear receptor modulation and prognostic significance in primary breast cancer. *J Natl Cancer Inst* **102**, 54-68 (2010).
18. Hartgers, F.C., *et al.* DC-STAMP, a novel multimembrane-spanning molecule preferentially expressed by dendritic cells. *Eur J Immunol* **30**, 3585-3590 (2000).
19. Hartgers, F.C., *et al.* Genomic organization, chromosomal localization, and 5' upstream region of the human DC-STAMP gene. *Immunogenetics* **53**, 145-149 (2001).
20. Staeger, H., Brauchlin, A., Schoedon, G. & Schaffner, A. Two novel genes FIND and LIND differentially expressed in deactivated and Listeria-infected human macrophages. *Immunogenetics* **53**, 105-113 (2001).
21. Yagi, M., *et al.* DC-STAMP is essential for cell-cell fusion in osteoclasts and foreign body giant cells. *J Exp Med* **202**, 345-351 (2005).
22. Eleveld-Trancikova, D., *et al.* The dendritic cell-derived protein DC-STAMP is highly conserved and localizes to the endoplasmic reticulum. *J Leukoc Biol* **77**, 337-343 (2005).
23. Jansen, B.J., *et al.* OS9 interacts with DC-STAMP and modulates its intracellular localization in response to TLR ligation. *Mol Immunol* **46**, 505-515 (2009).
24. Litovchick, L., Friedmann, E. & Shaltiel, S. A selective interaction between OS-9 and the carboxyl-terminal tail of meprin beta. *J Biol Chem* **277**, 34413-34423 (2002).
25. Friedmann, E., Salzberg, Y., Weinberger, A., Shaltiel, S. & Gerst, J.E. YOS9, the putative yeast homolog of a gene amplified in osteosarcomas, is involved in the endoplasmic reticulum (ER)-Golgi transport of GPI-anchored proteins. *J Biol Chem* **277**, 35274-35281 (2002).

26. Eleveld-Trancikova, D., *et al.* DC-STAMP interacts with ER-resident transcription factor LUMAN which becomes activated during DC maturation. *Mol Immunol* **47**, 1963-1973 (2010).
27. Raggio, C., *et al.* Luman, the cellular counterpart of herpes simplex virus VP16, is processed by regulated intramembrane proteolysis. *Mol Cell Biol* **22**, 5639-5649 (2002).
28. Kukita, T., *et al.* RANKL-induced DC-STAMP is essential for osteoclastogenesis. *J Exp Med* **200**, 941-946 (2004).
29. Eleveld-Trancikova, D., *et al.* The DC-derived protein DC-STAMP influences differentiation of myeloid cells. *Leukemia* **22**, 455-459 (2008).
30. Sawatani, Y., *et al.* The role of DC-STAMP in maintenance of immune tolerance through regulation of dendritic cell function. *Int Immunol* **20**, 1259-1268 (2008).
31. Lutz, M.B., *et al.* An advanced culture method for generating large quantities of highly pure dendritic cells from mouse bone marrow. *J Immunol Methods* **223**, 77-92 (1999).
32. Lu, R., Yang, P., O'Hare, P. & Misra, V. Luman, a new member of the CREB/ATF family, binds to herpes simplex virus VP16-associated host cellular factor. *Mol Cell Biol* **17**, 5117-5126 (1997).
33. Jin, D.Y., *et al.* Hepatitis C virus core protein-induced loss of LZIP function correlates with cellular transformation. *EMBO J* **19**, 729-740 (2000).
34. DenBoer, L.M., *et al.* Luman is capable of binding and activating transcription from the unfolded protein response element. *Biochem Biophys Res Commun* **331**, 113-119 (2005).
35. Wen, A.Y., Sakamoto, K.M. & Miller, L.S. The role of the transcription factor CREB in immune function. *J Immunol* **185**, 6413-6419 (2010).
36. Kasahara, T., Yagisawa, H., Yamashita, K., Yamaguchi, Y. & Akiyama, Y. IL1 induces proliferation and IL6 mRNA expression in a human astrocytoma cell line: positive and negative modulation by chorela toxin and cAMP. *Biochem Biophys Res Commun* **167**, 1242-1248 (1990).
37. Isshiki, H., *et al.* Constitutive and interleukin-1 (IL-1)-inducible factors interact with the IL-1-responsive element in the IL-6 gene. *Mol Cell Biol* **10**, 2757-2764 (1990).
38. Schindler, R., *et al.* Correlations and interactions in the production of interleukin-6 (IL-6), IL-1, and tumor necrosis factor (TNF) in human blood mononuclear cells: IL-6 suppresses IL-1 and TNF. *Blood* **75**, 40-47 (1990).
39. Xing, Z., *et al.* IL-6 is an antiinflammatory cytokine required for controlling local or systemic acute inflammatory responses. *J Clin Invest* **101**, 311-320 (1998).
40. Kobayashi, Y., *et al.* Identification of calcium-activated neutral protease as a processing enzyme of human interleukin 1 alpha. *Proc Natl Acad Sci U S A* **87**, 5548-5552 (1990).
41. Thornberry, N.A., *et al.* A novel heterodimeric cysteine protease is required for interleukin-1 beta processing in monocytes. *Nature* **356**, 768-774 (1992).
42. Smith-Garvin, J.E., Koretzky, G.A. & Jordan, M.S. T cell activation. *Annu Rev Immunol* **27**, 591-619 (2009).
43. Humphreys, N.E. & Grencis, R.K. IL-1-dependent, IL-1R1-independent resistance to gastrointestinal nematodes. *Eur J Immunol* **39**, 1036-1045 (2009).
44. Corinti, S., Albanesi, C., la Sala, A., Pastore, S. & Girolomoni, G. Regulatory activity of autocrine IL-10 on dendritic cell functions. *J Immunol* **166**, 4312-4318 (2001).
45. Liu, H., Hu, B., Xu, D. & Liew, F.Y. CD4+CD25+ regulatory T cells cure murine colitis: the role of IL-10, TGF-beta, and CTLA4. *J Immunol* **171**, 5012-5017 (2003).
46. Allez, M. & Mayer, L. Regulatory T cells: peace keepers in the gut. *Inflamm Bowel Dis* **10**, 666-676 (2004).

CHAPTER 5

Analysis of genes regulated by the transcription factor LUMAN identifies ApoA4 as a target gene in dendritic cells

**Sanecka A, Ansems M, van Hout-Kuijer MA,
Looman MW, Prosser AC, Welten S, Gilissen C,
Sama IE, Huynen MA, Veltman JA, Jansen BJ,
Eleveld-Trancikova D, Adema GJ**

*Molecular Immunology (2011),
doi:10.1016/j.molimm.2011.12.003*

Abstract

Dendritic cells (DCs) are professional antigen presenting cells of the immune system that play a crucial role in initiating immune responses and maintaining self tolerance. Better understanding of the molecular basis of DC immunobiology is required to improve DC-based immunotherapies. We previously described the interaction of transcription factor LUMAN (also known as CREB3 or LZIP) with the DC-specific transmembrane protein DC-STAMP in DCs. Target genes of LUMAN and its role in DCs are currently unknown. In this study we set out to identify genes regulated by LUMAN in DCs using microarray analysis. Expression of a constitutively active form of LUMAN in mouse DC cell line D2SC/1 identified Apolipoprotein A4 (ApoA4) as its target gene. Subsequent validation experiments, bioinformatics-based promoter analysis, and silencing studies confirmed that ApoA4 is a true target gene of LUMAN in bone marrow-derived DCs (BMDCs).

Introduction

Dendritic cells (DCs) are key regulators of immunological responses in our body. They bridge the innate and adaptive immune systems, and maintain the balance between immunity and tolerance¹. DCs are particularly abundant in tissues forming the interface with the external environment. They constantly monitor the extracellular space detecting incoming pathogens. Antigen uptake in the presence of inflammation and danger signals results in DC maturation². The transition from immature to a mature state involves physiological, functional and morphological changes. Many of them are driven by transcription factors (TFs). To allow fast reprogramming, DCs make use of so-called “ready to go” transcription factors which are present in immature DCs in an inactive state. Binding of pathogen associated molecular patterns (PAMPs) to pattern recognition receptors (PRRs) leads to the initiation of signaling cascades and the subsequent activation of TFs such as NFκβ. In immature DCs, NFκβ is sequestered in the cytoplasm by binding to an inhibitor. Its activation is achieved through stimulus-responsive proteolysis of the inhibitors³. All known PAMPs and the resulting inflammatory cytokines are potent activators of the NF-κB pathway⁴.

Recently we described the interaction of DC-STAMP with the transcription factor LUMAN (CREB3/LZIP) in DCs⁵. LUMAN belongs to the bZIP superfamily of TFs and is the prototype member of the CREB3 subfamily⁶. The physiological roles of LUMAN were primarily deduced through overexpression studies conducted in cultured cells and LUMAN interaction partners⁷. LUMAN was reported to interact with transcriptional coactivator HCF1⁸, hepatitis C virus core protein⁹ and CC chemokine receptor 1¹⁰. Messenger RNA of LUMAN is ubiquitously expressed while the protein was shown to be expressed only in trigeminal ganglionic neurons and in monocytes^{10,11}. We recently have reported expression of LUMAN at the protein level in DCs and have shown that LUMAN is activated upon DC maturation⁵. The inactive form of LUMAN resides in the endoplasmic reticulum (ER) of immature DCs. LUMAN is activated in a process called regulated intramembrane proteolysis (RIP), which involves translocation to the Golgi compartment and subsequent proteolytic cleavage¹². Upon RIP, the cleaved active form of LUMAN can translocate to the nucleus to regulate gene expression. Currently, target genes of LUMAN in DCs are not known.

To investigate the role of the DC-STAMP/LUMAN pathway in DCs we set out to find target genes of LUMAN. For this purpose, we overexpressed the active form of LUMAN in the mouse DC cell line (D2SC/1) using retroviral gene delivery. Altered

gene expression was studied using microarray-based expression profiling. Amongst the surprisingly low number of differentially expressed genes identified, we here report ApoA4 as a direct target gene of LUMAN in mouse bone marrow-derived DCs (mBMDCs).

Material and methods

Cell lines and cell culture

The human embryonic kidney cell line HEK293 was cultured in DMEM (Invitrogen) supplemented with 10% heat-inactivated FCS (Greiner Bio-One), 1% of non-essential amino acids (NEAA) (Invitrogen) and 0.5% antibiotic-antimycotic (Invitrogen). The mouse embryonic fibroblast cell line NIH3T3 was cultured in DMEM supplemented with 5% heat-inactivated FCS, and 0.5% antibiotic-antimycotic. HEK293FT cells (Invitrogen) were cultured in DMEM supplemented with 10% heat-inactivated FCS, 1% NEAA, 0.5% antibiotic-antimycotic, 1% ultra-glutamine (Lonza), and 1 mM sodium pyruvate (Invitrogen). Cells were kept under selection with 500 µg/ml of Geneticin (G418) (Invitrogen). Phoenix packaging cells were cultured in IMDM (Invitrogen) supplemented with 5% heat-inactivated FCS and 0.5% antibiotic-antimycotic. D2SC/1 cells were cultured in IMDM supplemented with 5% heat-inactivated FCS and 0.5% antibiotic-antimycotic.

Generation of bone marrow-derived DCs and stimulations

Mouse BMDCs were generated from bone marrow progenitor cells, according to the modified protocol of Lutz *et al.*¹³. Bone marrow cells were flushed from the femurs and tibias of 6- to 8-week-old female C57BL/6 mice (Charles River WIGA GmbH), washed and counted. Cells were plated at a concentration of 4×10^6 cells per 10 cm Petri dish in 13 ml of RPMI-1640 medium (Invitrogen) supplemented with 10% FCS, 1% ultra-glutamine, 28 µM of β-mercaptoethanol (Sigma-Aldrich), 0.5% antibiotic-antimycotic and 20 ng/ml of murine recombinant GM-CSF (PeproTech). After 3 days, 4 ml of fresh medium was added containing fresh GM-CSF to final concentration of 8.75 ng/ml. For transduction experiments non-adherent and loosely adherent cells at day 6 of culture were used. For activation of endogenous LUMAN non-adherent and loosely adherent cells at day 7 of culture were harvested and plated in 12 well culture plates (Corning) 10^6 cells/well in 1.5 ml of mBMDC culture medium. Different concentrations of Brefeldin A (BFA), tunicamycin (Tm) and thapsigargin (TG) were tested (all from Sigma) for optimal induction of ApoA4 expression without severely influencing the vitality of the cells (data not shown).

Retroviral supernatants and transduction of D2SC/1 cells

pLZRS-IRES-ΔNGFR and pLZRS-EGFP-IRES-ΔNGFR vectors were kindly provided by J.H. Jansen from Central Hematology Laboratory, RUNMC, Nijmegen, the Netherlands¹⁴. Murine LUMANDp (aa 1–238) was cloned into pLZRS-IRES-ΔNGFR retroviral expression vector. The IRES (internal ribosomal entry site) allows for separate expression of LUMANDp or GFP and

a truncated version of the nerve growth factor receptor (Δ NGFR) that lacks intracellular domains. Phoenix packaging cells were transfected with expression vectors using polyethylenimine (PEI) (Polysciences) as a transfection agent. At day 3 after transfection cells were harvested, replated for expansion and kept under selection of puromycin (1 μ g/ml) for 5 days. Next, cells were harvested and replated for virus production in medium without puromycin for 24 h. Supernatant was collected, cell debris was removed by centrifugation and supernatant containing virus particles was filtered through a 0.45 μ m filter. Aliquots were stored at -80°C until use.

For transduction, cells were cultured on retronectin (Takara Bio Inc., Japan) coated 35 mm Petri dishes together with 2 ml of thawed virus containing supernatant for indicated time and then washed with PBS. The percentage of GFP⁺ and Δ NGFR⁺ cells after transduction was monitored by FACS analysis (BD FACSCalibur Flow Cytometer). tNGFR expression was detected using the supernatant of the 20.4 hybridoma (American Type Culture Collection) producing anti-human NGFR antibody. Expression of LUMANDp was confirmed by qPCR.

RNA isolation for microarray, quality control, and microarray hybridization

Total RNA was isolated from D2SC/1 cells using the RNeasy Mini kit (Qiagen) according to the manufacturer's protocol. The quality of RNA was tested using the Agilent2100 Bioanalyzer following the manufacturer's protocol. All samples had a 28S:18S ration >1.5 , thus passing quality standards for further processing. Two micrograms of total RNA was labeled according to the GeneChip Whole Transcript (WT) Sense Target Labeling Assay as provided by the manufacturer (Affymetrix, Santa Clara, CA), and hybridized to Mouse Exon 1.0 ST Arrays overnight before scanning in on Affymetrix GCS 3000 7G scanner. The Mouse Exon 1.0 ST Array contains $\sim 1,200,000$ probe sets with an average of 4 probes per exon and an average of about 40 probes per gene. All hybridizations were carried out at the Microarray Facility of the Department of Human Genetics, Nijmegen Centre of Molecular Life Sciences, Radboud University Nijmegen Medical Centre, Nijmegen, the Netherlands.

Analysis of microarrays

The Affymetrix CEL files were imported into Affymetrix Expression Console version 1.1 where control probes were extracted using the default RMA algorithm in order to perform quality analysis checks. The area under the curve (AUC) of the receiver operator characteristic was calculated using the positive and negative control probes. All arrays had an AUC score above the empirically defined threshold of 0.85 indicating a good separation of the positive controls from the negative control probes. Subsequently, CEL files were imported into Partek (Partek Genomic Suite software, version 6.4; Partek Inc., St. Louise, MO) where only core exons were extracted and normalized using the RMA algorithm with GC background correction. Core transcript intensities were calculated by calculating the mean \log_2 intensities of the corresponding probe sets.

Lentiviral supernatants and transduction of mBMDCs

Two SureSilencing shRNA plasmids encoding the shRNA sequence targeting murine LUMAN: shLUMANred (5'-GGAGATGTCTAGGCTGATACT-3'), shLUMANgreen (5'-GCCGAGGAAGATTCG-

TAACAA-3') and negative control Scrambled shRNA (shScr) (5'-GGAATCTCATTCGATGCAT-AC-3') plasmid were obtained from SuperArray Bioscience. Using Gateway technology, DNA encoding sequences for short-hairpin BLOCK-iT-U6-RNAi Entry vector were introduced into the pLenti6/BLOCK-iT-DEST vector (Invitrogen), following the manufacturer's protocol. cDNA encoding for murine full length LUMAN (LUMANfl), murine dominant positive form of LUMAN (LUMANDp) (aa 1–238) and GFP were introduced to the pLenti6/V5-DEST Gateway Vector (Invitrogen) using pENTR-1A vector (Invitrogen).

The individual vectors were co-transfected with packaging vectors into the HEK293FT cells according to the manufacturer's instructions. Virus was produced in HEK293FT culture medium supplemented with 82.5 µg/ml of water-soluble cholesterol (Sigma-Aldrich) and collected from tissue culture supernatant 24 and 48 hours after transfection. Cell debris was removed by centrifugation and supernatant containing virus particles was filtered through a 0.45 µm filter. Aliquots were stored at -80°C until use.

Viral titers were determined by transduction of NIH3T3 cells with serial dilutions of the virus stock in the presence of 10 µg/ml of polybrene (Sigma-Aldrich). Two days after transduction the cells were cultured under selection with 2 µg/ml Blasticidin (Invitrogen) for 12 days. Medium was refreshed every third day. To determine the titer, the number of colonies was determined after crystal violet staining. The titer ranged between 2×10^5 and 13×10^5 transfection units (TU)/ml

Lentiviral knock-down and overexpression of LUMAN in mBMDCs

Mouse BMDCs were harvested after 6 days of culture and 1.2×10^6 cells were resuspended in 700 µl of virus supernatant containing 10 µg/ml of DEAE-dextran (Pharmacia Biotech AB) to facilitate viral infection. Cell-virus suspensions were plated on 12-well tissue culture plates (700 µl/well) and centrifuged for 90 minutes at 2200 rpm and 37°C. After centrifugation, virus supernatant was replaced by mBMDC culture medium. The infection procedure was repeated the following day. As a negative control, mBMDC culture medium with DEAE-dextran was used. The multiplicity of infection (MOI) for silencing of LUMAN was matched with the MOI of the scrambled shRNA control in each experiment.

RNA isolation and quantitative real-time PCR (qPCR)

Total RNA was isolated from at least 6×10^5 cells using a Quick-RNA MiniPrep kit (Zymo Research). RNA quantity and purity were determined using a NanoDrop spectrophotometer. Two micrograms of total RNA were treated with DNase-I (Invitrogen) and cDNA was synthesized using random primers and SuperScript Moloney murine leukemia virus reverse transcriptase (II-MMLV) (Invitrogen). Messenger RNA levels for the genes of interest were determined with a Bio-rad CFX96 (Bio-rad) using Fast Start SYBR Green kit (Roche) and primers for one of the following genes: porphobilinogen deaminase (PBGD) (forward: 5'-CCTACCATACTACCTCCTG-GCTT TAC-3'; reverse: 5'-TTTGGGTGAAAGACAACAGCAT-3'), LUMAN (forward: 5'-AC AAC-TACTCCCTTCCACAG-3'; reverse: 5'-TTCTCCAAGAGCTTCTTCTC-3'), ApoA4 (forward: 5'-CCAATGTGGTGTGGGATTACTT-3'; reverse: 5'-CCTCTCAGT TTCCTTGGCTAGA-3'). Data were analyzed with Bio-rad CFX manager version 1.6 (Bio-rad) and checked for correct amplifica-

tion and dissociation of the products. PBGD served as a reference gene. mRNA levels relative to PBGD were calculated as: $2^{-(\Delta Ct)}$.

Promoter analysis of the apolipoprotein cluster

Putative promoter regions extending 2 kb upstream of the transcription start site (TSS) of mouse apolipoproteins (apoa5, apoc3, apoa1 and apoa4) were extracted from the Genome Browser track of the UCSC July 2007 mouse genome assembly [<http://genome.ucsc.edu>]¹⁵. The genomic coordinates of the promoter regions used are as follows: apoa5 (chr9: 46074691–46076690); apoc3 (chr9: 46043381–46045380); apoa1 (chr9: 46034713–46036712) and apoa4 (chr9: 46046927–46048926), all on mouse chromosome 9. From the same genome browser track, 2 kb promoter sequences of all reference genes in the mouse genome were obtained. Subsequently, the algorithm Clover¹⁶ was used to screen for over-represented transcription factor binding sites (TFBSs) in the apolipoprotein promoter sequences using a pre-compiled library of TFBS motifs. The library contained 521 TFBS motifs (position-specific weight matrices) culled from the JASPAR core database (2005)¹⁷ and TRANSFAC version 7.0 database¹⁸. Our inputs to the Clover algorithm were the following: promoter sequences of the apolipoproteins (2 kb upstream of the TSS of their corresponding genes) as test set of sequences; the 521 TFBS motifs for screening; and for statistical calculations, promoter sequences (2 kb upstream of the TSS) of all genes in the mouse genome were used as background. All results obtained were filtered at a TFBS instance threshold score ≥ 5 for recognizing a specific TFBS, and a significant p-value ≤ 0.05 for over-represented motifs in the test set of sequences relative to the background. An instance score > 0 indicates a better match of a test sequence to a TFBS motif than randomly expected.

Phylogenetic conservation of the same 2 kb promoter region upstream of the TSS of the reference genes of mouse apoa5, apoc3, apoa1 and apoa4 were downloaded (November 2011) from the Phastcons tract, phastCons30wayPlacental, of the July 2007 mouse genome assembly of UCSC genome browser. Phastcons scores range from 0 to 1, the higher the score the more conserved a nucleotide base¹⁹. The conservation tract for placental mammals was used to observe the extent of conservation of predicted TFBS sites in the apolipoprotein promoter regions. Depiction of the TFBS sites so-obtained in the promoter sequences of the apolipoproteins was further performed using inhouse Python scripts.

Results

Identification of ApoA4 as a potential target gene of LUMAN

We previously reported on the interaction of DC-STAMP with the transcription factor LUMAN expressed in DCs⁵. To investigate this novel pathway in DCs we set out to identify potential target genes of LUMAN.

A mouse DC cell line (D2SC/1)^{20,21} was retrovirally transduced to overexpress the dominant positive form of LUMAN (LUMANdp). Transduction efficiency was between 35 and 60% as determined by FACS analysis 18 h post transduction (data not shown).

Altered gene expression between D2SC/1 cells transduced with either LUMANDp or with a control GFP vector was examined using a mouse exon microarray. Gene expression was analyzed at 0, 6 and 18 h after transduction. Pairwise comparisons between the LUMANDp samples and the GFP samples for 6 h and 18 h time points were made using the following criteria; one of the two expression values (log 2) is >5.0 (i.e. the gene is expressed), and the gene shows a 2 or more fold difference in expression relative to GFP.

Surprisingly, the number of differentially expressed genes was low at both time points (Supplementary Table 1). At 6 h after transduction only 40 differentially expressed genes were found of which 25 were upregulated and 15 downregulated in LUMANDp samples in comparison to the GFP samples. At 18 h post transduction 39 genes were upregulated and 24 genes downregulated of which only one gene was present at the 6 h time point. Although LUMAN mRNA expression was clearly upregulated in cells transduced with LUMANDp retrovirus at 6 and 18 h post-transduction (Fig. 1A), the 6 h post transduction time point was supposedly too early for active LUMANDp protein expression and/or function.

Herp and EDEM genes that were previously reported as the target genes of LUMAN in HeLa and HEK293 cell lines, respectively^{22,23} were not differentially expressed in D2SC/1 cells overexpressing active form of LUMAN (Fig. 1A). One of the most strongly upregulated genes at the 18 h time point was Apolipoprotein A4 (ApoA4) (Fig. 1A). Since apolipoproteins have been frequently implicated in regulation of immune responses²⁴⁻²⁸ we set out to verify the ApoA4 gene as a LUMAN target gene in DCs.

Validation of the microarray was performed by real-time quantitative PCR (qPCR) using both the microarray samples (Exp1) and samples from an independent experiment (Exp2). Besides the 6 and 18 h time points, which were taken for microarray analysis, for qPCR analysis we also took along 24 h samples. In correlation with the microarray results, levels of LUMAN mRNA were increased more than 4 times 6 h after transduction with LUMANDp (Fig. 1B). The strong upregulation of ApoA4 mRNA was detected at 18 h and 24 h post-transduction with the active form of LUMAN confirming the microarray data (Fig. 1B). Consistent with the microarray data, no effect on the EDEM and Herp genes expression was observed (data not shown). These data suggest that ApoA4, but not Herp and EDEM gene expression, is regulated by LUMANDp in murine DCs.

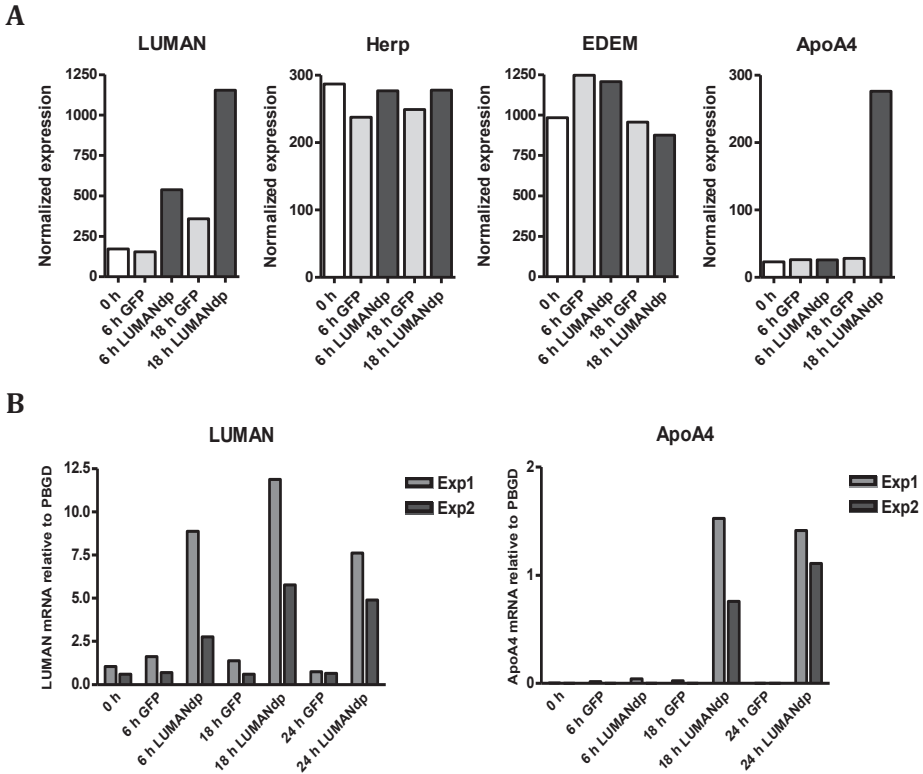


Figure 1. ApoA4 is upregulated upon overexpression of LUMANdp. D2SC/1 cells were infected with retrovirus to overexpress active form of LUMAN (LUMANdp) or GFP as a negative control. **A)** Data represent normalized gene expression of LUMAN, Herp, EDEM and ApoA4 mRNA at 0, 6 and 18 hours post transduction on mouse exon microarray. **B)** Validation of microarray experiment by qPCR, samples from experiment used for microarray (Exp1) and independent experiment (Exp2) were tested for mRNA expression of LUMAN and ApoA4. Data represent expression of LUMAN and ApoA4 mRNA at 0, 6, 18 and 24 hours post transduction in relation to PBGD.

LUMAN specifically regulates Apolipoprotein A4 expression

ApoA4 is a member of the apolipoprotein family. It forms a gene cluster together with ApoA1, ApoC3 and ApoA5 on chromosome 9 in the mouse^{29,30} (Fig. 2A). Other apolipoprotein family members such as ApoE are similar in structure and function to ApoA4 although they are located in a distinct gene cluster³¹. The microarray data from D2SC/1 cells transduced with the dominant positive form of LUMAN were therefore analyzed for altered expression of the apolipoprotein family genes. From the whole apolipoprotein family, only ApoA4 mRNA expression levels were affected by LUMANdp expression (Fig. 2B). These results were confirmed independently

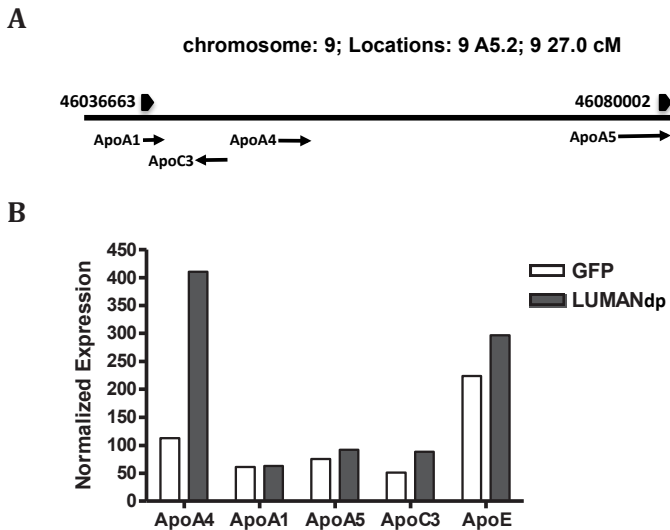


Figure 2. ApoA4 upregulation upon overexpression of LUMANDp is specific for ApoA4 in apolipoprotein family. A) Representation of apolipoproteins cluster on murine chromosome 9. B) Normalized expression of apolipoprotein family genes 18 hours post transduction in microarray samples (legend of the Fig. 1A).

by qPCR on both the microarray samples and samples from another independent experiment (data not shown).

To determine if ApoA4 is an immediate downstream target of the transcription factor LUMAN, the promoter of mouse ApoA4 and its gene cluster was examined for the presence of the previously published LUMAN binding sites CREB and C/EBP^{6,8,9,23} using bioinformatics approaches. Analysis identified the CREB site, Tax/CREB, in the proximity of the start of ApoA4 transcription (Fig. S1). Tax is a transactivator protein of the human T-cell lymphotropic virus type I (HTLV-I) whose binding to the ubiquitous transcriptional factor, CREB, has been shown to lead to the formation of a multiprotein complex with far greater DNA recognition specificity than that of CREB alone³². Binding sites for C/EBP, which has been shown to enhance transcription from CRE site⁸, were also present in the promoter region of ApoA4 (Fig. S1). The promoters of the other apolipoprotein family genes examined did not contain this unique combination of CREB and C/EBP sites (Fig. S1), although individual sites are represented in some of the other apolipoprotein promoter sequence(s) (Fig. S1). Further bioinformatics analysis of the mouse ApoA4 promoter region indicates that the Tax/CREB binding site within 500 bp upstream of the TSS is strongly conserved

in placental mammals (Fig. S1). Some phylogenetic conservation of C/EBP and Tax/CREB binding sites was also discerned. Collectively, our data show that only ApoA4 and none of the other apolipoprotein family members examined contain conserved consensus binding sites to which LUMAN could bind.

Overexpression of the active form of LUMAN results in ApoA4 expression in mBMDC

Further investigation into the role of LUMAN in the regulation of ApoA4 expression was carried out in primary mouse bone marrow-derived dendritic cells (mBMDCs). Lentiviral transduction of mBMDCs for the overexpression of LUMAN protein was optimized to yield $\pm 30\%$ positive mBMDCs (data not shown). The effectiveness of transduction for LUMAN was confirmed by qPCR (Fig. 3A). Murine BMDCs were transduced with lentivirus encoding the dominant positive form of LUMAN (LUMANdp), the full length LUMAN (LUMANfl) or GFP as negative controls. Up to 9 fold increase in LUMAN mRNA levels was observed in cells transduced with virus encoding either the full length or the active form of LUMAN compared to endogenous LUMAN expression in cells transduced with GFP (Fig. 3A). Subsequently, we investigated the expression of ApoA4 mRNA in mBMDCs transduced with LUMAN. ApoA4 mRNA was detected only in mBMDCs transduced with the active form of LUMAN (Fig. 3B), indicating that ApoA4 is also a target of LUMAN in primary mBMDCs. Overexpression of the LUMANfl did not result in ApoA4 expression demonstrating that activation of LUMAN is necessary to induce ApoA4 expression.

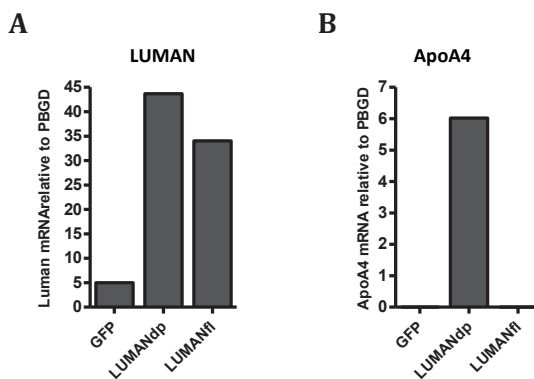


Figure 3. ApoA4 is expressed in mBMDC expressing LUMANdp but not LUMANfl. mBMDC were infected with lentivirus to overexpress full length LUMAN (LUMANfl), active form of LUMAN (LUMANdp) or GFP (control). Expression of LUMAN and ApoA4 transcripts was determined using qPCR. Data represent expression relative to PBGD. Data shown are representative for at least three independent experiments

Brefeldin A (BfA) induced activation of endogenous LUMAN protein results in ApoA4 induction

Brefeldin A (BfA) has been persistently shown to promote LUMAN cleavage by inducing fusion of ER to the Golgi apparatus^{12,33,34}. Therefore, induction of ApoA4 expression following BfA exposure of mBMDC endogenously expressing LUMAN was investigated in time (Fig. 4A). Low levels of ApoA4 mRNA were first observed at 12 h after treatment with 1 μ g/ml BfA. This expression was further elevated in later time points up to 20 h (Fig. 4A). Several reports^{12,23,35,36} indicated that LUMAN, in contrast with other bZIP TFs is not activated by ER stress. Indeed, treatment of mBMDC with the ER stressors thapsigargin (TG) and tunicamycin (Tm) does not result in ApoA4 expression (Fig. 4B).

To study the contribution of LUMAN in BfA mediated induction of ApoA4 we performed LUMAN knock down experiment in mBMDC. mBMDC were transduced with lentivirus encoding for LUMAN targeting shRNA or a non-targeting scrambled control sequence (shScr). Lentiviral infection did not result in maturation of mBMDCs (data not shown). Two different shRNAs targeting different sequences of LUMAN were used; shLUMANred and shLUMANGreen, which resulted in LUMAN mRNA knock-down of 90% and 60%, respectively (Fig. 5A). Luman knock-down mBMDC showed a significant decrease in induction of ApoA4 in response to BfA treatment. Moreover, the decrease in ApoA4 expression was correlated with the level of LUMAN knock-down efficiency resulting in lower ApoA4 mRNA levels (Fig. 5B). Taken together, these data demonstrate that BfA treatment of mBMDCs leads to expression of ApoA4 mRNA. By silencing LUMAN we proved that this ApoA4 expression is driven by the activation of the transcription factor LUMAN.

Discussion

Herein we investigated the target genes of LUMAN in DCs using overexpression of the active form of LUMAN in D2SC/1 cells. The microarray analysis indicated ApoA4 as a potential target gene of LUMAN. The validation experiments, bioinformatics analysis of ApoA4 promoter, as well as overexpression and silencing studies in mBMDC confirmed that ApoA4 is a direct target gene of the transcription factor LUMAN in DCs. Expression of the other genes of the apolipoprotein family was not affected by LUMAN. As ApoA4 is considered an anti-inflammatory agent in the immune system, its induction by LUMAN suggests a role for LUMAN in quenching inflammation.

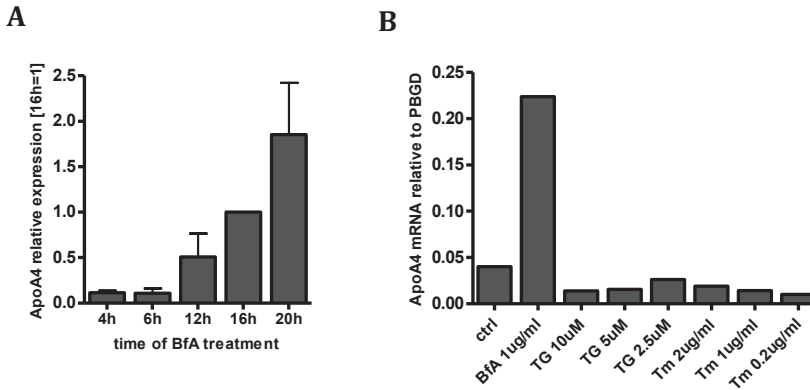


Figure 4. Activation of endogenous Luman in mBMDC with BfA. **A)** ApoA4 expression in mBMDC treated with 1ug/ml of BfA was determined by qPCR. Expression level at 16 hours of BfA treatment was set at one. Data represent mean \pm SEM of three independent experiments. **B)** mBMDC were treated for 16h with indicated concentrations of BfA, taspigargin (Tg) or Tunicamycin (Tm). ApoA4 expression was measured by qPCR. Data represent expression relative to PBGD. Data shown are representative of three independent experiments.

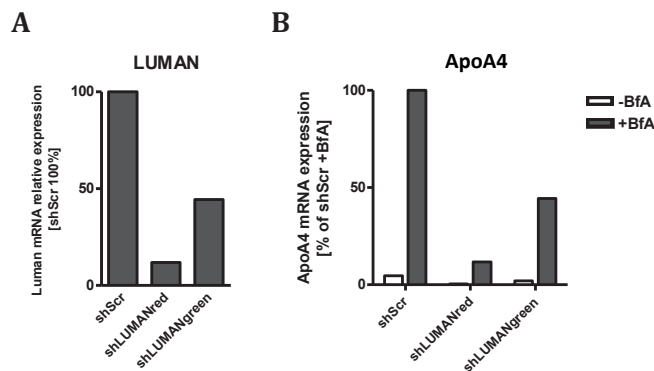


Figure 5. Silencing of LUMAN attenuates the BfA driven expression of ApoA4. mBMDC were infected with lentivirus expressing shRNA targeting LUMAN (shLUMANred, shLUMANGreen) or control shRNA (shScr). **A)** Silencing efficiency was confirmed by qPCR. Data represent LUMAN expression in cells targeted with LUMAN-specific shRNAs relative to shScr; **B)** Effect of LUMAN silencing on ApoA4 expression upon BfA treatment was determined in mBMDCs targeted with shRNA. Levels of ApoA4 mRNA are shown on the graph in relation to levels in shScr +BfA sample. Data shown are representative of at least three independent experiments.

A surprisingly low number of genes was differentially expressed upon overexpression of the active form of LUMAN in D2SC/1 cells. We observed less than 70 differentially expressed genes. Interestingly, overexpression of another bZIP family transcription factor XBP1 in muscle cells resulted in about 500 differentially expressed genes³⁷. On the other hand, expression of active form of ATF6 in HeLa cells or full length LUMAN protein in HEK 293 cell line were also shown to result in a low number of differentially expressed genes^{22,38}. In our study we have used the active form of LUMAN in DCs instead of natural stimuli to activate full length LUMAN. This may have led to the relatively low number of differentially expressed genes observed. Signals that activate LUMAN may be necessary for activation or recruitment of other regulatory proteins that co-operate with LUMAN in transcriptional regulation. This way we may have selected for those genes that are regulated by LUMAN *per se* and do not require other transcription factors, that may be induced by the natural stimuli activating the LUMAN pathway. We have previously shown LUMAN activation upon maturation of human DCs⁵. Unfortunately, no antibodies detecting endogenous mouse LUMAN are currently available to confirm this finding in mice.

Several lines of evidence indicate that ApoA4 is a direct, physiological target of LUMAN in murine DCs. First, expression profiling and qPCR analyses of D2SC/1 cells and mBMDCs indicated that ApoA4 expression is induced upon overexpression of the dominant positive form of LUMAN. Second, we found CREB and C/EBP binding sites within the 2 kb promoter region of murine ApoA4 gene. These sites have previously been shown to promote LUMAN binding⁸. The combination of CREB and C/EBP binding sites was unique for the ApoA4 promoter in the group of apolipoprotein promoters analyzed. The identification of a high-scoring and phylogenetically conserved (in mammals) CREB site within 500 bp of the transcription start site of ApoA4 is interesting because TFBS at such regions have been found to be highly conserved amongst mammals, and are likely to be functional^{39,40}. However, to confirm if this predicted site in ApoA4 promoter is indeed bound by LUMAN, chromatin immunoprecipitation or luciferase assay based studies will be necessary. Of note analysis of the promoter region of human apolipoproteins indicates that, despite its conservation in placental mammals, this particular CREB site was not found in the promoter region of human APOA4.

Third, we found that ApoA4 expression is induced by Brefeldin A treatment, which was shown to activate the cleavage and activation of LUMAN^{5,12,33,34}. Moreover, shRNA-mediated silencing of LUMAN dramatically reduced the BfA-induced expression of ApoA4. Confirmation of the induction of murine ApoA4 on protein

level awaits the development of anti mouse ApoA4 antibodies.

ApoA4 belongs to apolipoprotein family of lipid binding proteins which play an important role in lipid transport and metabolism⁴¹⁻⁴⁶. Members of this family have been implicated in regulation of the immune responses and many autoimmune diseases²⁴⁻²⁸. ApoE was reported to enhance endogenous lipid antigen presentation and subsequent NKT cell activation²⁵. ApoA1 was shown to modulate immune cell function by regulating cellular cholesterol balance²⁸. ApoA4 is located within the same gene cluster on the chromosome 9 with ApoA1, ApoC3 and ApoA5⁴⁷. ApoA4 expression was also found in peripheral blood mononuclear cells (PBMCs) of systemic lupus erythematosus (SLE) patients⁴⁸. Interestingly, ApoA4 was shown to reduce secretion of proinflammatory cytokines from human PBMCs⁴⁹ suggesting that ApoA4 may be part of an anti-inflammatory feedback loop. We have previously shown a functional interaction of LUMAN with DC-STAMP in human monocyte-derived DCs and reported LUMANS activation upon maturation of DCs⁵. Timing of LUMAN activation at late time points (16 h) after TLR ligation is in line with potential negative feedback properties. Herein we revealed ApoA4 as a novel target gene of LUMAN in DCs. Therefore, it is tempting to speculate that ApoA4 induction by the DC-STAMP/LUMAN pathway is part of a negative feedback loop used by DCs to resolve inflammation. In line with this anti-inflammatory role of ApoA4, our recent results demonstrated that DC-STAMP knock-down mBMDCs secrete less IL-6, IL-12, TNF- α and IL-10 and showed impaired T-cell activation potential⁵⁰.

LUMAN belongs to the bZIP family of transcription factors many of which become activated during ER-stress and participate in the unfolded protein response (UPR)^{51,52}. Multiple reports suggested that LUMAN is not activated by the ER stress^{12,23,35,36}, although others suggested that LUMAN can take part in UPR by regulating expression of EDEM and Herp proteins that are involved in aspects of ER-associated degradation (ERAD)^{22,23}. In our experiments LUMANdp did not effect expression of EDEM and Herp in DCs. Rather, ApoA4 expression was induced by the LUMAN activator BfA but was not detected following ER-stress in mBMDCs. This finding is in line with our data in human DC that LUMAN is not activated by ER-stressors, e.g., thapsigargin or tunicamycin (data not shown). These data suggest that activation of LUMAN as well as pool of genes regulated by LUMAN may differ between different cell types.

Recently, the liver-specific homologue of LUMAN, CREB-H was shown to regulate ApoA4 gene expression⁵³. Other apolipoprotein genes located on chromosome 9 were unaffected by overexpression of active form of CREB-H in liver, like we show for

LUMAN in DCs. As CREB-H's DNA-binding domain (b-ZIP region) is most homologous to that of LUMAN (84%)⁵⁴, it is tempting to speculate that CREB-H and LUMAN bind to the same region in ApoA4 promoter in liver tissue and DC respectively.

Additionally, CREB-H was also shown to be activated by LPS and proinflammatory cytokines⁵² implicating its involvement in cross-talk between ER-stress and innate immune pathways. Further research is necessary to fully understand the role of LUMAN in ER-stress and its link to innate immune response pathways.

Acknowledgements

This work was financially supported by VICI grant 918-66-615 (awarded to G.J.A.) from the Netherlands Organization for Scientific Research (NWO). IS was supported by the Virgo consortium, an Innovative Cluster approved by the Netherlands Genomics Initiative and partially funded by the Dutch government (BSIK 03012), The Netherlands.

References

1. Banchereau, J. & Steinman, R.M. Dendritic cells and the control of immunity. *Nature* **392**, 245-252 (1998).
2. Reis e Sousa, C. Dendritic cells as sensors of infection. *Immunity* **14**, 495-498 (2001).
3. Baeuerle, P.A. & Baltimore, D. Activation of DNA-binding activity in an apparently cytoplasmic precursor of the NF-kappa B transcription factor. *Cell* **53**, 211-217 (1988).
4. Baldwin, A.S., Jr. The NF-kappa B and I kappa B proteins: new discoveries and insights. *Annu Rev Immunol* **14**, 649-683 (1996).
5. Eleveld-Trancikova, D., et al. DC-STAMP interacts with ER-resident transcription factor LUMAN which becomes activated during DC maturation. *Mol Immunol* **47**, 1963-1973 (2010).
6. Burbelo, P.D., et al. LZIP-1 and LZIP-2: two novel members of the bZIP family. *Gene* **139**, 241-245 (1994).
7. Chan, C.P., Kok, K.H. & Jin, D.Y. CREB3 subfamily transcription factors are not created equal: Recent insights from global analyses and animal models. *Cell Biosci* **1**, 6 (2011).
8. Lu, R., Yang, P., O'Hare, P. & Misra, V. Luman, a new member of the CREB/ATF family, binds to herpes simplex virus VP16-associated host cellular factor. *Mol Cell Biol* **17**, 5117-5126 (1997).
9. Jin, D.Y., et al. Hepatitis C virus core protein-induced loss of LZIP function correlates with cellular transformation. *EMBO J* **19**, 729-740 (2000).
10. Ko, J., et al. Human LZIP binds to CCR1 and differentially affects the chemotactic activities of CCR1-dependent chemokines. *FASEB J* **18**, 890-892 (2004).
11. Lu, R. & Misra, V. Potential role for luman, the cellular homologue of herpes simplex virus VP16 (alpha gene trans-inducing factor), in herpesvirus latency. *J Virol* **74**, 934-943 (2000).
12. Raggio, C., et al. Luman, the cellular counterpart of herpes simplex virus VP16, is processed by regulated intramembrane proteolysis. *Mol Cell Biol* **22**, 5639-5649 (2002).
13. Lutz, M.B., et al. An advanced culture method for generating large quantities of highly pure dendritic cells from mouse bone marrow. *J Immunol Methods* **223**, 77-92 (1999).
14. Nigten, J., et al. ID1 and ID2 are retinoic acid responsive genes and induce a G0/G1 accumulation in acute promyelocytic leukemia cells. *Leukemia* **19**, 799-805 (2005).
15. Karolchik, D., Hinrichs, A.S. & Kent, W.J. The UCSC Genome Browser. *Curr Protoc Bioinformatics* **Chapter 1**, Unit 1 4 (2007).
16. Frith, M.C., et al. Detection of functional DNA motifs via statistical over-representation. *Nucleic Acids Res* **32**, 1372-1381 (2004).
17. Sandelin, A., Alkema, W., Engstrom, P., Wasserman, W.W. & Lenhard, B. JASPAR: an open-access database for eukaryotic transcription factor binding profiles. *Nucleic Acids Res* **32**, D91-94 (2004).
18. Matys, V., et al. TRANSFAC: transcriptional regulation, from patterns to profiles. *Nucleic Acids Res* **31**, 374-378 (2003).
19. Siepel, A., et al. Evolutionarily conserved elements in vertebrate, insect, worm, and yeast genomes. *Genome Res* **15**, 1034-1050 (2005).
20. Steinbach, F., et al. Dendritic cells presenting equine herpesvirus-1 antigens induce protective anti-viral immunity. *J Gen Virol* **79** (Pt 12), 3005-3014 (1998).
21. Paglia, P., Girolomoni, G., Robbiati, F., Granucci, F. & Ricciardi-Castagnoli, P. Immortalized dendritic cell line fully competent in antigen presentation initiates primary T cell responses in vivo. *J Exp Med* **178**, 1893-1901 (1993).
22. Liang, G., et al. Luman/CREB3 induces transcription of the endoplasmic reticulum (ER) stress response protein Herp through an ER stress response element. *Mol Cell Biol* **26**, 7999-8010 (2006).
23. DenBoer, L.M., et al. Luman is capable of binding and activating transcription from the unfolded protein response element. *Biochem Biophys Res Commun* **331**, 113-119 (2005).
24. Emancipator, K., Csako, G. & Elin, R.J. In vitro inactivation of bacterial endotoxin by human lipoproteins and apolipoproteins. *Infect Immun* **60**, 596-601 (1992).
25. Chuang, K., Elford, E.L., Tseng, J., Leung, B. & Harris, H.W. An expanding role for apolipoprotein E in sepsis and inflammation. *Am J Surg* **200**, 391-397 (2010).
26. van den Elzen, P., et al. Apolipoprotein-mediated pathways of lipid antigen presentation. *Nature* **437**, 906-910 (2005).
27. Zhang, H.L., Wu, J. & Zhu, J. The immune-modulatory role of apolipoprotein E with emphasis on multiple sclerosis and experimental autoimmune encephalomyelitis. *Clin Dev Immunol* **2010**, 186813 (2010).

28. Wilhelm, A.J., *et al.* Apolipoprotein A-I and its role in lymphocyte cholesterol homeostasis and autoimmunity. *Arterioscler Thromb Vasc Biol* **29**, 843-849 (2009).
29. Karathanasis, S.K. Apolipoprotein multigene family: tandem organization of human apolipoprotein AI, CIII, and AIV genes. *Proc Natl Acad Sci U S A* **82**, 6374-6378 (1985).
30. van der Vliet, H.N., *et al.* Apolipoprotein A-V: a novel apolipoprotein associated with an early phase of liver regeneration. *J Biol Chem* **276**, 44512-44520 (2001).
31. Pearson, K., *et al.* Structure of human apolipoprotein A-IV: a distinct domain architecture among exchangeable apolipoproteins with potential functional implications. *Biochemistry* **43**, 10719-10729 (2004).
32. Paca-Uccaralerkun, S., *et al.* In vitro selection of DNA elements highly responsive to the human T-cell lymphotropic virus type I transcriptional activator, Tax. *Mol Cell Biol* **14**, 456-462 (1994).
33. De Lemos-Chiarandini, C., *et al.* A Golgi-related structure remains after the brefeldin A-induced formation of an ER-Golgi hybrid compartment. *Eur J Cell Biol* **58**, 187-201 (1992).
34. Audas, T.E., Li, Y., Liang, G. & Lu, R. A novel protein, Luman/CREB3 recruitment factor, inhibits Luman activation of the unfolded protein response. *Mol Cell Biol* **28**, 3952-3966 (2008).
35. Chen, X., Shen, J. & Prywes, R. The luminal domain of ATF6 senses endoplasmic reticulum (ER) stress and causes translocation of ATF6 from the ER to the Golgi. *J Biol Chem* **277**, 13045-13052 (2002).
36. Nadanaka, S., Okada, T., Yoshida, H. & Mori, K. Role of disulfide bridges formed in the luminal domain of ATF6 in sensing endoplasmic reticulum stress. *Mol Cell Biol* **27**, 1027-1043 (2007).
37. Acosta-Alvear, D., *et al.* XBP1 controls diverse cell type- and condition-specific transcriptional regulatory networks. *Mol Cell* **27**, 53-66 (2007).
38. Okada, T., Yoshida, H., Akazawa, R., Negishi, M. & Mori, K. Distinct roles of activating transcription factor 6 (ATF6) and double-stranded RNA-activated protein kinase-like endoplasmic reticulum kinase (PERK) in transcription during the mammalian unfolded protein response. *Biochem J* **366**, 585-594 (2002).
39. Tharakaraman, K., Bodenreider, O., Landsman, D., Spouge, J.L. & Marino-Ramirez, L. The biological function of some human transcription factor binding motifs varies with position relative to the transcription start site. *Nucleic Acids Res* **36**, 2777-2786 (2008).
40. Jansen, B.J., *et al.* MicroRNA genes preferentially expressed in dendritic cells contain sites for conserved transcription factor binding motifs in their promoters. *BMC Genomics* **12**, 330 (2011).
41. Hegele, R.A. Plasma lipoproteins: genetic influences and clinical implications. *Nat Rev Genet* **10**, 109-121 (2009).
42. Tso, P., Sun, W. & Liu, M. Gastrointestinal satiety signals IV. Apolipoprotein A-IV. *Am J Physiol Gastrointest Liver Physiol* **286**, G885-890 (2004).
43. Qin, X., Swertfeger, D.K., Zheng, S., Hui, D.Y. & Tso, P. Apolipoprotein AIV: a potent endogenous inhibitor of lipid oxidation. *Am J Physiol* **274**, H1836-1840 (1998).
44. Ferretti, G., Bacchetti, T., Bicchiera, V. & Curatola, G. Effect of human Apo AIV against lipid peroxidation of very low density lipoproteins. *Chem Phys Lipids* **114**, 45-54 (2002).
45. Duverger, N., *et al.* Protection against atherogenesis in mice mediated by human apolipoprotein A-IV. *Science* **273**, 966-968 (1996).
46. Ostos, M.A., *et al.* Antioxidative and antiatherosclerotic effects of human apolipoprotein A-IV in apolipoprotein E-deficient mice. *Arterioscler Thromb Vasc Biol* **21**, 1023-1028 (2001).
47. Zannis, V.I., Kan, H.Y., Kritis, A., Zanni, E.E. & Kardassis, D. Transcriptional regulatory mechanisms of the human apolipoprotein genes in vitro and in vivo. *Curr Opin Lipidol* **12**, 181-207 (2001).
48. Dai, Y., *et al.* A proteomic study of peripheral blood mononuclear cells in systemic lupus erythematosus. *Lupus* **17**, 799-804 (2008).
49. Recalde, D., *et al.* Human apolipoprotein A-IV reduces secretion of proinflammatory cytokines and atherosclerotic effects of a chronic infection mimicked by lipopolysaccharide. *Arterioscler Thromb Vasc Biol* **24**, 756-761 (2004).
50. Sanecka, A., *et al.* DC-STAMP knock-down deregulates cytokine production and T-cell stimulatory capacity of LPS-matured dendritic cells. *BMC Immunol* **12**, 57 (2011).
51. Bailey, D. & O'Hare, P. Transmembrane bZIP transcription factors in ER stress signaling and the unfolded protein response. *Antioxid Redox Signal* **9**, 2305-2321 (2007).
52. Zhang, K., *et al.* Endoplasmic reticulum stress activates cleavage of CREBH to induce a systemic inflammatory response. *Cell* **124**, 587-599 (2006).

53. Lee, J.H., *et al.* The transcription factor cyclic AMP-responsive element-binding protein H regulates triglyceride metabolism. *Nat Med* (2011).
54. Omori, Y., *et al.* CREB-H: a novel mammalian transcription factor belonging to the CREB/ATF family and functioning via the box-B element with a liver-specific expression. *Nucleic Acids Res* **29**, 2154-2162 (2001).

Supplementary figures

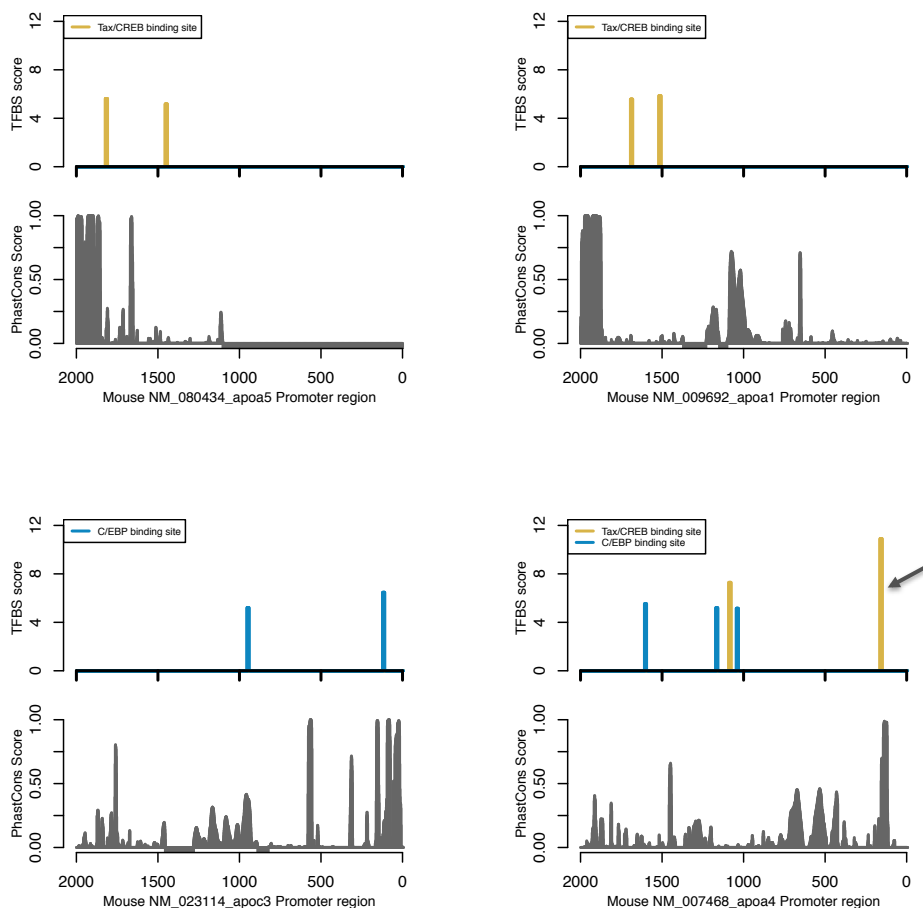


Figure S1. Promoter of mApoA4 contains CREB site. The upper subgraph for each apolipoprotein promoter depicts the TFBSs with a motif instance score threshold of at least 5 in the apolipoprotein promoter regions. The scale of the y-axis ranges from 0 to 12 for each subgraph, the higher the TFBS score, the stronger the motif match for the site. For clarity, only CREB and C/EBP related sites are shown. On the lower subgraphs the PhastCons scores are depicted. They range from 0 to 1, the higher the score the more conserved a nucleotide base.

A			B		
	Gene name	6h GFP vs 6h LUMANDp Fold induction		Gene name	18h GFP vs 18h LUMANDp Fold induction
1	Rsl1	5.94	1	Apoa4	9.88
2	Ubc	4.81	2	Nfyc	5.04
3	Creb3	3.47	3	Gstp2	3.83
4	Supt4h1	3.37	4	Sec23a	3.29
5	Rpa3	2.46	5	Sec24d	3.25
6	Celf1	2.44	6	Creb3	3.19
7	Gm4708	2.40	7	Lysmd1	3.03
8	Spcs1	2.39	8	Atg2a	3.02
9	Gsta3	2.33	9	Magea4	3.00
10	Olf476	2.31	10	Olf1286	2.96
11	Vmn1r22	2.31	11	Psm2	2.74
12	Olf1415	2.27	12	Gabrb2	2.72
13	Cdk10	2.24	13	5930434B04Rik	2.64
14	2610318N02Rik	2.21	14	Tas2r113	2.50
15	Nt5c2	2.19	15	Gbf1	2.42
16	Gstp2	2.18	16	Zfp59/Mfg2	2.42
17	Gm11428	2.17	17	Zfp9	2.33
18	Fdps	2.16	18	Tnfrsf23	2.32
19	Tmem9	2.16	19	Olf707	2.22
20	Gtf2h4	2.12	20	Sec24a	2.22
21	Zfp143	2.11	21	1110003E01Rik	2.22
22	Try5	2.10	22	Golga4	2.21
23	Nubpl	2.10	23	Chpf	2.21
24	B330016D10Rik	2.05	24	Dync1h1	2.18
25	Olf586	2.05	25	Tmem67	2.17
26	B230325K18Rik	-2.03	26	Macf1	2.15
27	Olf1338	-2.04	27	lft20	2.13
28	4833413D08Rik	-2.05	28	Olf1160	2.12
29	AY036118	-2.06	29	Ggcx	2.12
30	Olf3	-2.06	30	Ick	2.11
31	Ucn3	-2.07	31	Irgq	2.10
32	Vmn1r183	-2.11	32	Ppp2r5a	2.09
33	Cetn4	-2.11	33	Ldhd	2.07
34	D930031A20Rik	-2.21	34	Strbp	2.06
35	Cyp2c40	-2.22	35	Hmgn5	2.03
36	Mup20	-2.24	36	Arf4	2.01
37	Serpina1e	-2.31	37	Ttc5	2.01
38	Klk1	-2.33	38	A630007B06Rik	2.01
39	Ahcy	-2.36	39	Akap9	2.01
40	4921509C19Rik	-2.85	40	Snrrp35	-2.02
			41	Hist1h4m	-2.02
			42	Rbpj	-2.03
			43	Olf935	-2.04
			44	Olf651	-2.07
			45	B3galt6	-2.08
			46	Vmn1r59	-2.08
			47	B230220N19Rik	-2.09
			48	Ccl4	-2.09
			49	Usp-ps	-2.10
			50	Ncf2	-2.10
			51	Fabp5	-2.10
			52	Olf552	-2.10
			53	Olf1	-2.16
			54	Gm11428	-2.17
			55	Vmn1r35	-2.18
			56	BC003266	-2.28
			57	Polr2h	-2.33
			58	Rpl35a	-2.33
			59	Refbp2	-2.40
			60	Olf1057	-2.50
			61	Hist1h2ac	-2.53
			62	Ccl7	-2.77
			63	Hist1h3g	-2.83

Table S1. Lists of differentially expressed genes. Genes differentially expressed after retroviral overexpression of LUMANDp in D2SC/1 cells in comparison with genes expressed by cells transduced with GFP after 6 hours **A**) and 18 hours **B**) post transduction. Results are presented as a fold increase or decrease.

CHAPTER 6

**General discussion
and future perspectives**

General discussion

The immune system developed to protect us from pathogens, cancer and autoimmune diseases. In order to function properly the balance between tolerance and immunity must be maintained. Dendritic cells (DCs) are the professional antigen presenting cells of the immune system that play a strategic role in keeping this balance. They link innate and acquired immune responses as well as induce tolerance to self-antigens. During recent years DCs attracted much interest in the medical community because of their potential use in moderating immune responses. Engineered DC based vaccines could tip the balance between immunity and tolerance *e.g.*, in favour of transplant or against growing tumour. DCs were first described almost 40 years ago¹. However, new DC subsets are still being discovered, and novel proteins of unknown function preferentially expressed by DCs have been identified. Better understanding of DC immunobiology will help to design and improve DC-based immunotherapy. This thesis describes the studies directed to reveal the function of DC-STAMP in DCs biology.

DC-STAMP expression

DC-STAMP known also as TM7SF4 and FIND was identified as a transmembrane protein preferentially expressed by DCs². Subsequent work showed that macrophages and osteoclasts are also positive for DC-STAMP^{3,4} indicating that DC-STAMP expression is restricted to the cells derived from common myeloid precursors. Nevertheless, fresh monocytes and some subtypes of DCs, like Langerhans cells, are essentially negative for DC-STAMP. Transduction of a GFP transgene under the control of the DC-STAMP promoter into hematopoietic stem cells (HSCs) resulted in the predominant expression of transgene in DCs among different spleen cell populations⁵. CD8 positive DCs were shown to have higher expression of DC-STAMP than the CD8 negative DC subsets⁵. As CD8 positive DCs are important for cross-presentation^{6,7} it would be of interest to investigate possible role of DC-STAMP in this process.

DC-STAMP promoter

Expression of DC-STAMP appears to be regulated differently in each cell type. While RANKL is a potent inducer of DC-STAMP in osteoclasts, IL-4 induces its expression in macrophages^{3,4}. Analysis of the chromatin modifications, including

histone H3 trimethylation on lysine 4 (H3K4me3) and 27 (H3K27me3), associated with the promoter of DC-STAMP gene has shown an increased histone H3K4 methylation in macrophages and DCs in comparison with monocytes⁸. This type of histone methylation in gene promoters is correlated with higher transcriptional activity⁸, thus explaining the much higher expression of DC-STAMP in macrophages and DCs relative to monocytes.

During differentiation of DCs from bone marrow cells expression of DC-STAMP increases and is synchronized with CD11c expression⁹. Additionally, mRNA levels of both transcripts are downregulated upon maturation of DCs^{10,11}. This suggests that DC-STAMP gene may be linked with CD11c gene in regulatory network underlying the functional maturation of DCs. This hypothesis is supported by bioinformatics based comparison of murine CD11c and DC-STAMP promoters recently performed by Edelmann *et al.*, which identified an evolutionarily conserved promoter framework shared between these two genes¹⁰.

It was previously shown that DC-STAMP promoter could successfully drive transgene expression in DCs^{5,10}. Research of our group investigating the use of DC-associated promoters in genetic vaccines demonstrated potential use of DC-STAMP promoter in a specific targeting of DCs *in vivo*¹¹ (V. Moulin *et al.*, manuscript submitted for publication). Additionally, DCs expressing OVA antigen under the control of DC-STAMP promoter were shown to induce strong CD8⁺ T cells proliferation¹¹. Thus utilization of DC-STAMP promoter as a tool to target tumour antigens to DCs should be considered. Targeting DCs *in vivo* could form the basis of novel antitumor treatment strategies aimed at boosting immune responses alternative to the time-consuming and expensive immunotherapy strategy with *ex vivo* loaded DCs.

DC-STAMP family (paralogues and orthologues)

DC-STAMP is highly conserved among different species with 95% of homology between the murine and the human DC-STAMP protein. Highly conserved, presumably orthologous proteins are present in all mammals for which a sequence is available¹².

DC-STAMP is the founding member a novel family of proteins, as at its identification no homology with other protein families was observed. Subsequently, new members were added to the DC-STAMP family. DC-STAMP domain containing protein 1 and 2 (DC-ST1 and DC-ST2) are now classified as DC-STAMP family members¹². This

classification is based on the presence of highly conserved domain located between 242-421 amino acids of human DC-STAMP which covers the last two putative transmembrane domains and part of cytoplasmic tail (*DC-STAMP* (PF07782) <http://pfam.sanger.ac.uk>)¹³. Osteoclast stimulatory transmembrane protein (OC-STAMP), a DC-STAMP-like protein also expressed in osteoclasts, was proposed to be another novel member of the DC-STAMP family¹².

DC-STAMP structure

The structure of DC-STAMP protein remains largely unsolved. Human DC-STAMP contains 470 amino acids and based on the presence of the hydrophobic regions it is predicted to comprise from 4 to 7 transmembrane domains with a 70 amino acids long C-terminus². DC-STAMP was shown to contain three putative N-glycosylation sites². In Chapter 3 using tunicamycin treatment and western blot analysis we showed that DC-STAMP protein is indeed glycosylated. Additionally, our unpublished results from studies of DC-STAMP mutants strongly suggest that all three predicted sites are occupied by the sugar chains (data not shown).

Post-translational modifications (PTMs) play an important role in regulation of protein function. Protein phosphorylation is the most ubiquitous form of PTM employed in most of biological processes that allows dynamic activation of signalling pathways. Since DC-STAMP was shown to have potential phosphorylation site for PKC² it would be of interest to investigate whether DC-STAMP is indeed a substrate for PKC and what would be the role of this modification.

Recently, it was proposed that DC-STAMP may form homodimers as well as heterodimers with OC-STAMP in osteoclasts¹⁴. This dimerization partner may be important for the observed fusion process in osteoclasts that has been attributed to DC-STAMP (see below). It would be interesting to test if DC-STAMP is present as a dimer also in DCs. More insight into structure of DC-STAMP and its PTMs would most likely provide important new insights in its function.

Fusogenic properties of DC-STAMP

DC-STAMP is called the “master fusogen” for osteoclast differentiation. Osteoclasts are multinuclear giant cells derived from monocytic precursor, and are uniquely designed to resorb bone^{15,16}. An essential event in osteoclasts development is multinucleation, induced by cell–cell fusion of mononuclear osteoclasts¹⁷. This

process is analogous to the fusion events that take place between macrophages to form giant cells, and involves the coordinated activity of several adhesion molecules, fusion proteins, and signaling proteins. DC-STAMP was shown to be necessary for fusion of osteoclasts as well as foreign body giant cells¹⁸. Mice lacking DC-STAMP have symptoms of osteopetrosis characterized by increased bone mass caused by decreased osteoclasts activity and lack of multinucleated osteoclasts¹⁹. How DC-STAMP exerts its fusogenic function is not yet fully understood.

DC-STAMP is believed to localize to the plasma membrane of osteoclasts. However, no clear microscopy picture showing colocalization of DC-STAMP with one of the cell membrane markers was ever published. Our overexpression studies of tagged DC-STAMP from many different cell lines and DCs doubt the localisation of DC-STAMP on the cell surface and strongly suggest its localization within ER-Golgi membranes. Additionally the results of our yeast-2-hybrid analysis revealing two ER-resident interacting partners (Chapter 2 & 3) strengthen the ER localisation of DC-STAMP in DCs. Nevertheless, appropriate colocalization studies in osteoclasts need to be performed to put an end to this debate. This putative cell membrane localization and presumed 7-transmembrane structure led to hypothesis that DC-STAMP might function as a G protein-coupled receptor with unknown ligand.

The DC-STAMP gene is a direct target of the transcription factor NFATc1 in osteoclasts^{20,21} and is highly induced in osteoclasts during differentiation^{4,18}. Monocyte chemoattractant protein-1 (MCP1/CCL2) was also shown to regulate DC-STAMP expression in osteoclasts²², while treatment of RAW264.7 cells with TNF α , LPS and RANKL induces fusion without increasing expression of DC-STAMP²³. Thus, it is not clear if an increase in DC-STAMP expression is necessary for the fusion itself. Recent studies have shown that RANKL stimulation of RAW264.7 cells induced two functionally different populations of mononuclear osteoclast precursor cells with distinct DC-STAMP expression levels, DC-STAMP high and DC-STAMP low cells¹⁴. DC-STAMP high cells are mononuclear donors that cannot form osteoclasts by themselves, while DC-STAMP low cells are master fusogens¹⁴. It is possible that stimuli that induce fusion could induce production of the putative ligand for DC-STAMP to initiate pro-fusion signalling²⁴.

Fusogenic properties of DC-STAMP go beyond osteoclasts. As DC-STAMP was shown to be involved in fusion of foreign body giant cells as well, it may also be involved in the formation of giant cells during chronic inflammatory conditions such as tuberculosis. A role for DC-STAMP in fusion of cells during malignancies has also been proposed. In multiple myeloma, a hematologic malignancy in which

tumor progression may account for uncontrolled osteoclastogenesis, the expression of DC-STAMP was shown to be upregulated in peripheral macrophages, while DCs and myeloma plasma cells showed high fusogenic susceptibility and under specific conditions could trans-differentiate to osteoclasts²⁵. Additionally, DC-STAMP was upregulated in papillary thyroid cancer²⁶, also featuring multinucleated giant cells^{27,28}.

Taken together, these data suggest that DC-STAMP, predominantly important for fusion of osteoclasts, in the pathogenic conditions may play a role in fusion of other cells *i.e.*, macrophages.

DC-STAMP interacting partners

OS9

OS-9 is an ubiquitously expressed protein originally identified in a screen for genes upregulated in osteosarcoma²⁹ and myeloid leukemia³⁰. Many interacting partners of OS9 have been described³¹⁻³³. Our data presented in Chapter 2 show interaction of DC-STAMP with OS9 and its involvement in the translocation of DC-STAMP towards the Golgi compartment.

Recent studies imply a role for OS9 in ER associated degradation (ERAD), a process in which potentially toxic, misfolded proteins are translocated from the ER into the cytosol for proteosomal degradation. OS9 was shown to recognize and bind misfolded glycoproteins in the ER³⁴⁻³⁸. As DC-STAMP is a glycosylated protein, it is important to answer the question whether OS9 interacts with DC-STAMP only when misfolded. Our data mapping the interacting regions between OS9 and DC-STAMP (Chapter 2) argue against such a role in case of DC-STAMP. The fact that the cytoplasmic tail of DC-STAMP, which is sufficient to interact with OS9, is not glycosylated and that the domain of OS9 responsible for binding misfolded proteins³⁹ is outside of the region necessary for interaction with DC-STAMP strongly suggest that interaction of OS9 with DC-STAMP is not based simply on binding to its misfolded form.

Rather, our data suggests that OS9 is necessary for the transport of DC-STAMP out of Golgi compartment upon maturation of DCs. The fact that OS9 was previously implicated in ER-to-Golgi transport of different proteins in mammalian and yeast cells^{31,33,40} supports these findings. Nevertheless, how OS-9 regulates DC-STAMP translocation is not fully understood. One hypothesis is that DC-STAMP exerts its function in the ER at the moment of DCs maturation and it is transported towards the

Golgi compartment (observation in mature DCs, Chapter 2) to be removed as it is no longer required. This is supported by immunofluorescence data presented in Chapter 2 where levels of DC-STAMP are dramatically decreased after TLR stimulation. As OS9 was shown to promote proteosomal degradation of hypoxia inducible factor 1 α (HIF-1 α)³² it is possible that it also directs DC-STAMP removal from the ER. Additionally, stability of HIF-1 α in DCs was recently shown to be influenced by TLR ligation⁴¹. It is not known if OS9 is involved in this process. Further investigation is required to determine whether OS9 besides promoting DC-STAMP relocalization is involved in driving degradation of DC-STAMP. Silencing studies of OS9 in DCs would definitely broaden our knowledge on this subject.

Another debate concerns OS9 localization. OS9 is considered as an ER associated molecule. As no apparent transmembrane domain is detected in predicted OS9 structure, suggesting that OS9 does not span the ER membranes. Nevertheless, it is still controversial on which site of the ER membrane OS9 localizes. Interaction with SEL1L (ER luminal protein), would suggest that OS9 must be present in the lumen of the ER³⁶. On the other hand, many reports, including our studies showed interaction of OS9 with cytoplasmic proteins³¹⁻³³. Possible explanations of these contradicting reports are that OS9 flips between luminal and cytoplasmic site of the ER or is present on both sites of the ER membrane.

LUMAN

In Chapter 3 we described the interaction of the transcription factor LUMAN with DC-STAMP and the activation of LUMAN in mature DCs. As understanding the nature of this interaction could help to reveal the function of DC-STAMP, we investigated the target genes of LUMAN in DCs in Chapter 5.

LUMAN is the prototype of the CREB3 subfamily of membrane bound bZIP transcription factors. This subfamily comprises LUMAN itself (CREB3/LZIP), OASIS (CREB3L1), BBF2H7 (CREB3L2), CREB-H (CREB3L3) and AlbZIP (CREB3L4) transcription factors⁴². A knockout mouse model has been reported for all subfamily members beside LUMAN. LUMAN is activated in a process called regulated intramembrane proteolysis (RIP). Activation of transcription factors by RIP ensures a rapid response to stimuli. However, there are several other regulatory points in addition to RIP. For example the N-terminal active form of the CREB3 subfamily transcription factors can form distinct dimers with different transcriptional activity⁴³. It is not clear whether dimerization of LUMAN protein occurs and if it is necessary for its function.

Members of the bZIP family have been implicated in regulating gene expression in the unfolded protein response (UPR)^{44,45}. LUMAN also has been suggested to take part in UPR in non-immune cells by regulating the expression of the ER degradation-enhancing alpha-mannosidase-like 1 (EDEM) and homocysteine-induced endoplasmic reticulum (Herp) proteins that are involved in different aspects of ER-associated degradation (ERAD)^{46,47}. Our studies described in Chapter 5 did not show a clear involvement of LUMAN in these processes in DCs. Thus, we postulate that in DCs the role of LUMAN goes beyond ER-stress. Recently, a concept of cross-talk between the innate immune system and ER-stress pathways came forward⁴⁸. TLR triggering was shown to be able to activate ER-stress pathways in macrophages⁴⁹. Moreover, an intact UPR is necessary for differentiation of DCs and DC survival upon TLR ligation⁵⁰. We hypothesize that in DCs LUMAN may be involved in cross-talk between the innate immune response and the ER-stress pathways.

Several studies pointed to an essential role of the CREB3 subfamily members, OASIS and BBF2H7 in protein secretion⁵¹⁻⁵⁵. Our microarray data (Chapter 5, Table S1) revealed enhanced expression of Sec24a, Sec24d and Sec23a, all proteins involved in intracellular trafficking and protein secretion⁵⁶, following expression of constitutively active LUMAN. Furthermore golgin autoantigen 4 (Golga4/Golgin-245) and Golgi-specific brefeldin A-resistance factor 1 (Gbf1) genes important for vesicle-mediated transport^{57,58} were upregulated in this setting. Although it remains to be investigated whether these genes are true targets of LUMAN, their differential expression and interaction of LUMAN with OS9 (Chapter 3) is suggesting the involvement of LUMAN in regulation of ER-to-Golgi transport.

LUMAN mRNA is ubiquitously expressed. Its protein was shown to be expressed only in neurons, monocytes and dendritic cells. There is no report showing the protein expression of LUMAN in osteoclasts however we cannot exclude the possibility that “master fusogen” function of DC-STAMP is mediated by LUMAN. Studies of fusion of osteoclasts and macrophages in absence of LUMAN (silencing/knock-out mouse) could give the answer to that question.

DC-STAMP and LUMAN activation in dendritic cells

The role of DC-STAMP in fusion of osteoclasts and foreign body giant cells was described but its role in DCs remained greatly undefined. In Chapter 3, based on similarities with SREB/SCAP model⁶⁰ we proposed a model of how DC-STAMP and its interacting proteins could function in DCs. In this model DC-STAMP interacts with LUMAN and OS9 in the ER of immature DCs. Upon maturation DC-STAMP and

LUMAN leave the ER, while OS9 localization is not influenced. Upon arrival in the Golgi compartment, LUMAN is cleaved by Golgi-residing proteases and its active form translocates to the nucleus to regulate gene expression.

One of the questions that remain to be answered is the precise function of DC-STAMP in the DC-STAMP/LUMAN pathway in DCs. One possibility is that DC-STAMP facilitates the translocation of LUMAN to the Golgi compartment needed for LUMAN activation and thus fulfils a role as transporter/chaperone for LUMAN. For now it is not known if DC-STAMP physically interacts with LUMAN after leaving the ER. Protein interaction studies in mature DCs would help to resolve this question. If DC-STAMP is a transporter, LUMAN translocation to the Golgi/nucleus in the absence of DC-STAMP should be impaired.

Another possibility holds that DC-STAMP keeps LUMAN in the ER and is responsible for the release of LUMAN from the ER in response to activating signals. It will be interesting to test if the lack of DC-STAMP protein results in the spontaneous release of LUMAN from the ER. Our unpublished results from overexpression studies of LUMAN protein in cell lines where DC-STAMP is not expressed (HEK293, CHO) showed that lack of DC-STAMP does not lead to direct LUMAN activation in these non-immune cells. Studies are further hampered by the fact that the exact nature of the signals required for LUMAN activation is still largely elusive. DCs deficient in DC-STAMP would be valuable tools to answer this question.

Recent data from our lab show that in human monocyte-derived DCs LUMAN becomes activated during the maturation of DCs (Chapter 3 and manuscript in preparation). An intriguing question is whether DC-STAMP is responsible for sensing directly or indirectly the signals leading to DC activation.

An immunoreceptor tyrosine-based inhibitory motif (ITIM) was identified by Chiu *et al* in the cytoplasmic tail of DC-STAMP⁶³. Interestingly, same group claims that DC-STAMP associates with CD16, the molecule bearing a counteracting immunoreceptor tyrosine-based activation motif (ITAM). Taken together this gives an indication that DC-STAMP may function as a signaling molecule.

Overexpression of DC-STAMP was shown to block differentiation of granulocytes while allowing development of myeloid cells⁶¹ suggesting the importance of DC-STAMP in development of myeloid precursors towards CD11c⁺ cells. On the other hand, it was reported that lack of DC-STAMP does not inhibit differentiation or proliferation of DCs in DC-STAMP knock-out mice¹⁹. Although, total number of DCs in DC-STAMP knock-out mice was not investigated/shown. Studies on DC-STAMP

deficient DCs suggest that DC-STAMP regulates antigen presentation activity in DCs and maintenance of immune self-tolerance¹⁹. Our data from DC-STAMP silencing studies presented in Chapter 4 showed that DC-STAMP is important for cytokine production in LPS matured DCs. To understand how DC-STAMP exerts this function additional studies are needed. A potential explanation for DC-STAMP's role in cytokine regulation could be related to the fact that DC-STAMP is a protein with highly fusogenic properties. It is possible that in DCs DC-STAMP also exerts its fusogenic function. DCs do not readily fuse but phagosome formation was shown to occur via fusion of ER and plasmalemma underneath phagocytic cups⁶⁴. It has been shown that for secretion of cytokines like IL-6 and TNF α , a proper function of phagosome is important⁶⁵⁻⁶⁷. It is possible that DC-STAMP as an ER residing protein with fusogenic properties would play a role in that complex process. In this situation DC-STAMP deficiency could have a negative impact on cytokine production. Testing intracellular cytokine levels could provide a clue about the potential deregulated secretion.

On the other hand, in light of interaction between DC-STAMP and LUMAN it is tempting to speculate that LUMAN may be involved in the observed deregulated cytokine production by DC-STAMP knock-down DCs. It would be very interesting to look at the effect of LUMAN silencing in these cells. Our preliminary data suggest that mBMDC with LUMAN knock-down have decreased production of TNF α upon LPS stimulation similar to the DC-STAMP knock-down DCs. Moreover, our microarray data of D2SC1 cells overexpressing active form of LUMAN indicated increase in the IL-1 β production (data not shown). This effect on cytokine production may be mediated by transcription factor activity of LUMAN. Regulation of cytokine production by LUMAN might occur directly by binding CREB sites present in promoters of many cytokine genes by LUMAN or by influencing NF- κ B activity. Supporting the second possibility is a report showing that LUMAN increased NF- κ B dependent luciferase activity in response to Lkn-1 chemokine in HOS/CCR1 cells and THP-1 cells⁶². Cleavage of LUMAN protein, which is a hallmark of its activation, in mature DCs and its localization to the nucleus, strongly suggests its importance in DC immunobiology.

Our recent data show that activation of LUMAN in mature DCs is triggered by number of stimuli like LPS, INF γ , Poly I:C and PGE2 (D. Eleveld-Trancikova *et al.*, manuscript in preparation) suggesting that this is more general event not so much dependent on pathway by which immature DCs were triggered for maturation. Tolerogenic signals like treatment with IL-10 and dexamethasone does not lead to

the activation of LUMAN. Additionally, kinetic of LUMAN activation is not influenced by the type of tested stimuli and the cleaved product of LUMAN is observed earliest 16 hours upon adding the stimuli. The nature of the signal that triggers translocation of LUMAN to Golgi for its activation is not known. We believe that signalling pathways activated upon TLR stimulation induce the production of the activating signal (Fig. 1). Time needed for the production of the signal would explain the 16 hours delay in the LUMANS activation. In Chapter 5 we described ApoA4 as a target gene of LUMAN in murine DCs. ApoA4 was shown to reduce secretion of proinflammatory cytokines from human PBMCs, which suggested its anti-inflammatory properties⁵⁹. The cytokine secretion by DCs is the fast outcome of stimulation with TLR ligands that is important, among others, for an initiation of the inflammation. The delayed activation of LUMAN and subsequent control of the ApoA4 expression suggest that LUMAN potentially plays a role in a feedback loop controlling the inflammatory responses in DCs (Fig. 1).

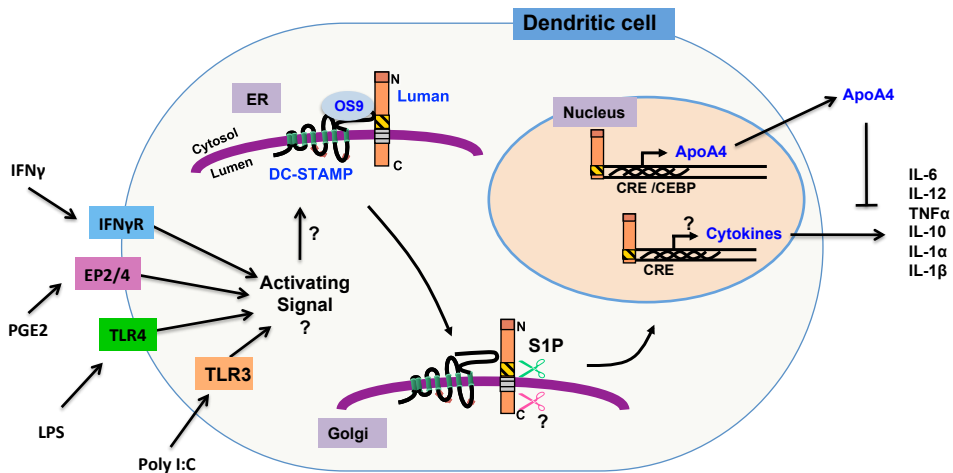


Figure 1. Hypothetical model of DC-STAMP/LUMAN/OS9 interaction and function in DCs. Stimulation of DC with different TLR ligands (LPS, Poly I:C) or PGE2 and IFN γ leads to induction of signalling pathways resulting in production of the undefined LUMAN's "activation signal". This signal potentially sensed by DC-STAMP provokes translocation of DC-STAMP/LUMAN complex from the ER to the Golgi compartment. OS9 facilitates translocation of DC-STAMP and LUMAN but does not leave the ER. Golgi-residing proteases (S1P and perhaps another one) can release N-terminal part of LUMAN. Active form of LUMAN can translocate to the nucleus to regulate transcription of ApoA4 and different cytokines. Additionally, ApoA4 may influence the release/production of cytokines, forming a feedback loop helping to resolve ongoing inflammation.

Conclusions and future directions

We investigated the role of DC-STAMP and its interacting partners LUMAN and OS9 in the immunobiology of DCs. While some pieces of the puzzle start fitting into place, a lot of work still has to be done to complete the riddle. Our and others work showed that DC-STAMP is a very versatile protein. Its function as a “master fusogen” was described in osteoclasts and foreign body giant cells. DC-STAMP knock-out mice beside the osteopetrosis phenotype, at older age show symptoms of autoimmune diseases, consistent with the postulated role of DC-STAMP within the immune system. We have shown that decrease in DC-STAMP expression in dendritic cells alters their cytokine production and function as activators of Th1 responses upon LPS stimulation.

In this thesis we often have looked at DC-STAMP through the prism of the transcription factor LUMAN. Nevertheless, it is accountable that the role DC-STAMP plays in the LUMAN activation covers only a small part of DC-STAMP’s functions. Availability of DC-STAMP knock-out mice, preferably mice in which DC-STAMP has been specifically eliminated from DCs, would open a wide window of opportunities. Challenging such mice with infectious agents, like bacteria or fungi, or with tumour cells will certainly provide further insight into the role of DC-STAMP in the immune system. Creation of LUMAN knockout mice and parallel experiments to those in DC-STAMP deficient mice would help to extract the essence of the DC-STAMP and LUMAN interaction and would facilitate the analysis of the role OS9 herein. Insight into these pathways in DCs would help to better understand molecular basis of DC immunobiology, and could possibly lead to better design of DC-based immunotherapies.

References

1. Steinman, R.M. & Cohn, Z.A. Identification of a novel cell type in peripheral lymphoid organs of mice. I. Morphology, quantitation, tissue distribution. *J Exp Med* **137**, 1142-1162 (1973).
2. Hartgers, F.C., *et al.* DC-STAMP, a novel multimembrane-spanning molecule preferentially expressed by dendritic cells. *Eur J Immunol* **30**, 3585-3590 (2000).
3. Staeger, H., Brauchlin, A., Schoedon, G. & Schaffner, A. Two novel genes FIND and LIND differentially expressed in deactivated and Listeria-infected human macrophages. *Immunogenetics* **53**, 105-113 (2001).
4. Kukita, T., *et al.* RANKL-induced DC-STAMP is essential for osteoclastogenesis. *J Exp Med* **200**, 941-946 (2004).
5. Dresch, C., Edelmann, S.L., Marconi, P. & Brocker, T. Lentiviral-mediated transcriptional targeting of dendritic cells for induction of T cell tolerance in vivo. *J Immunol* **181**, 4495-4506 (2008).
6. Pooley, J.L., Heath, W.R. & Shortman, K. Cutting edge: intravenous soluble antigen is presented to CD4 T cells by CD8- dendritic cells, but cross-presented to CD8 T cells by CD8+ dendritic cells. *J Immunol* **166**, 5327-5330 (2001).
7. Schnorrer, P., *et al.* The dominant role of CD8+ dendritic cells in cross-presentation is not dictated by antigen capture. *Proc Natl Acad Sci U S A* **103**, 10729-10734 (2006).
8. Tserel, L., *et al.* Genome-wide promoter analysis of histone modifications in human monocyte-derived antigen presenting cells. *BMC Genomics* **11**, 642 (2010).
9. Eleveld-Trancikova, D., *et al.* The dendritic cell-derived protein DC-STAMP is highly conserved and localizes to the endoplasmic reticulum. *J Leukoc Biol* **77**, 337-343 (2005).
10. Edelmann, S.L., Nelson, P.J. & Brocker, T. Comparative promoter analysis in vivo: identification of a dendritic cell-specific promoter module. *Blood* (2011).
11. Moulin, V., *et al.* Targeting Dendritic Cells with Antigen via Dendritic Cell-Associated Promoters. *Submitted to* (2011).
12. Yang, M., *et al.* Osteoclast stimulatory transmembrane protein (OC-STAMP), a novel protein induced by RANKL that promotes osteoclast differentiation. *J Cell Physiol* **215**, 497-505 (2008).
13. Finn, R.D., *et al.* The Pfam protein families database. *Nucleic Acids Research* **38**, D211-D222.
14. Mensah, K.A., Ritchlin, C.T. & Schwarz, E.M. RANKL induces heterogeneous DC-STAMP(lo) and DC-STAMP(hi) osteoclast precursors of which the DC-STAMP(lo) precursors are the master fusogens. *J Cell Physiol* **223**, 76-83 (2010).
15. Teitelbaum, S.L. Bone resorption by osteoclasts. *Science* **289**, 1504-1508 (2000).
16. Miyamoto, T. & Suda, T. Differentiation and function of osteoclasts. *Keio J Med* **52**, 1-7 (2003).
17. Boyle, W.J., Simonet, W.S. & Lacey, D.L. Osteoclast differentiation and activation. *Nature* **423**, 337-342 (2003).
18. Yagi, M., *et al.* DC-STAMP is essential for cell-cell fusion in osteoclasts and foreign body giant cells. *J Exp Med* **202**, 345-351 (2005).
19. Sawatani, Y., *et al.* The role of DC-STAMP in maintenance of immune tolerance through regulation of dendritic cell function. *Int Immunol* **20**, 1259-1268 (2008).
20. Yagi, M., *et al.* Induction of DC-STAMP by alternative activation and downstream signaling mechanisms. *J Bone Miner Res* **22**, 992-1001 (2007).
21. Kim, K., Lee, S.H., Ha Kim, J., Choi, Y. & Kim, N. NFATc1 induces osteoclast fusion via up-regulation of Atp6v0d2 and the dendritic cell-specific transmembrane protein (DC-STAMP). *Mol Endocrinol* **22**, 176-185 (2008).
22. Miyamoto, K., *et al.* MCP-1 expressed by osteoclasts stimulates osteoclastogenesis in an autocrine/paracrine manner. *Biochem Biophys Res Commun* **383**, 373-377 (2009).
23. Hotokezaka, H., *et al.* Molecular analysis of RANKL-independent cell fusion of osteoclast-like cells induced by TNF-alpha, lipopolysaccharide, or peptidoglycan. *J Cell Biochem* **101**, 122-134 (2007).
24. Oursler, M.J. Recent advances in understanding the mechanisms of osteoclast precursor fusion. *J Cell Biochem* **110**, 1058-1062 (2010).
25. Silvestris, F., Ciavarella, S., Strippoli, S. & Dammacco, F. Cell fusion and hyperactive osteoclastogenesis in multiple myeloma. *Adv Exp Med Biol* **714**, 113-128.
26. Lee, K.Y., Huang, S.M., Li, S. & Kim, J.M. Identification of differentially expressed genes in papillary thyroid cancers. *Yonsei Med J* **50**, 60-67 (2009).
27. Gaffey, M.J., Lack, E.E., Christ, M.L. & Weiss, L.M. Anaplastic thyroid carcinoma with osteoclast-like giant cells. A clinicopathologic, immunohistochemical, and ultrastructural study. *Am J Surg Pathol* **15**, 160-168 (1991).

28. Guiter, G.E. & DeLellis, R.A. Multinucleate giant cells in papillary thyroid carcinoma. A morphologic and immunohistochemical study. *Am J Clin Pathol* **106**, 765-768 (1996).
29. Su, Y.A., Hutter, C.M., Trent, J.M. & Meltzer, P.S. Complete sequence analysis of a gene (OS-9) ubiquitously expressed in human tissues and amplified in sarcomas. *Mol Carcinog* **15**, 270-275 (1996).
30. Kimura, Y., Nakazawa, M. & Yamada, M. Cloning and characterization of three isoforms of OS-9 cDNA and expression of the OS-9 gene in various human tumor cell lines. *J Biochem* **123**, 876-882 (1998).
31. Litovchick, L., Friedmann, E. & Shaltiel, S. A selective interaction between OS-9 and the carboxyl-terminal tail of meprin beta. *J Biol Chem* **277**, 34413-34423 (2002).
32. Baek, J.H., *et al.* OS-9 interacts with hypoxia-inducible factor 1alpha and prolyl hydroxylases to promote oxygen-dependent degradation of HIF-1alpha. *Mol Cell* **17**, 503-512 (2005).
33. Nakayama, T., Yaoi, T., Kuwajima, G., Yoshie, O. & Sakata, T. Ca2(+)-dependent interaction of N-copine, a member of the two C2 domain protein family, with OS-9, the product of a gene frequently amplified in osteosarcoma. *FEBS Lett* **453**, 77-80 (1999).
34. Alcock, F. & Swanton, E. Mammalian OS-9 is upregulated in response to endoplasmic reticulum stress and facilitates ubiquitination of misfolded glycoproteins. *J Mol Biol* **385**, 1032-1042 (2009).
35. Bernasconi, R., Pertel, T., Luban, J. & Molinari, M. A dual task for the Xbp1-responsive OS-9 variants in the mammalian endoplasmic reticulum: inhibiting secretion of misfolded protein conformers and enhancing their disposal. *J Biol Chem* **283**, 16446-16454 (2008).
36. Christianson, J.C., Shaler, T.A., Tyler, R.E. & Kopito, R.R. OS-9 and GRP94 deliver mutant alpha1-antitrypsin to the Hrd1-SEL1L ubiquitin ligase complex for ERAD. *Nat Cell Biol* **10**, 272-282 (2008).
37. Hosokawa, N., Kamiya, Y., Kamiya, D., Kato, K. & Nagata, K. Human OS-9, a lectin required for glycoprotein endoplasmic reticulum-associated degradation, recognizes mannose-trimmed N-glycans. *J Biol Chem* **284**, 17061-17068 (2009).
38. Mueller, B., Klemm, E.J., Spooner, E., Claessen, J.H. & Ploegh, H.L. SEL1L nucleates a protein complex required for dislocation of misfolded glycoproteins. *Proc Natl Acad Sci U S A* **105**, 12325-12330 (2008).
39. Satoh, T., *et al.* Structural basis for oligosaccharide recognition of misfolded glycoproteins by OS-9 in ER-associated degradation. *Mol Cell* **40**, 905-916 (2010).
40. Friedmann, E., Salzberg, Y., Weinberger, A., Shaltiel, S. & Gerst, J.E. YOS9, the putative yeast homolog of a gene amplified in osteosarcomas, is involved in the endoplasmic reticulum (ER)-Golgi transport of GPI-anchored proteins. *J Biol Chem* **277**, 35274-35281 (2002).
41. Spirig, R., *et al.* Effects of TLR agonists on the hypoxia-regulated transcription factor HIF-1alpha and dendritic cell maturation under normoxic conditions. *PLoS One* **5**, e0010983.
42. Burbelo, P.D., *et al.* LZIP-1 and LZIP-2: two novel members of the bZIP family. *Gene* **139**, 241-245 (1994).
43. Vinson, C., Acharya, A. & Taparowsky, E.J. Deciphering B-ZIP transcription factor interactions in vitro and in vivo. *Biochim Biophys Acta* **1759**, 4-12 (2006).
44. Bailey, D. & O'Hare, P. Transmembrane bZIP transcription factors in ER stress signaling and the unfolded protein response. *Antioxid Redox Signal* **9**, 2305-2321 (2007).
45. Zhang, K., *et al.* Endoplasmic reticulum stress activates cleavage of CREBH to induce a systemic inflammatory response. *Cell* **124**, 587-599 (2006).
46. Liang, G., *et al.* Luman/CREB3 induces transcription of the endoplasmic reticulum (ER) stress response protein Herp through an ER stress response element. *Mol Cell Biol* **26**, 7999-8010 (2006).
47. DenBoer, L.M., *et al.* Luman is capable of binding and activating transcription from the unfolded protein response element. *Biochem Biophys Res Commun* **331**, 113-119 (2005).
48. Martinon, F. & Glimcher, L.H. Regulation of innate immunity by signaling pathways emerging from the endoplasmic reticulum. *Curr Opin Immunol* **23**, 35-40 (2010).
49. Martinon, F., Chen, X., Lee, A.H. & Glimcher, L.H. TLR activation of the transcription factor XBP1 regulates innate immune responses in macrophages. *Nat Immunol* **11**, 411-418 (2010).
50. Iwakoshi, N.N., Pypaert, M. & Glimcher, L.H. The transcription factor XBP-1 is essential for the development and survival of dendritic cells. *J Exp Med* **204**, 2267-2275 (2007).
51. Murakami, T., *et al.* Distinct mechanisms are responsible for osteopenia and growth retardation in OASIS-deficient mice. *Bone* **48**, 514-523 (2010).
52. Murakami, T., *et al.* Signalling mediated by the endoplasmic reticulum stress transducer OASIS is involved in bone formation. *Nat Cell Biol* **11**, 1205-1211 (2009).

53. Saito, A., *et al.* Regulation of endoplasmic reticulum stress response by a BBF2H7-mediated Sec23a pathway is essential for chondrogenesis. *Nat Cell Biol* **11**, 1197-1204 (2009).
54. Tanegashima, K., Zhao, H., Rebbert, M.L. & Dawid, I.B. Coordinated activation of the secretory pathway during notochord formation in the *Xenopus* embryo. *Development* **136**, 3543-3548 (2009).
55. Fox, R.M., Hanlon, C.D. & Andrew, D.J. The CrebA/Creb3-like transcription factors are major and direct regulators of secretory capacity. *J Cell Biol* **191**, 479-492.
56. Spang, A. The life cycle of a transport vesicle. *Cell Mol Life Sci* **65**, 2781-2789 (2008).
57. Gleeson, P.A., *et al.* p230 is associated with vesicles budding from the trans-Golgi network. *J Cell Sci* **109** (Pt 12), 2811-2821 (1996).
58. Kawamoto, K., *et al.* GBF1, a guanine nucleotide exchange factor for ADP-ribosylation factors, is localized to the cis-Golgi and involved in membrane association of the COPI coat. *Traffic* **3**, 483-495 (2002).
59. Recalde, D., *et al.* Human apolipoprotein A-IV reduces secretion of proinflammatory cytokines and atherosclerotic effects of a chronic infection mimicked by lipopolysaccharide. *Arterioscler Thromb Vasc Biol* **24**, 756-761 (2004).
60. Brown, M.S. & Goldstein, J.L. The SREBP pathway: regulation of cholesterol metabolism by proteolysis of a membrane-bound transcription factor. *Cell* **89**, 331-340 (1997).
61. Eleveld-Trancikova, D., *et al.* The DC-derived protein DC-STAMP influences differentiation of myeloid cells. *Leukemia* **22**, 455-459 (2008).
62. Jang, S.W., Kim, Y.S., Lee, Y.H. & Ko, J. Role of human LZIP in differential activation of the NF-kappaB pathway that is induced by CCR1-dependent chemokines. *J Cell Physiol* **211**, 630-637 (2007).
63. Chiu, Y.G., *et al.* Dendritic Cell-Specific Transmembrane Protein (DC-STAMP) Is An Immunoreceptor Tyrosine-Based Inhibitory Motif (ITIM)-Bearing Molecule Regulating Osteoclast Development Thru the SHP-1 Signaling Cascade in *Arthritis Rheum*, Vol. **60** 1241 (2009).
64. Gagnon, E., *et al.* Endoplasmic reticulum-mediated phagocytosis is a mechanism of entry into macrophages. *Cell* **110**, 119-131 (2002).
65. Murray, R.Z., Kay, J.G., Sangermani, D.G. & Stow, J.L. A role for the phagosome in cytokine secretion. *Science* **310**, 1492-1495 (2005).
66. Manderson, A.P., Kay, J.G., Hammond, L.A., Brown, D.L. & Stow, J.L. Subcompartments of the macrophage recycling endosome direct the differential secretion of IL-6 and TNFalpha. *J Cell Biol* **178**, 57-69 (2007).
67. Stow, J.L., Low, P.C., Offenhauser, C. & Sangermani, D. Cytokine secretion in macrophages and other cells: pathways and mediators. *Immunobiology* **214**, 601-612 (2009).

Summary

Our body is constantly challenged by various bacteria, viruses, fungi and parasites. The main role of the immune system is to protect us from the attacks of those pathogens. Additionally, the immune system needs to deal with dangers coming from the cells of our own body to prevent carcinogenesis and to regulate its own actions to protect us from autoimmunity. Dendritic cells (DCs) are the cells of the immune system that play a strategic role in keeping the balance between immunity and tolerance. This dual function of DCs makes them attractive for use in immunotherapies against cancer and autoimmune diseases. Better understanding of DC immunobiology is vital for improvement of DC-based immunotherapies. DC-STAMP is a protein preferentially expressed by DCs. The research described in this thesis focused on resolving the function of DC-STAMP in DC immunobiology.

Chapter 2 identifies OS9 as a novel binding partner of DC-STAMP. OS9 is an ER associated protein implicated in ER-to-Golgi transport. We demonstrate that in immature DCs DC-STAMP and OS9 colocalize in the ER and that DC maturation leads to translocation of DC-STAMP towards the Golgi compartment while localization of OS9 remains unaffected. Using deletion mutants we provided evidence that OS9 plays a role in the redistribution of DC-STAMP upon TLR stimulation.

In **Chapter 3** we present the identification of another interacting partner of DC-STAMP, the transcription factor LUMAN. LUMAN belongs to the CREB/ATF gene family of ER-resident transcription factors. Their activation is governed by a process called regulated intramembrane proteolysis (RIP). To undergo RIP, LUMAN must be transported from the ER to the Golgi compartment where its active form can be liberated by Golgi-residing proteases. In this study we showed localization of LUMAN protein in the ER of immature DCs, its cleavage and translocation to the nucleus upon DC maturation. As DC-STAMP was shown to translocate to the Golgi compartment upon DCs maturation (Chapter 2) and to influence LUMAN cleavage, we postulate a function of DC-STAMP in LUMAN activation.

In **Chapter 4** we characterize the effect of DC-STAMP silencing in mouse bone marrow derived DCs (mBMDCs) on their phenotype and function. Using lentiviral delivery of shRNA we knocked down the expression of DC-STAMP and showed that DC-STAMP is important for proper cytokine production by DC after LPS stimulation. Moreover, we observed a decreased ability of DC-STAMP knock-down mature mBMDCs to stimulate T cell proliferation and differentiation into Th1 type T cells. Our data indicate that DC-STAMP is important for regulation of immune responses driven by mature DCs.

In **Chapter 5** we set out to identify the target genes of LUMAN in DCs. We overexpressed the active form of LUMAN and analysed its effect on the gene expression profile of DC using microarrays. Our approach revealed Apolipoprotein A4 (ApoA4) as a specific target gene of LUMAN in DCs. As ApoA4 is considered to be an anti-inflammatory protein we postulate that LUMAN may be part of a feedback loop necessary for resolving the ongoing inflammation.

Finally, in **Chapter 6** a general discussion and future perspectives on the topics presented in this thesis are given

Samenvatting

Ons lichaam wordt continu belaagd door verschillende bacteriën, virussen, schimmels en parasieten. De belangrijkste rol van het immuunsysteem is ons te beschermen tegen deze pathogenen. Daarnaast beschermt het immuunsysteem ons tegen gevaren vanuit ons eigen lichaam, zoals het ontstaan van kanker. Bovendien reguleert het zijn eigen acties om ons te beschermen tegen auto-immuunziekten. Dendritische cellen (DC's) zijn cellen van het immuunsysteem die een strategische rol spelen in het bewaren van de balans tussen immuniteit en tolerantie. Deze tweedelige functie van DC's maakt ze interessant om te gebruiken in immunotherapie tegen zowel kanker en auto-immuunziekten. Meer inzicht in DC immunobiologie is daarom essentieel voor de verbetering van immunotherapien die op DCs gebaseerd zijn. DC-STAMP is een eiwit dat voornamelijk tot expressie komt in DC's. Het onderzoek beschreven in dit proefschrift was gericht op het ontrafelen van de functie van DC-STAMP in DC immunobiologie.

In **Hoofdstuk 2** laten we zien dat OS9 een nieuwe bindingspartner is van DC-STAMP. OS9 is een ER (endoplasmatisch reticulum) geassocieerd eiwit dat betrokken is bij de transport van eiwitten van het ER naar het Golgi-apparaat. We laten zien dat in zogenaamde onrijpe DCs zowel DC-STAMP als OS9 aanwezig is in het ER. Rijping van DCs leidt tot verplaatsing van DC-STAMP naar het Golgi-apparaat, terwijl OS9 in het ER blijft. Door gebruik te maken van deletiemutanten demonstreren we dat OS9 een rol speelt in de redistributie van DC-STAMP na TLR (Toll-like Receptor) stimulatie.

In **Hoofdstuk 3** presenteren we de identificatie van een andere bindingspartner van DC-STAMP, de transcriptiefactor LUMAN. LUMAN maakt deel uit van de CREB/ATF genfamilie van transcriptiefactoren die aanwezig zijn in het ER. De activatie van deze transcriptiefactoren wordt geregeld door het zogenoemde RIP (gereguleerde intramembraan proteolyse) proces. Om RIP te ondergaan moet LUMAN getransporteerd worden van het ER naar het Golgi-apparaat waar zijn actieve vorm bevrijd kan worden door de daar aanwezige proteases. In deze studie tonen we aan dat LUMAN aanwezig is in het ER van onrijpe DCs. Ook laten we zien dat tijdens de rijping van DCs LUMAN geactiveerd wordt en zich verplaatst naar de celkern. Omdat we gedemonstreerd hebben dat DC-STAMP zich kan verplaatsten naar het Golgi-apparaat tijdens DC rijping en dat het bovendien een rol speelt bij de bevrijding van LUMAN uit het Golgi-apparaat stellen we dat DC-STAMP een functie heeft in LUMAN activatie.

In **Hoofdstuk 4** karakteriseren we het effect op het fenotype en de functie van

DCs uit het beenmerg van muizen na verlaging van de expressie van DC-STAMP. Gebruikmakend van lentivirale overdracht van shRNA hebben we de expressie van DC-STAMP in DC's onderdrukt en aangetoond dat DC-STAMP belangrijk is voor een goede cytokine productie van DC's na LPS stimulatie. Daarnaast zien we een verminderd vermogen van deze DC's om T cel proliferatie en differentiatie in Th1 type T cellen te stimuleren. Onze data tonen aan dat DC-STAMP belangrijk is voor de regulering van immuunreacties die gedreven worden door rijpe DCs.

In **Hoofdstuk 5** proberen we de targetgenen van LUMAN in DC's te identificeren. Na overexpressie van de actieve vorm van LUMAN hebben we de effecten hiervan geanalyseerd in het genexpressie profiel van DC's met behulp van microarrays. Onze aanpak laat zien dat Apolipoproteïn A4 (ApoA4) een specifiek targetgen van LUMAN in DCs is. Omdat ApoA4 gezien wordt als een ontstekingsremmend eiwit stellen we dat LUMAN deel kan uitmaken van een negatieve terugkoppeling die nodig is voor het weer remmen van bestaande ontstekingen.

Hoofdstuk 6 sluit af met een algemene discussie en toekomstperspectieven van de in dit proefschrift gepresenteerde onderwerpen.

Podsumowanie

Organizm człowieka jest nieustannie narażony na atak ze strony chorobotwórczych organizmów takich jak wirusy, bakterie, grzyby czy pasożyty. Główną rolą naszego układu odpornościowego jest walka z tymi patogenami. Dodatkowo, układ immunologiczny musi radzić sobie z niebezpieczeństwem, którego źródłem są własne komórki, tak jak w przypadku nowotworów oraz chorób autoimmunizacyjnych. Utrzymanie dynamicznej równowagi pomiędzy reakcjami immunologicznymi a mechanizmami odpowiedzialnymi za jej wyciszenie, jest niezbędne do prawidłowego funkcjonowania organizmu. Ważną rolę w utrzymaniu tej równowagi odgrywają komórki dendrytyczne. Komórki te mogą zarówno inicjować odpowiedź immunologiczną, jak również jej zapobiegać. Ta dwójka funkcja odpowiada za niezwykle zainteresowanie komórkami dendrytycznymi, zarówno wśród naukowców jak i lekarzy. Dzieje się tak, ponieważ komórki dendrytyczne można wykorzystywać z jednej strony w celach terapeutycznych – zarówno w leczeniu nowotworów i chorób autoimmunizacyjnych, z drugiej strony – w zapobieganiu odrzuceniu przeszczepów. Dogłębna charakterystyka mechanizmów rządzących immunobiologią komórki dendrytycznej jest niezbędna zarówno do ulepszenia istniejących, jak również do opracowania nowych terapii.

Wyniki zaprezentowane w niniejszej pracy są efektem projektu badawczego, którego celem było scharakteryzowanie funkcji białka DC-STAMP, obecnego w komórkach dendrytycznych. DC-STAMP jest transbłonowym białkiem, zlokalizowanym w retikulum endoplazmatycznym (ER), a ekspresja tego białka ograniczona jest głównie do komórek dendrytycznych, makrofagów i osteoklastów. Jednym ze sposobów poznania funkcji białka jest identyfikacja innych białek, które z nim oddziałują. Dlatego też postanowiliśmy zidentyfikować i scharakteryzować białka oddziałujące z DC-STAMP.

Rozdział drugi dotyczy charakterystyki białka OS9, które oddziałuje z DC-STAMP. OS9 jest białkiem zlokalizowanym w ER i bierze udział w transporcie białek między ER a aparatem Golgiego. W tym rozdziale wykazaliśmy, że w niedojrzałych komórkach dendrytycznych białka OS9 i DC-STAMP znajdują się w fizycznym kontakcie i lokalizują się w ER. W trakcie dojrzewania komórki dendrytycznej DC-STAMP jest transportowane w kierunku aparatu Golgiego, natomiast lokalizacja OS9 pozostaje bez zmian. Przy użyciu mutantów delecyjnych wykazaliśmy, że fizyczne połączenie OS9 z DC-STAMP warunkuje transport DC-STAMP z ER do aparatu Golgiego. Wyniki te sugerują, że OS9 odgrywa rolę w transporcie DC-STAMP do aparatu Golgiego w czasie dojrzewania komórek dendrytycznych, które jest wywołane stymulacją

poprzez ligandy Toll-podobnych receptorów (TLR).

W **Rozdziale trzecim** opisane zostało drugie białko oddziaływujące z DC-STAMP, będące czynnikiem transkrypcyjnym, o nazwie LUMAN. Białko LUMAN należy do rodziny czynników transkrypcyjnych CREB/ATF. W postaci nieaktywnej jest ono związane z błoną ER. Aby doszło do jego aktywacji, LUMAN musi być przetransportowany do aparatu Golgiego, gdzie zachodzi hydroliza jego nieaktywnej postaci. Uwolniona, aktywna N-terminalna domena białka jest transportowana do jądra komórkowego, gdzie wiąże się do elementów regulatorowych docelowych genów. Na podstawie wyników tej części projektu badawczego dowiedliśmy, że białko LUMAN w niedojrzałych komórkach dendrytycznych jest zlokalizowane w ER. W dojrzałych komórkach dendrytycznych jego aktywną formę zaobserwowaliśmy w jądrze komórkowym. Dodatkowo wykazaliśmy, że obecność DC-STAMP wpływa na hydrolityczną aktywację białka LUMAN. W związku z tym, że DC-STAMP tak samo jak LUMAN, podczas dojrzewania komórek dendrytycznych jest transportowany z ER do aparatu Golgiego, stwierdziliśmy że DC-STAMP jest odpowiedzialny za regulację aktywności czynnika transkrypcyjnego LUMAN.

Rozdział czwarty poświęcony jest opisowi identyfikacji funkcji białka DC-STAMP w komórkach dendrytycznych poprzez wyciszenie jego ekspresji. W wyniku obniżonej ekspresji białka DC-STAMP, stymulowane LPSEM mysie komórki dendrytyczne charakteryzowały się zaburzoną produkcją cytokin i chemokin. Dodatkowo, komórki te miały obniżoną zdolność pobudzania limfocytów T do podziału i do różnicowania się w kierunku limfocytów pomocniczych typu Th1. Nasze wyniki wskazują, że DC-STAMP pełni ważną funkcję w regulacji odpowiedzi immunologicznej indukowanej przez dojrzałe komórki dendrytyczne.

Rozdział piąty dotyczy identyfikacji genów regulowanych przez czynnik transkrypcyjny LUMAN w komórkach dendrytycznych. W celu jego charakterystyki wprowadziliśmy do komórek dendrytycznych aktywną wersję czynnika LUMAN i przy użyciu mikromacierzy DNA przeprowadziliśmy analizę różnic w ekspresji genów. W ten sposób udało nam się wykazać, że genem regulowanym przez czynnik LUMAN w komórkach dendrytycznych jest gen *Apolipoproteiny A4*. Apolipoproteina A4 jest, między innymi uważana za czynnik przeciwzapalny, dlatego też aktywacja jej ekspresji przez czynnik LUMAN, który jest aktywowany podczas dojrzewania komórek dendrytycznych, sugeruje jego udział w wygaszaniu stanu zapalnego.

Podsumowując, odkrycia zaprezentowane w niniejszej pracy rzucają nowe światło na rolę białek DC-STAMP, OS9 i LUMAN w immunobiologii komórek dendrytycznych. Do pełnego wyjaśnienia interakcji zachodzących pomiędzy tymi

trzema białkami oraz ich regulacji w obrębie komórek dendrytycznych niezbędne są dalsze badania.

Acknowledgements

Completing a PhD is a long, hard road with many twists and turns. Six years ago when I decided to step on this road I wasn't fully aware of how tough it's going to be. Nevertheless, now I am at the end of it and I have little to regret. Herein, I would like to thank all the people who helped me on the way, who made it easier, who made it happen.

First and foremost, I would like to thank my promotor. **Gosse**, thank you for all I've learned from you. Though the lessons you gave me sometimes were bitter, now I can feel the sweet taste of them. It was you who insisted that I start to use the "holy" Dutch AGENDA. I've learned to think independently and to plan better.

Next, I would like to thank my paranimfen. **Agata**, we've been friends for almost 10 years now. We studied together and shared a flat in Kraków. The first time I visited the Netherlands was to visit you. Second time I came I had stayed for over 5 years. If not you I wouldn't probably end up doing my PhD in this country, say nothing about meeting my husband :). Thank you for being always there for me, when I need to share good or bad news, complain, laugh or when I simply feel like talking polish. **Christina**, for all these years we could always escape from the lab to eat lunch together, release some steam and laugh – essential thing in the stressful life of every PhD student. I am glad that we can continue to do that via skype. Thank you for being my friend. Also big thanks to you and **Luis** for taking care of our "sweet" cat Rufus, for helping with moving and for all the good Cuban food.

Of course, this thesis would not have been possible without work and help of people who once belonged to the STAMP group. **Dada** and **Bas** thank you for all the input I got from you during my PhD. You pass on me all your knowledge about DC-STAMP and Co. Thank you for the critical comments and good advices. **Dada**, differences between our personalities sometimes caused turbulences in our little STAMP group but I want you to know that I am very grateful for all your help and support. **Maaïke vH**, you were part of the STAMP group when I joined. You introduced me to the culture lab, transfections, confocal microscopy and qPCR. Thank you for your technical support and kindness. **Amy** you've joined TIL just for the last year of my PhD when I really needed an extra help. Thank you for all the hopeless ApoA4 ELISAs, tons of great virus you made and countless FACS samples you run. It was fun working, cooking, watching movies, shopping and dancing with you. I still remember Polish pierogi we made and delicious salmon and grapefruit salad recipe I got from you. Pity that Perth is so far. I would also like to thank my student **Kathrin** who helped me a lot during her time at the TIL. **Katharina** and **Suzanne**, thank you for your effort you put in the DC-STAMP

project.

Next come the SCRIPT group. Girls, it was pleasure to swim in one aquarium. I miss all this crazy ideas, “intellectual” nonsenses and our discussions about life and science. Dear **Marleentje**, you took very good care of me when I’ve started at TIL. You showed me around, handled very well my emotional outbursts and “my cruel honesty”. You even held yourself from singing when I was around. Thank you for that ;). It took some time but we became friends and I hope that the miles between us won’t change it (doesn’t matter English or American ones). I am sorry that you won’t be there during my defence and the party. All the best to you and **Koen** on your new life adventure in America. **Saartje**, we sat opposite each other for almost 3 years divided only by the screens of our computers. I enjoyed our cat talks, dinners and wine tasting. It was fun to train together for the Marikenloop. Thanks, for slowing down when I couldn’t keep up. Good luck with your own defence and your new job. **Nina**, I am sorry that our “huwelijks bootjes” are drifting away ;). I enjoyed a lot sharing the desk with you and all the excitement of the wedding preparations. I hope you haven’t forgotten our agreement for the future when we are old and when friendship will survive only if all spilled coffee can be easily forgotten. **Maaïke L**, I always could count on your help when mysterious bands appeared on my gels, cloning didn’t work or when I needed to move flats or to visit IKEA. I always admired how many IP’s and gels you could run during one day and after that still full of energy to go for horse riding. Thanks for sharing your good spirit and knowledge.

I also would like to thank people from the mouse group **Martijn, Jori, Stefan, Wendy, Marjolijn, Michiel** for the supply of legs and spleens, and help with setting up my assays.

Wendy, we started as PhD students at the TIL together and I think we both felt a bit lonely in Nijmegen. Thank you for being my gym and dinner companion. I miss it. With you gym wasn’t boring though the spinning class is still “no, no” to me. Never loose your self-confidence. Soon we will celebrate your defence.

Iziah and **Christian** thank you for your professional bioinformatics support and patience when I ask for the n-time to reanalyse the data.

I also wish to thank all the current and former **TILLERS** for the great work atmosphere and many “gezellig” coffee breaks. Thank you for sharing your knowledge, protocols and reagents.

Special Big Thank You will go to the TIL party team: **Martijn, Wendy, Koen, Ben, Jori, Saartje, Joost, Barbara, Marjolein, Michiel, Stefan, Hans, Jurjen** I always had fun talking, dancing and drinking together with you. I miss Fridays at Aesculaaf, lab out’jes, Christmas dinners, kroegtijger and poker parties.

I also would like to thank **Ruurd** and **Alessandra** for their input into STAMP project during the time when Gosse couldn't be there.

Many thanks to the ladies of the Secretariat. Thank you **Jeanette** for squeezing me into Gosse's busy agenda and nice chit-chats when I was killing time waiting for another delayed meeting to start.

Next I would like to thank some friends from outside work. Thank you all for being there for me, believing in me and for your support. I know that even when we are far away from each other I can always count on you. **Asia**, you were my only Polish friend in Nijmegen. We met on the Dutch course, first month when I moved to Nijmegen. Soon we became friends. I loved our jazz dance classes, dinners, movie evenings and discussions about biology, economy and life in general. Thank you for all the quality time we had together. Nijmegen wasn't the same after you moved to Amsterdam. **Anna G** and **Anna Z**, I am so happy that after so many years when we lived in different countries we are now all in London and we see each other much more often.

Last but not least I would like to thank my family. **Mamo**, dziękuję Ci ze twoją miłość, wiarę we mnie, za to że pozwalając mi na samodzielność i zawsze mnie wspierałaś w moich wyborach. **Radek, Marcin, Aneta i Filip** bardzo się cieszę, że będziecie ze mną w tym bardzo ważnym dla mnie dniu. Dziękuję.

Finally, I would like to thank my husband. Dear **Patrick**, thank you for all the dinners waiting for me when I worked late and for the shelter in your arms when I had a bad day. The source of your patience must be deep. Thank you for all your love and support.

Anna

Curriculum Vitae

Anna Sanecka-Duin was born on March 6, 1981 in Staszów, Poland. In 2000, she started her studies towards her Master of Science in Biotechnology at the Jagiellonian University in Kraków. In 2004 she received the Erasmus/Socrates scholarship and spent 4 months as a trainee in the Max Planck Institute of Biochemistry in Martisried, Germany. Working under the supervision of Dr. Cord Brakebusch, she broadened her laboratory experience characterizing the effects of Rac-1 knock-out in mouse skin.

After going back to Poland she continued her studies and performed a 10 months practical training in the departments of Microbiology and Immunology under the supervision of Prof. Jan Potempa and Dr. Krzysztof Guzik. She studied the effect of protease SV8 from *Staphylococcus aureus* on phagocytosis of granulocytes by macrophages.

After she graduated from Jagiellonian University in 2005 she obtained Leonardo da Vinci scholarship and spent 4 months working in biotech company Cellerix in Tres Cantos, Madrid, Spain. During this traineeship she was working on development of retroviral gene delivery system.

After experiencing working in industry she moved back to academia and in August 2006 she obtained the PhD student position at the Department of Tumor Immunology in Nijmegen Center for Molecular Life Sciences (NCMLS), Radboud University Medical Centre under the supervision of Prof. Gosse J. Adema.

Since October 2011, she holds the position of Carrier Development Fellow at Medical Research Council, National Institute for Medical Research in London, UK. She is working in the Department of Parasitology in the group of Dr. Eva Frickel on characterization of *Toxoplasma gondii* specific CD8 T cells in the brain of chronically infected mice.

List of publications

- Hontelez S, **Sanecka A**, Netea M, van Spruel A, Adema GJ. **Molecular view on PRR crosstalk in anti-fungal immunity**. Cell Microbiology (2012) Jan 10. doi: 10.1111/j.1462-5822.2012.01748.x
- **Sanecka A**, Ansems M, van Hout-Kuijter MA, Looman MW, Prosser AC, Welten S, Gilissen C, Sama IE, Huynen MA, Veltman JA, Jansen BJ, Eleveld-Trancikova D, Adema GJ. **Analysis of genes regulated by the transcription factor LUMAN identifies ApoA4 as a target gene in dendritic cells**. Molecular Immunology (2011), doi:10.1016/j.molimm.2011.12.003
- **Sanecka A**, Ansems M, Prosser AC, Warner K, Danielski K, den Brok MH, Jansen BJ, Eleveld-Trancikova D, Adema GJ. **DC-STAMP knock-down deregulates cytokine production and T-cell stimulatory capacity of LPS-matured dendritic cells**. BMC Immunology (2011), 12:57
- Eleveld-Trancikova D, **Sanecka A**, van Hout-Kuijter MA, Looman MW, Hendriks IA, Jansen BJ, Adema GJ. **DC-STAMP interacts with ER-resident transcription factor Luman which becomes activated during DC maturation**. Molecular Immunology (2010), 47(1963-1973)
- Jansen BJ*, Eleveld-Trancikova D*, **Sanecka A**, van Hout-Kuijter MA, Hendriks IA, Looman MW, Leusen JH, Adema GJ. **OS9 interacts with DC-STAMP and modulates its intracellular localization in response to TLR ligation**. Molecular Immunology (2009), 46(505-515)
*equally contributed to this study
- Chrostek A, Wu X, Quondamatteo F, Hu R, **Sanecka A**, Niemann C, Langbein L, Haase I, Brakebusch C. **Rac1 is crucial for hair follicle integrity but is not essential for maintenance of the epidermis**. Molecular and Cellular Biology (2006), 26(6957-6970)

